ONWI-308

Modelling Rock Joint Behavior from In Situ Block Tests: Implications for Nuclear Waste Repository Design

Technical Report

September 1982

Nick Barton

Terra Tek, Inc.
University Research Park
420 Wakara Way
Salt Lake City, Utah 84108

ONWI
Office of Nuclear Waste Isolation

BATTELLE Project Management Division

BIBLIOGRAPHIC DATA

Barton, Nick, 1982. *Modelling Rock Joint Behavior from In Situ Block Tests: Implications for Nuclear Waste Repository Design,* ONWI-308, prepared by Terra Tek, Inc. for Office of Nuclear Waste Isolation, Battelle Memorial Institute, Columbus, OH.

NOTICE

Printed in the United States of America
Available from
National Technical Information Service
U.S. Department of Commerce
5285 Port Royal Road
Springfield, VA 22161

NTIS price codes
Printed copy: A06
Microfiche copy: A01

ONWI-308
Distribution Category UC-70

Modelling Rock Joint Behavior from In Situ Block Tests: Implications for Nuclear Waste Repository Design

Technical Report

September 1982

Nick Barton

Terra Tek, Inc.
University Research Park
420 Wakara Way
Salt Lake City, Utah 84108

The content of this report was effective as of September 1981. This report was prepared by Terra Tek, Inc. under Subcontract E512-04700 with Battelle Project Management Division, Office of Nuclear Waste Isolation under Contract No. DE-AC06-76-RLO1830-ONWI with the U.S. Department of Energy. This contract was administered by the Battelle Office of Nuclear Waste Isolation.

ACKNOWLEDGEMENTS

Significant impetus for this study was generated by the enthusiasm of Ron Hoffman and Don Maxwell of Science Applications, Inc., Oakland, CA. Funding was provided by the Office of Nuclear Waste Isolation, under Contract E512-04700. The support of Mike Wigley and Bill Ubbes is gratefully acknowledged. The constitutive modelling techniques developed during the course of this study have been validated against a large body of test data. The exceptional experimental studies of joint deformability performed by Stavros Bandis of Thessaloniki, Greece (formerly of Leeds University, England) are humbly acknowledged.

ABSTRACT

Realistic simulation of the mechanical and hydraulic properties of rock joints has been an important goal of numerical modelling for many years. In this report, simple, inexpensive index tests suitable for application to jointed core or jointed blocks of rock are described. These provide quantitative data on joint roughness, joint wall strength and residual friction angle, suitable for waste repository characterization. These three parameters form the basis of a new constitutive law of rock joint behavior which will enable numerical modellers to simulate the complete shear strength-displacement, dilation and closure of joints, including shear reversal and unloading cycles. Size effects are reviewed in detail and methods are developed for correcting the results of small scale tests to allow for limited sample size. The effects of shear displacement and dilation, normal closure and joint opening on permeability are modelled, so that fully coupled hydromechanical modelling can be achieved. The effects of extremely slow stress perturbations, periods of stick, and thermal loading on joint properties are also evaluated. The numerical modelling techniques are illustrated with numerous examples, and are validated against a large body of experimental data.

TABLE OF CONTENTS

1 INTRODUCTION

Realistic simulation of the mechanical and hydraulic properties of rock joints has been an important goal of numerical modelling for many years. Even simplified constitutive models demonstrate the extreme importance of joint characteristics. For example, a simple change of friction angle from 40° to 30° may alter not only the magnitudes of deformation, but also the type of deformation experienced by an excavation. When joint modelling is designed to also include different degrees of joint roughness, dilation and joint aperture, it is clear that realistic response will be dependent on correct constitutive models of the way these parameters interact with changes of stress. Numerical instability may be experienced if input parameters are not mutually compatible.

Potential siting of nuclear waste repositories in jointed media such as granite, basalt, or tuff places added emphasis on the importance of joint properties. It is known from mining and tunneling practice, from numerical models and physical models, that joint apertures vary in response to excavation, to thermal loading and to dynamic loading. The potential migration of groundwater across a repository will be strongly influenced by the zones of reduced permeability caused by joint closure, and by the zones of increased permeability caused by shear displacement.

The constitutive model of joint behavior described in detail in this report is designed to satisfy two important goals:

1. realistic simulation of observed phenomena
2. inexpensive joint data acquisition

Preliminary modelling can be based solely on the characterization of joints recovered in drillcore, together with the estimate of water conducting aperture obtainable from borehole pumping tests. Once access to the site is available, these preliminary joint characterization studies would be extended to obtain their directional variation. Simple block tests are described for extrapolating some of the data obtained from heated block tests to other locations at the site, thereby reducing the time and cost of site characterization, while increasing the number of sampling points.

2 EVIDENCE OF JOINT DISPLACEMENT FROM PHYSICAL MODELS

The deformation of a rockmass that can be measured when fluid is injected or withdrawn from a well, is a relatively complex phenomenon caused by the change of effective normal stress in the joints (or pore space). The degree of complexity is increased considerably when shear displacement accompanies "normal" changes of aperture. Joint shear displacements may be caused by excavation in anisotropic stress fields, by thermal loading and by dynamic loading. All these effects have been demonstrated in recent numerical modelling reported by Wahi et al. (1980).

If the relevant joints are smooth and planar (e.g. bedding joints in shale) shearing has obvious consequences for the stability of the blocks bounded by these joints, as clearly demonstrated by Wahi et al. (1980). However, if the relative joints are rough, with high wall strength as in granite, stability will not necessarily be reduced by the shearing process since roughness-induced dilation will increase the normal stress and "lock" the joints in some finite displaced position. The only significant consequence of this process is the aperture strain caused by the dilation. Permeability may be greatly enhanced locally.

Graphic examples of joint dilation caused by the shearing process are provided by physical models of excavation in jointed media. Barton and Hansteen (1979) have studied models consisting of up to 20,000 discreet interlocked blocks. Obvious cases of joint shear and dilation are provided by photographs of the ultimate failure of an unreinforced excavation subjected to severe dynamic loading, as shown in Figure 2-1. The deliberate choice of unfavorable joint orientations and highly anisotropic stress fields may also cause joint shear during the excavation process, as illustrated by the circled deformation vectors shown in Figure 2-2. Prototype-scale shear displacements of at least 50mm are evident, and a considerable length of joint (>50 meters) is involved. Severe dynamic loading of this model causes additional shear displacement along the diagonal joint, as seen in Figure 2-3.

The above examples are exaggerations of real processes due to the deliberate choice of unfavorable stress fields, unfavorable joint orientations and the choice of severe dynamic loading experienced only in the immediate vicinity of causative earthquake faults. However, the models illustrate in qualitative terms that shearing and dilation need to be modelled, even though

in practice, a well-engineered excavation may experience very small joint displacements. In general, the most important effect of these small joint displacements will be permeability enhancement rather than reduction of stability.

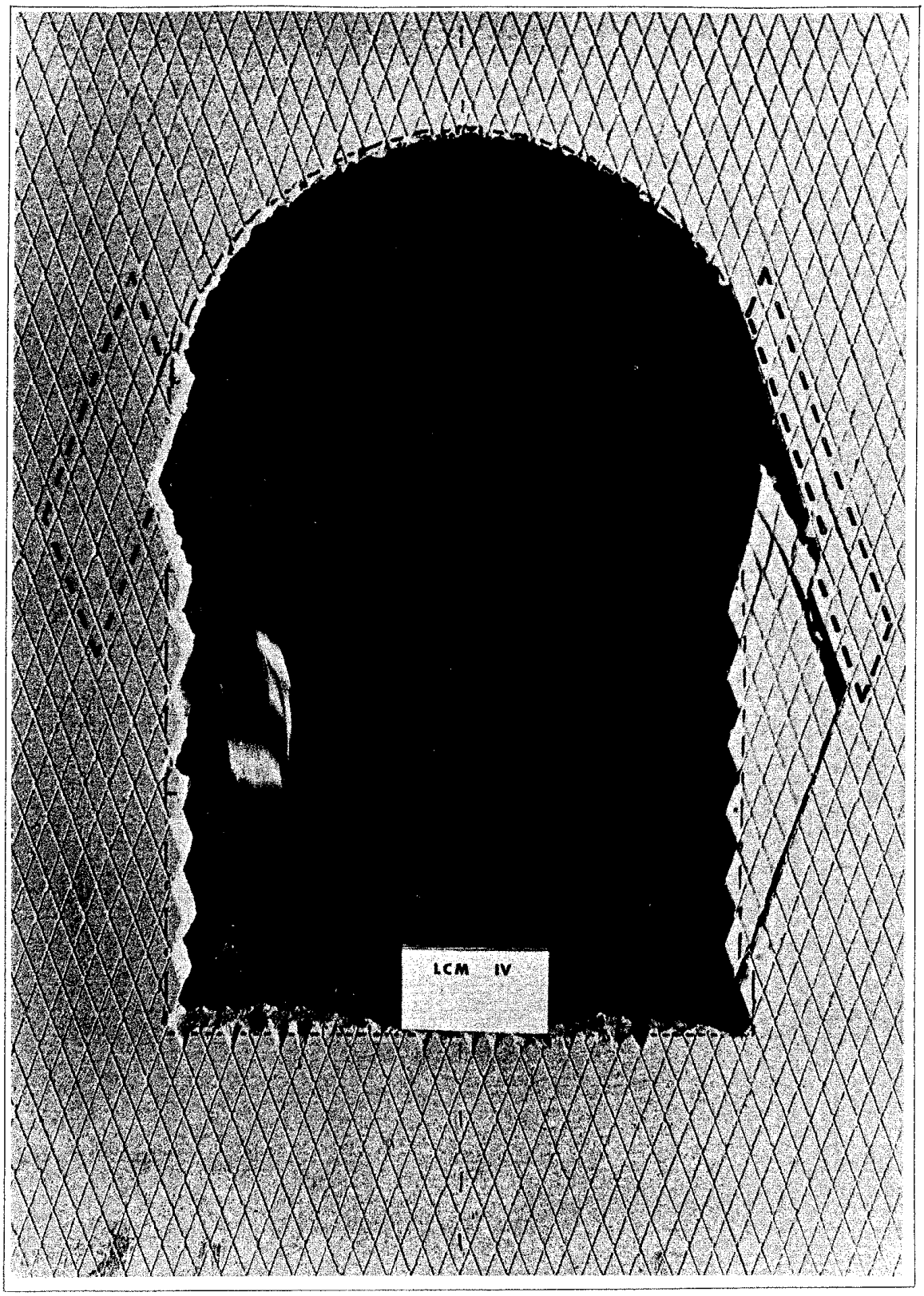

Figure 2.1. Dynamic loading of a two-dimensional jointed model demonstrating the dilation accompanying gross shear displacement (right wall) and a zone of shear strain (left wall - stippled). Joint lines were straight and parallel prior to excavation of the opening.

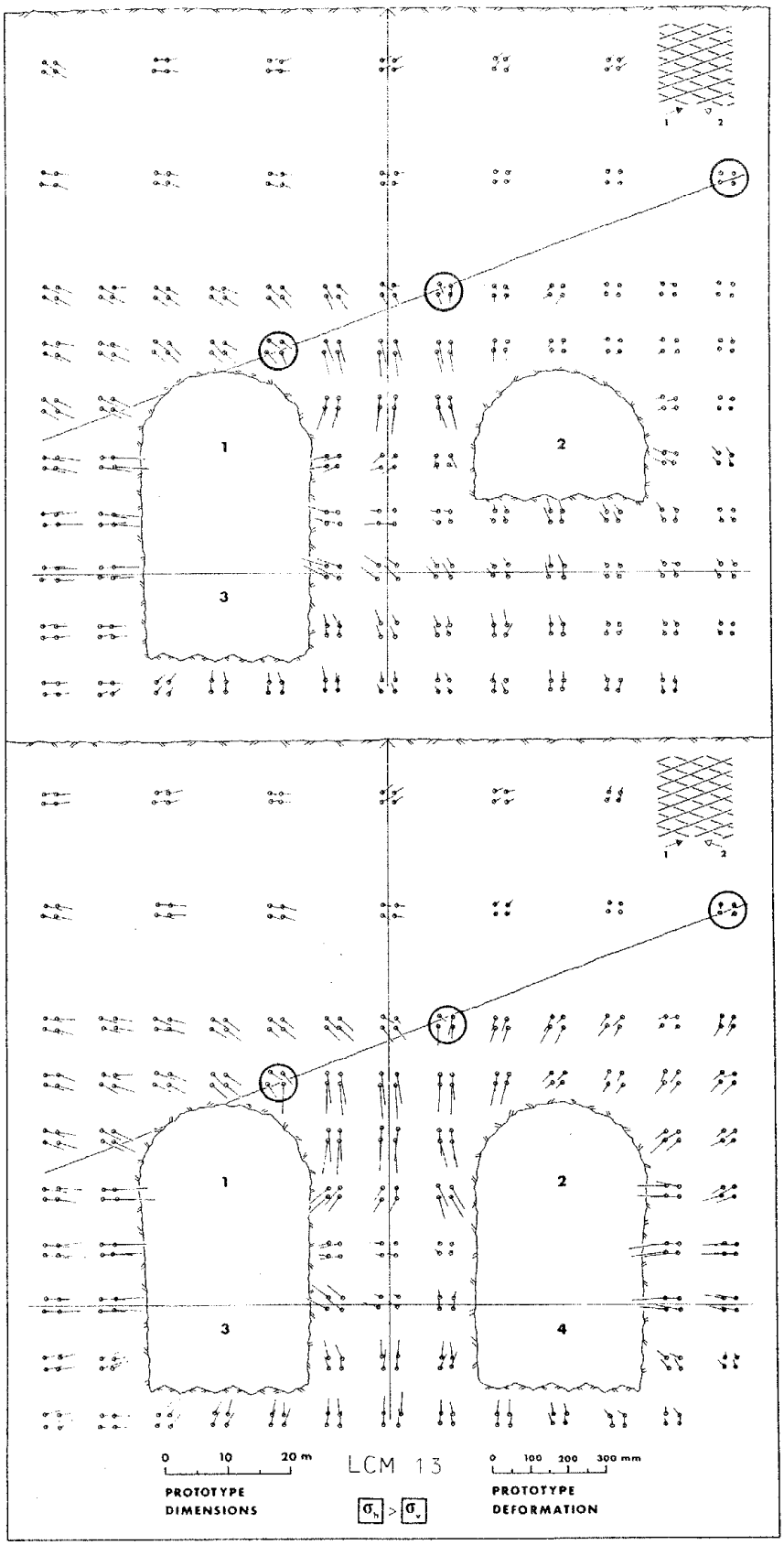

Figure 2.2. Shear displacement along a joint caused by the excavation process, when high horizontal stress is present, after Barton and Hansteen (1979).

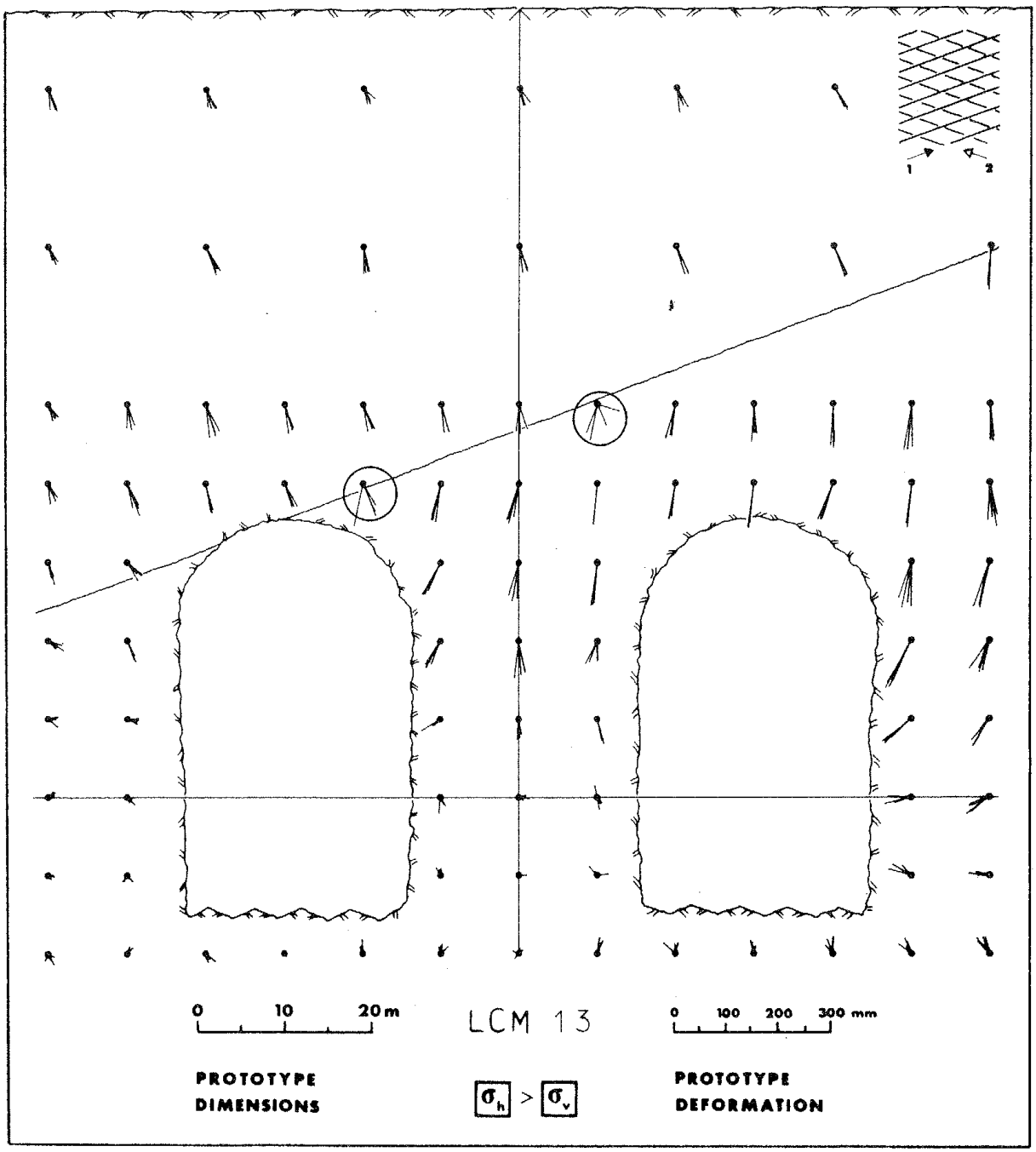

Figure 2.3. Net deformation of the model shown in Figure 2.2, caused by severe dynamic loading. Additional joint shear is evident.

3 QUANTITATIVE JOINT CHARACTERIZATION

The wide variation of peak shear strength of a typical suite of rock joints (Figure 3-1) tested at moderate engineering stress levels contrasts strongly from the narrow band of data typical of high stress tests (Figure 3-2). Byerlee's (1979) "law" for the shear strength of faults at high levels of stress:

$$\tau = 0.85\ \sigma_n \qquad (\sigma_n < 200\ \text{MPa})$$

$$\tau + 50 + 0.6\ \sigma_n \qquad (\sigma_n > 200\ \text{MPa})$$

is unlikely to be adequate for describing the highly individual performance of rock joints tested at moderate stress levels.

A simple, though quite complete method of characterizing the shear behavior of rock joints was developed some years ago (Barton, 1973). It consists of three components: ϕ_b, JRC and JCS. A basic or residual friction angle (ϕ_b or ϕ_r) for flat non-dilatent surfaces in fresh or weathered rock, respectively, forms the limiting value of shear strength. To this is added a roughness component (i). This is normal stress dependent and varies with the magnitude of the joint wall compressive strength (JCS), and with the joint roughness coefficient (JRC). The latter varies from about 0 to 20 for smooth to very rough surfaces respectively. The peak drained angle of friction (ϕ') at any given effective normal stress (σ'_n) is expressed as follows:

$$\phi' = \phi_r + i = \text{JRC}\ \log(\text{JCS}/\sigma'_n) + \phi_r \qquad \text{---------- 3-1}$$

Example

$$\phi_r = 25°,\ \text{JRC} = 10,\ \text{JCS} = 100\ \text{MPa},\ \sigma_n' = 1\ \text{MPa}$$

equation 3-1 gives $\phi' = 45°$

Examples of the strength envelopes generated with JRC values of 5, 10 and 20 are illustrated in Figure 3-3. The compression strength of the joint walls (JCS) has increased influence on the shear strength as the joint roughness increases. Values of JCS and its variation with weathering are measured with the Schmidt (L) hammer. Experimental details are given by Barton and Choubey (1977).

The residual friction angle (ϕ_r) of weathered joints is very difficult to determine experimentally due to the large displacements required, particularly if only small joint samples are available. A simple empirical approach has been developed as shown below.

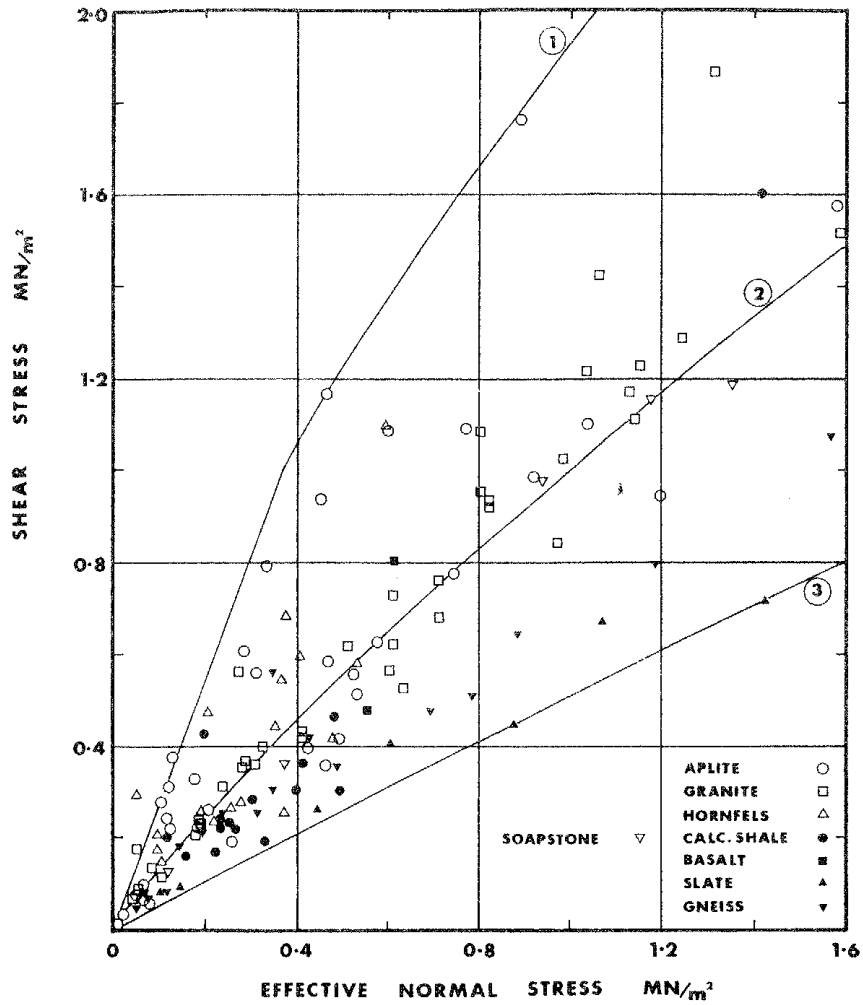

Figure 3.1. Peak shear strength of rock joints measured in the laboratory (sample lengths = 100mm) after Barton and Choubey (1977).

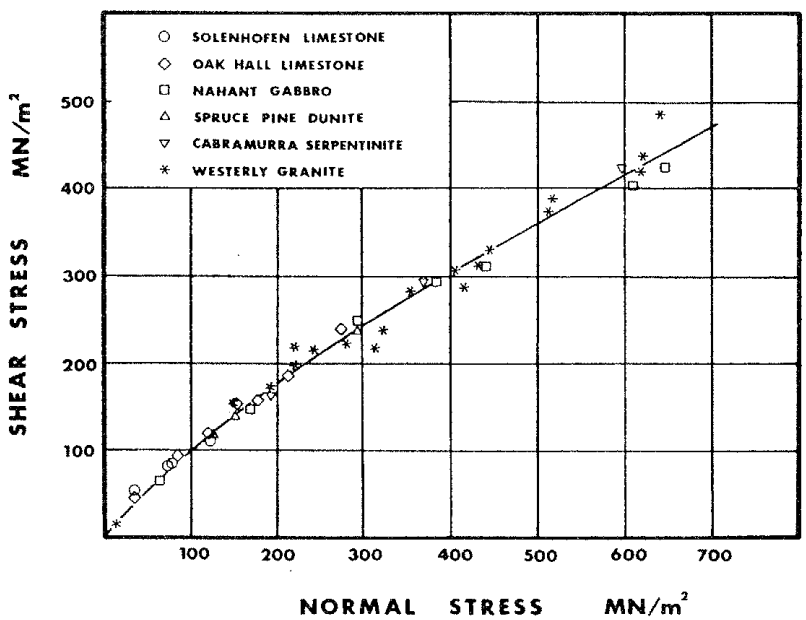

Figure 3.2. Peak shear strength of laboratory "faults", after Byerlee (1968).

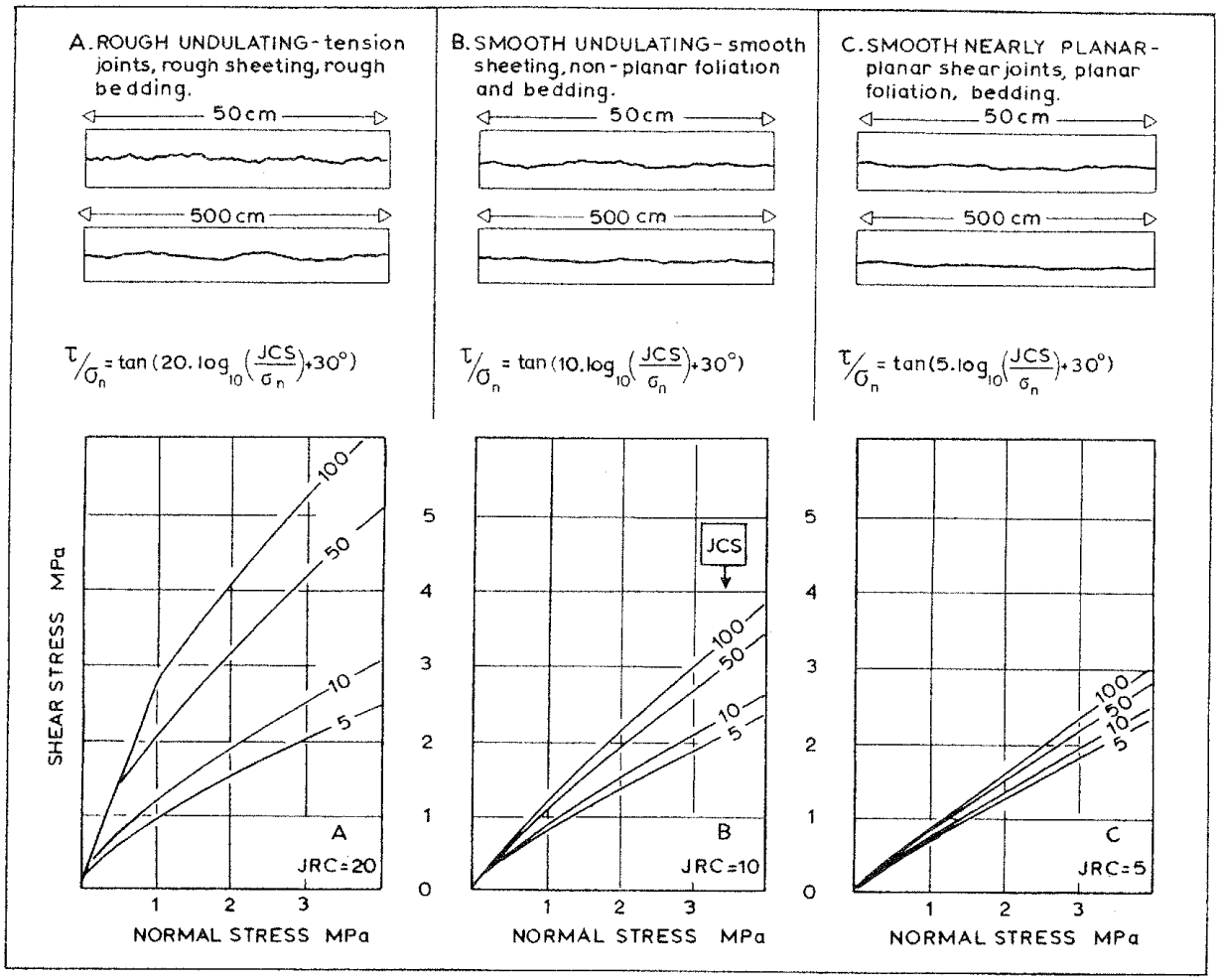

Figure 3.3. Method of estimating the peak shear strength of rock joints, based on the joint roughness coefficient JRC (20, 10 or 5), and on the joint wall compression strength JCS (100, 50, 10 or 5 MPa), after Barton (1973)(1 MPa = 145 psi).

$$\phi_r = (\phi_b - 20) + 20\, r_1/r_2 \quad \text{---------- 3-2}$$

where ϕ_b = basic (minimum) friction angle of flat unweathered rock surfaces (obtained from tilt tests on sawn blocks, or from triple core tilt tests - see Figure 3-4)

r_1 = Schmidt rebound on saturated, weathered joint walls

r_2 = Schmidt rebound on dry unweathered rock surfaces (i.e., saw cuts, fresh fracture surfaces, etc.)

Example:

$\phi_b = 30°$, $r_1 = 30$, $r_2 = 40$

equation 3-2 gives: $\phi_r = 25°$

The joint roughness coefficient (JRC) can be estimated in several different ways. For example, Barton and Choubey (1977) show a set of 10 increasingly rough joint profiles measured on 10cm long specimens, which can be physically compared with profiles measured on other joints (Figure 3-5). However, a more reliable method of determining JRC is by conducting tilt tests on jointed core, as illustrated in Figures 3-4 and 3-6.

The value of JRC is back-calculated directly from the tilt test by rearrangement of the peak strength equation:

$$JRC = \frac{\alpha° - \phi_r}{\log(JCS/\sigma_{no}')} \quad \text{---------- 3-3}$$

where $\alpha°$ = tilt angle when sliding occurs ($\alpha° = \arctan \tau/\sigma_{no}' = \phi'$)

σ_{no}' = effective normal stress acting across joint when sliding occurs

Example: $\alpha = 75°$, $\phi_r = 25°$, JCS = 100 MPa, $\sigma_{no}' = 0.001$ MPa

$$JRC = (75° - 25°)/5 = 10$$

The values of JRC, JCS, and ϕ_r are used to generate peak shear strength envelopes over the required range of stress. The table of values (overleaf) shows how the value of ϕ' varies inversely with the log of effective normal stress. This is a fundamental result for rock joints, rockfill, gravel, etc. (Barton and Kjærnsli, 1981).

Example : JRC = 10, JCS = 100 MPa, $\phi_r = 25°$. The table overleaf indicates:

Type of Test	σ_n'	ϕ'*
Approx. lab tilt test	0.001	75
Approx. field tilt test	0.01	65
	0.1	55
Approx. design loading	1.0	45
	10.0	35

*Note: ϕ' varies by JRC degrees ($^\circ$) for each ten-fold change in stress, in this case, 10°.

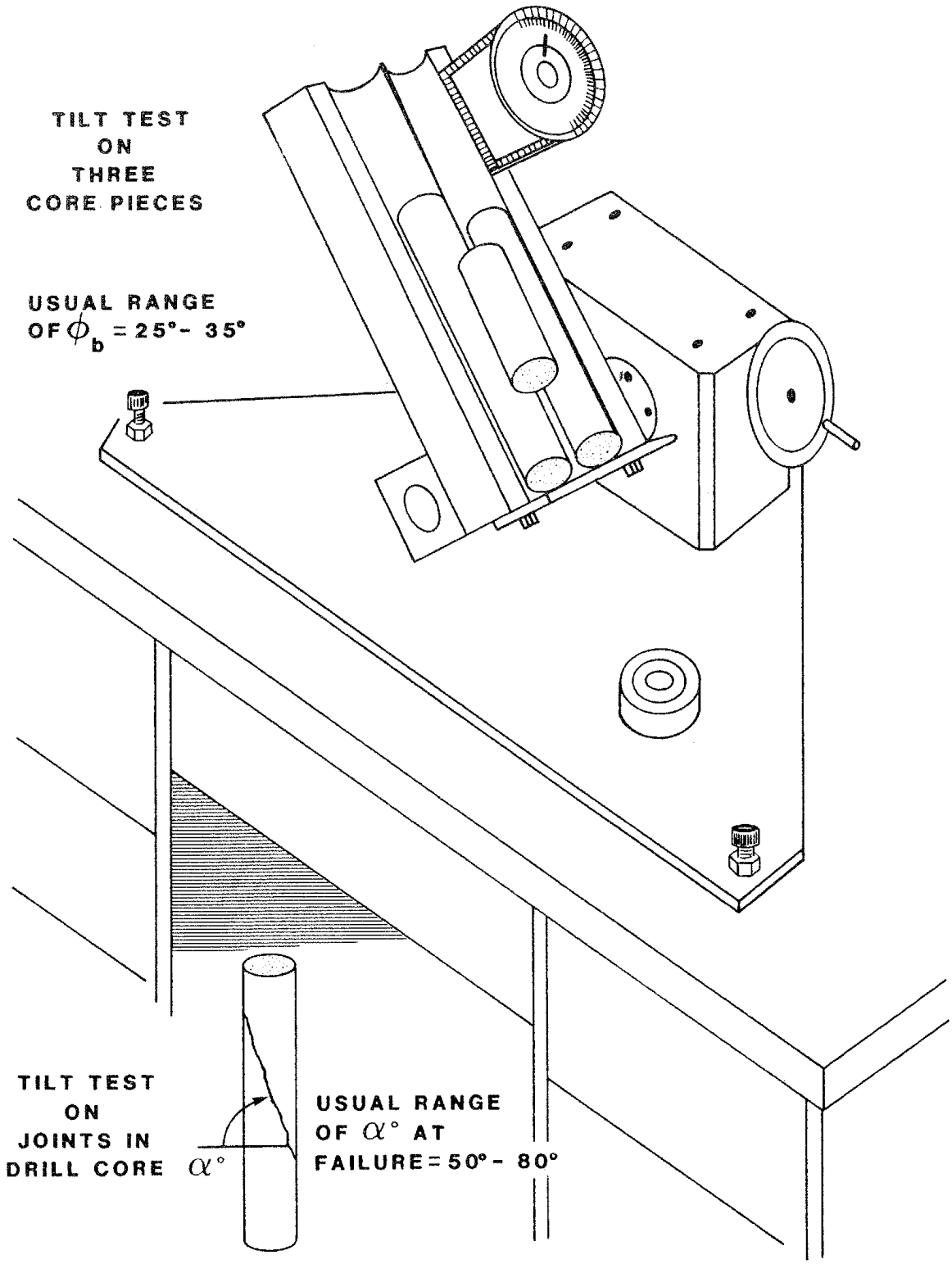

Figure 3.4. Tilt tests can be used to measure ϕ_b (of flat surfaces) and to measure the friction angle of joints intersecting drill core. These low stress tests are readily extrapolated to design stress levels.

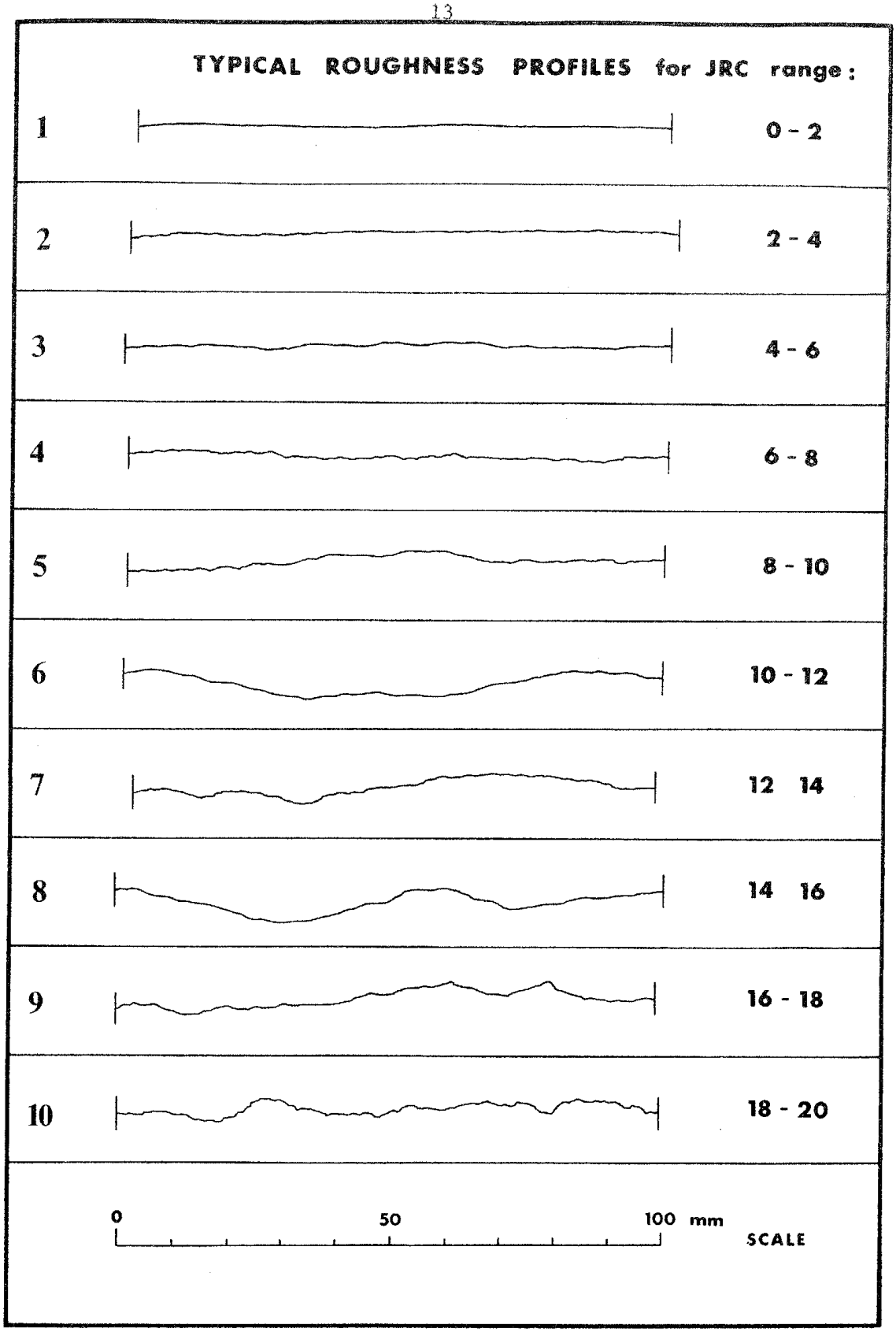

Figure 3.5. Typical JRC values for joint samples of different roughness, after Barton and Choubey, 1977.

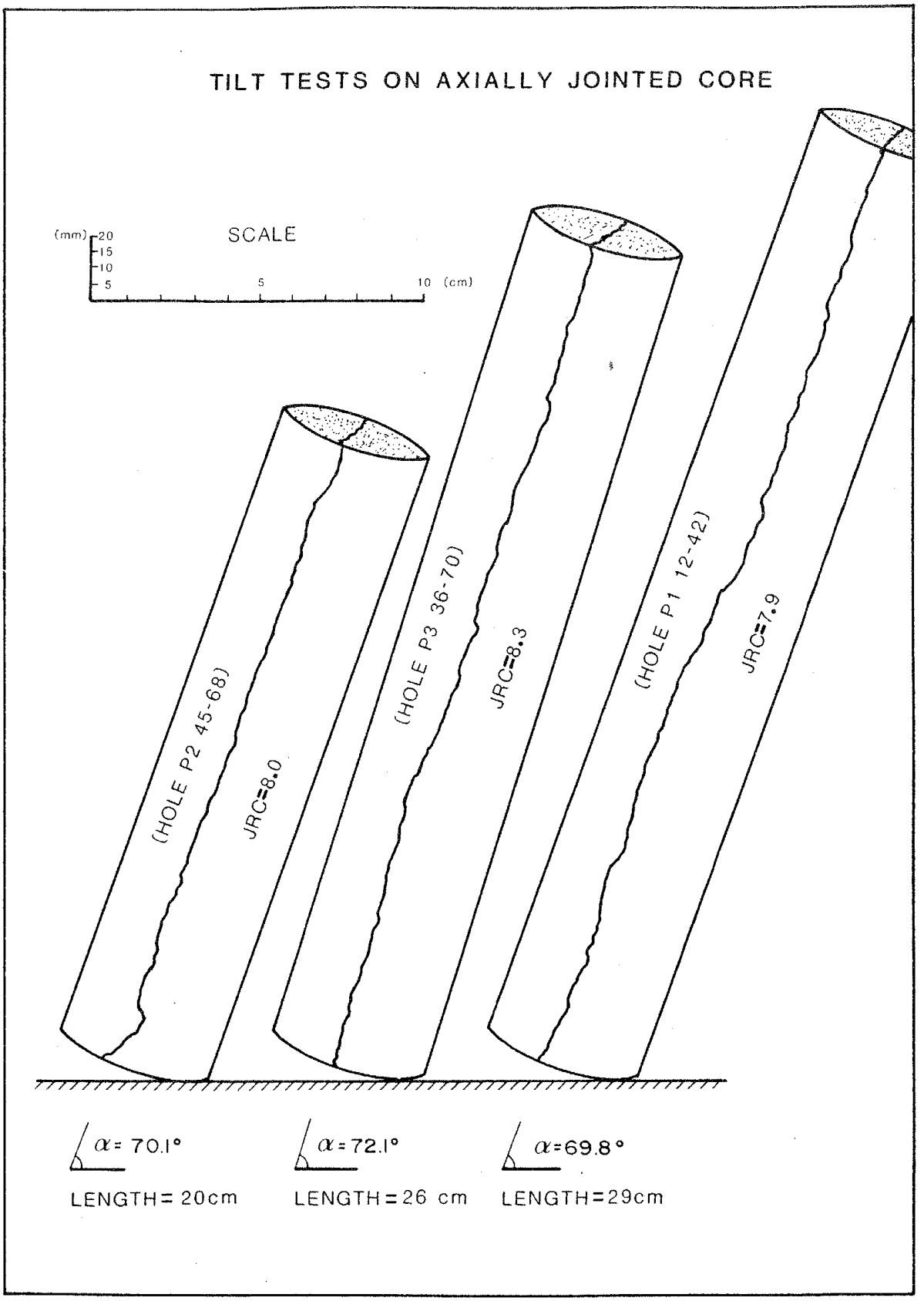

Figure 3.6. Tilt tests on axially jointed core obtained from Terra Tek's heated block test. The profiles are drawn at the mean tilt angles measured in each case.

4 SIZE-DEPENDENT JOINT PROPERTIES

Large-scale shear tests of joints in quartz diorite (Pratt, et al., 1974) and a comprehensive series of tests performed by Bandis (1980) have indicated that larger shear displacements are required to mobilize peak strength as the length of joint sample is increased. This means that larger but less steeply inclined asperities tend to control peak strength as the length of sample is increased. The photograph of model joint replicas of different size shown in Figure 4-1 indicates that during a shear test, the size of sample will determine both the distribution, number and size of contact areas. While this level of detail can obviously not be modelled numerically, its effect on joint behavior must be taken into account. The following possible size-dependent properties have to be considered:

1. shear displacement to mobilize peak strength (δ_{peak})
2. joint roughness coefficient (JRC)
3. joint wall compression strength (JCS)
4. shear stiffness (K_s)
5. dilation during shear (d_n)

A method of estimating (or measuring) the size-dependency of these parameters is needed, before a satisfactory constitutive law of behavior can be developed.

4.1 SIZE-DEPENDENCE OF DISPLACEMENT

A review of a large number of shear tests reported in the literature (650 data points) indicates that the displacement required to mobilize peak strength increases with sample size for a wide variety of surfaces. Surprisingly, quite planar joint surfaces and clay-filled discontinuities are also subject to this scale effect. The data presented in Figure 4-2 indicates that the ratio δ(peak)/L reduces gradually with increasing block or sample length (L).

When the data are grouped into the following three size categories:

1. laboratory size (30-300mm)
2. in situ size (300mm - 3m)
3. novel (3m - 12m)

and grouped into three surface categories, the variation of (peak) with size becomes clearly apparent, as shown in Table 4-1.

The importance of this size-effect in the numerical modelling of rockmass response requires little emphasis. A review of earthquake fault slip magnitudes (Nur, 1974) indicates that it possibly extends over dimensions of some orders of magnitude beyond the limits of testing. In Figure 4-3, the above groups of

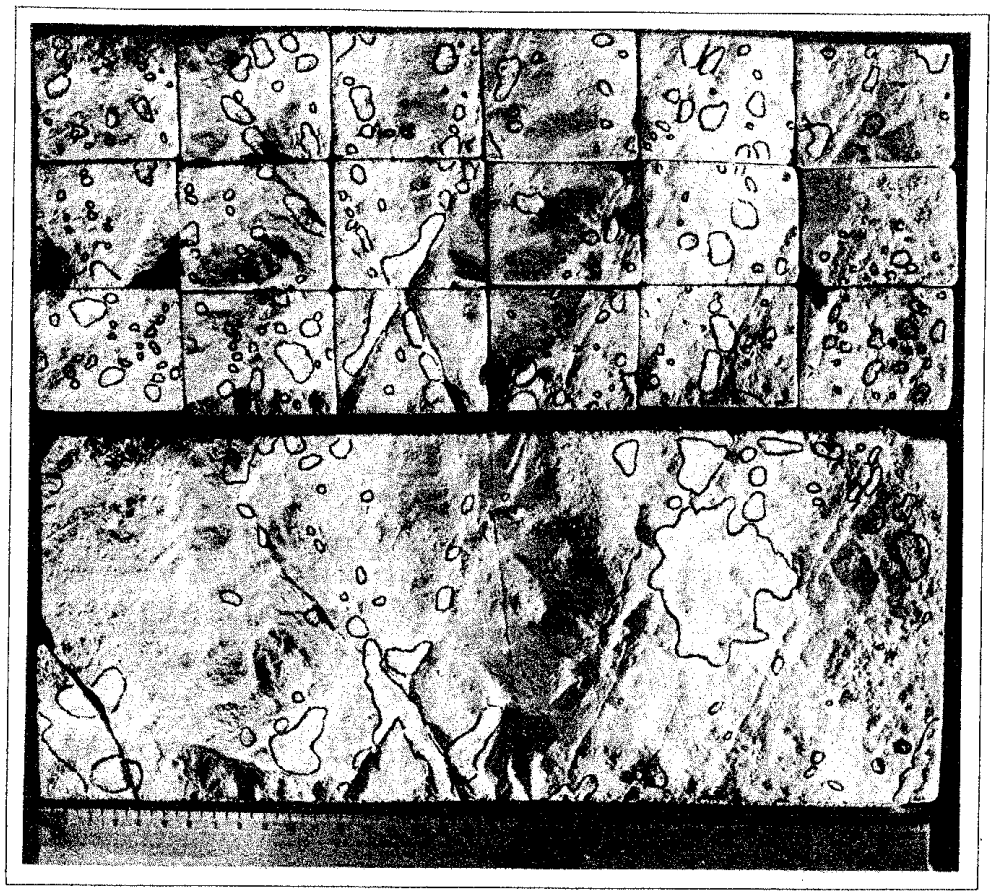

Figure 4.1. Photograph illustrating the distribution, number, and size of post-shear test contact areas on small and large joint samples, after Bandis et al. (1981). These model joints were cast directly from a rubber mold of a bedding plane in limestone.

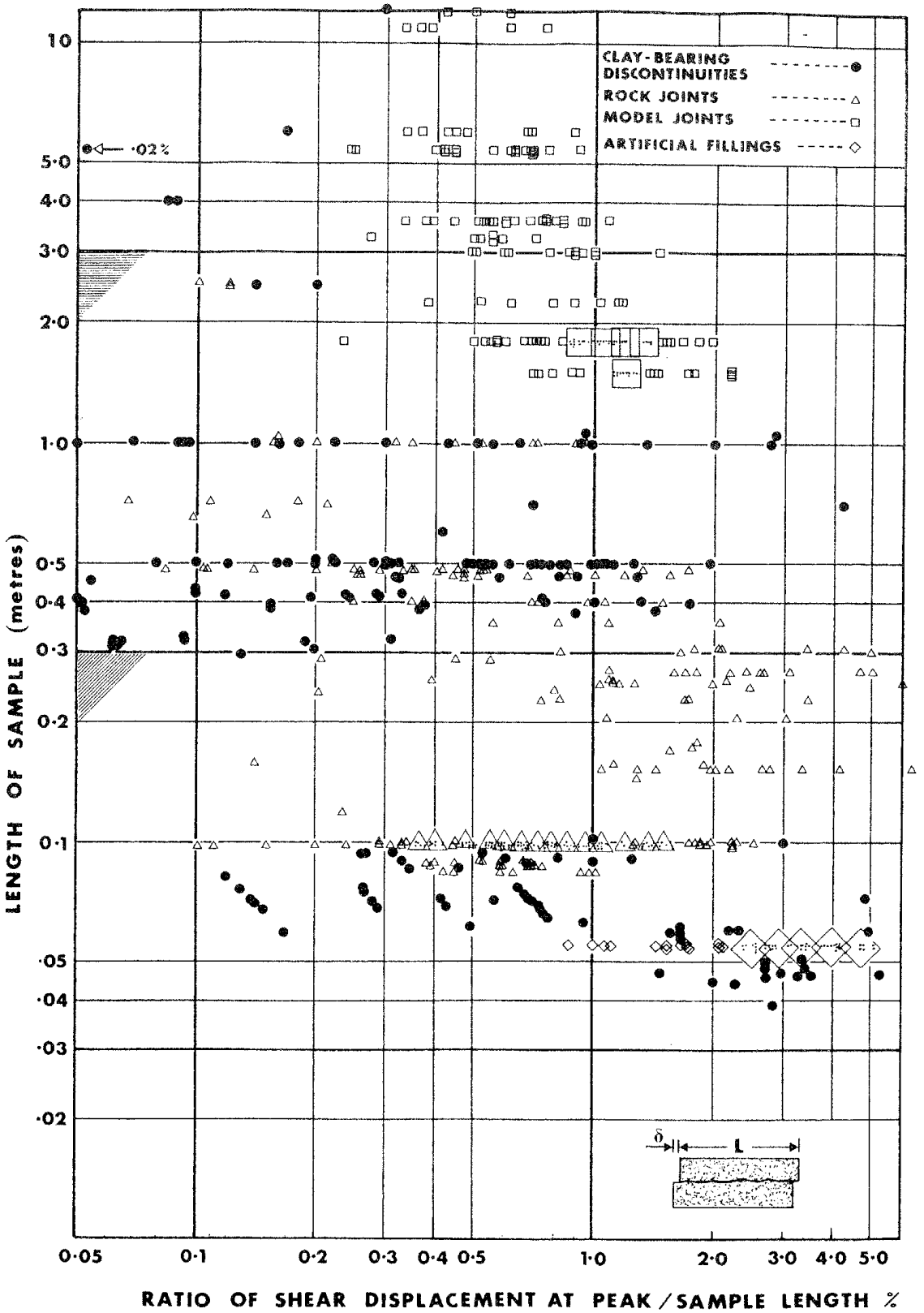

Figure 4.2. The displacement required to mobilize peak shear strength increases with sample size for a wide variety of joint and discontinuity types.

TABLE 4.1

Summary of Mean Peak Shear "Strains" for

Joints and Clay-filled Discontinuities

TYPE OF SAMPLE	LAB. SCALE (30-300mm)	IN SITU (0.3-3.0m)	NOVEL (3-12m)	ALL SIZES
(1) Filled discontinuities	1.31% (56)	0.55% (94)	0.13% (5)	0.81% (155)
(2) Rock Joints	1.28% (224)	0.72% (71)	--	0.98% (295)
(3) Model Joints	--	1.04% (96)	0.58% (66)	0.86% (162)

Numbers in parenthesis indicate the number of test results.

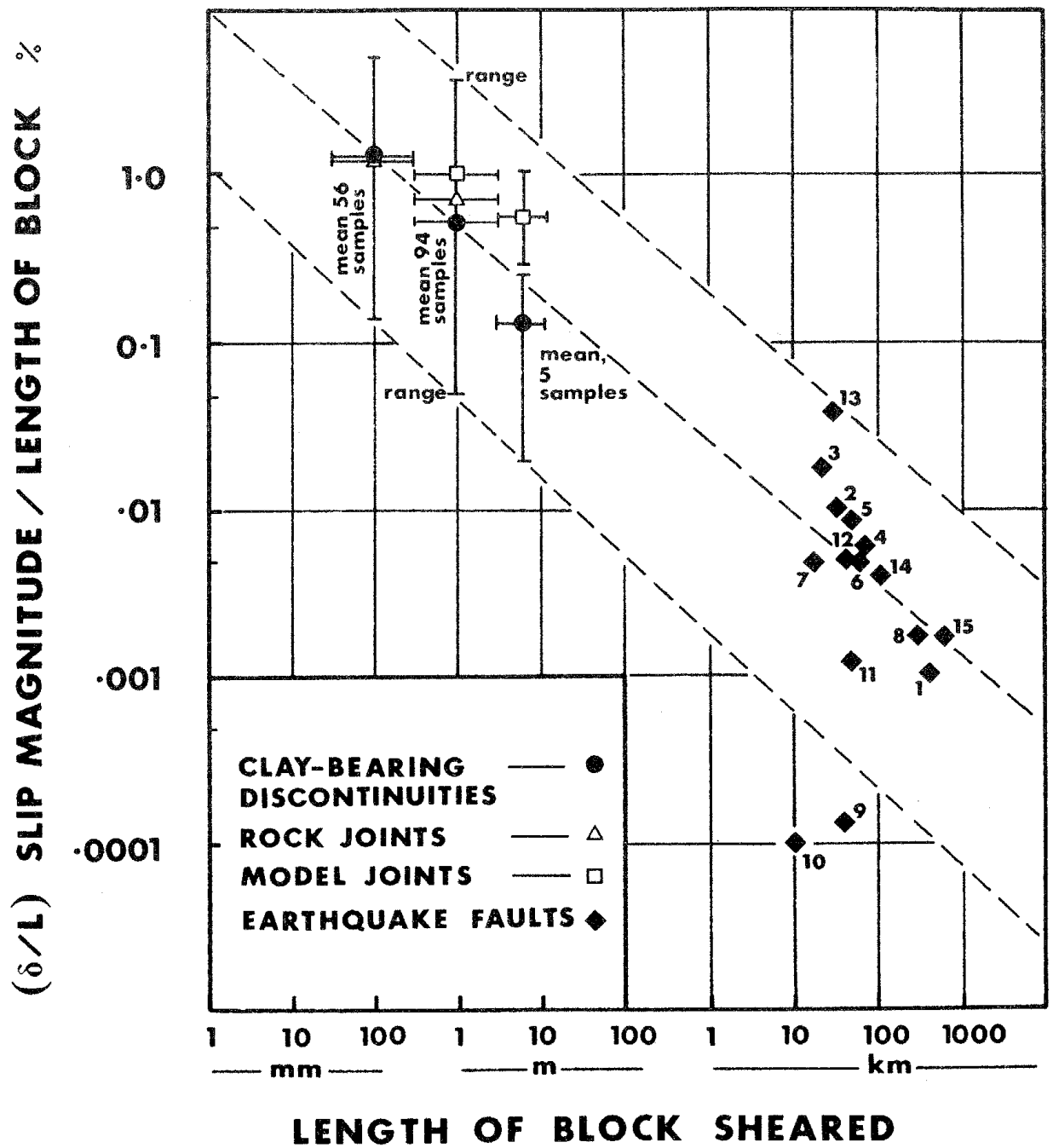

Figure 4.3. Block length apparently has a consistent effect on the slip magnitude required to mobilize strength. (Number of samples refer to clay bearing discontinuities only).

test data for mobilization of peak strength are plotted together with fault slip data. A reasonably consistent trend is apparent. An approximation to the mean trend of data is given by the following equation:

$$\delta(\text{peak}) = 0.004\ L^{0.6} \quad \text{---------- 4-1}$$

Analysis of data published by Bandis et al. (1981) indicates that the ratio $\delta(\text{peak})/L$ is related to the joint roughness coefficient (JRC) of the particular length of joint tested. The magnitude of $\delta(\text{peak})$ tends to be somewhat less when the JRC value is low, i.e. for smooth, planar surfaces. Improved fit to the data is obtained with the following equation:

$$\frac{\delta(\text{peak})}{L} = 1/500 \left(\frac{JRC}{L}\right)^{0.33} \quad \text{---------- 4-2}$$

where L = length of joint sample in meters

Example: L = 1m, JRC = 5, equation 4-2 gives $\delta(\text{peak}) = 0.0034$m

4.2 SIZE-DEPENDENCE OF JRC AND JCS

The shear strength-size investigations of joints in quartz diorite reported by Pratt et al. (1974) indicated a large reduction in peak shear strength, and a significant reduction in ultimate shear strength, as the size of in situ block was increased. Each test was performed in close proximity, in the same joint plane. Back-analysis of the data suggests that significant reductions of JRC (and possibly JCS) were occurring as size increased. Normal stress levels were in the range 1 - 10 MPa.

Barton and Choubey (1977) measured tilt angles of 59° during very low stress self-weight sliding tests on a 45cm long joint in granite (Figure 4-4). When the same joint was subdivided into eighteen blocks 10cm in length, an average angle of 69° was obtained from a combination of self-weight tilt and horizontal "push" tests. Back-analysis of these tests using equation 3-3 and assuming an unchanged value of JCS, suggests that JRC was 5.5 for the large sample and an average 8.7 for the small samples.

The peak shear strength (ϕ') of a rock joint as described in equation 3-1 can also be expressed as:

$$\phi' = \phi_r + d_n + S_a \quad \text{---------- 4-3}$$

where d_n = dilation angle at peak

S_a = asperity failure component

The shear tests on different size joint replicas reported by Bandis et al. (1981) indicated reduced values of d_n with increasing size of sample, but insufficient

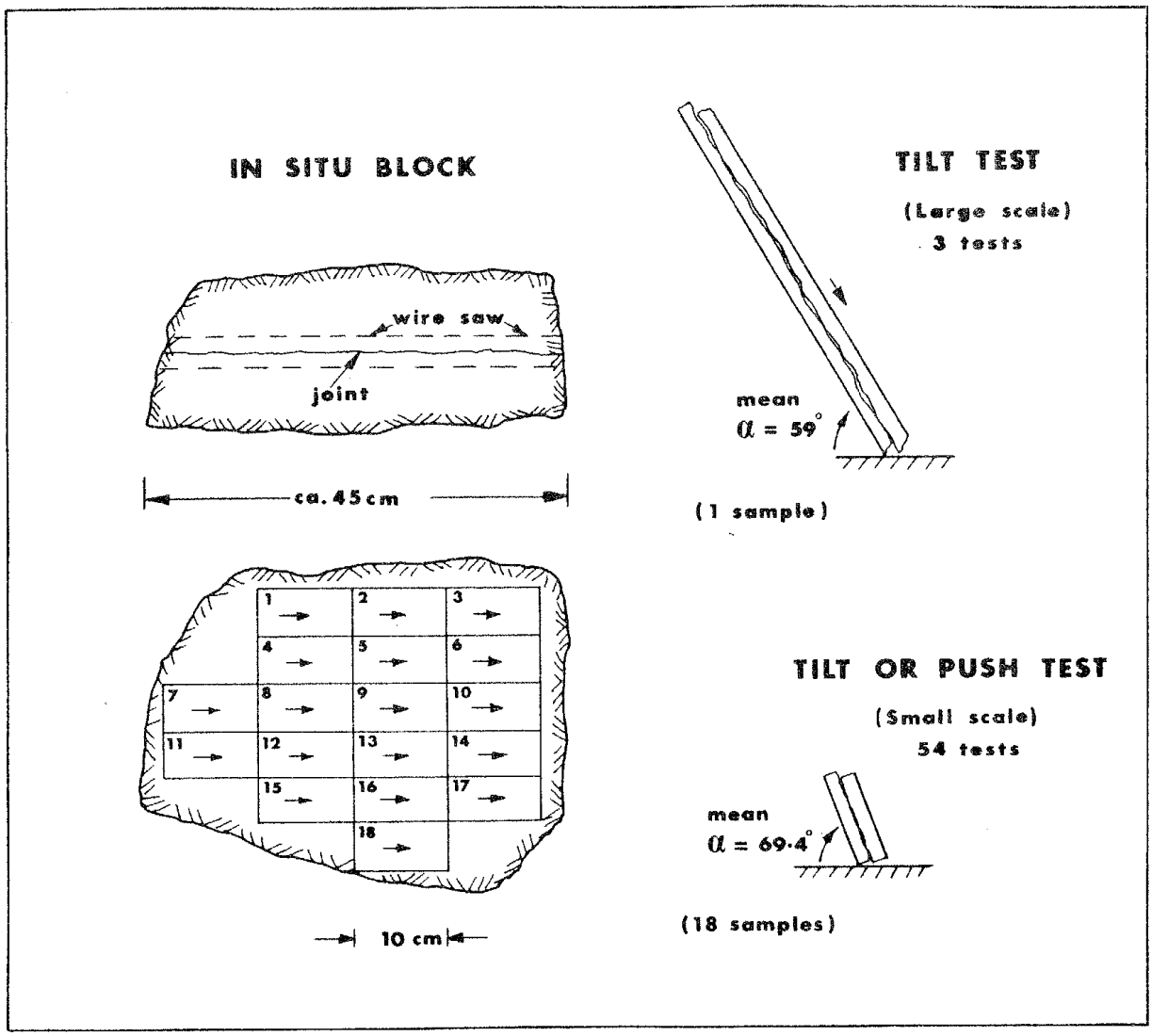

Figure 4.4. Size-effects on shear strength are also apparent at extremely low stress levels, after Barton and Choubey (1977).

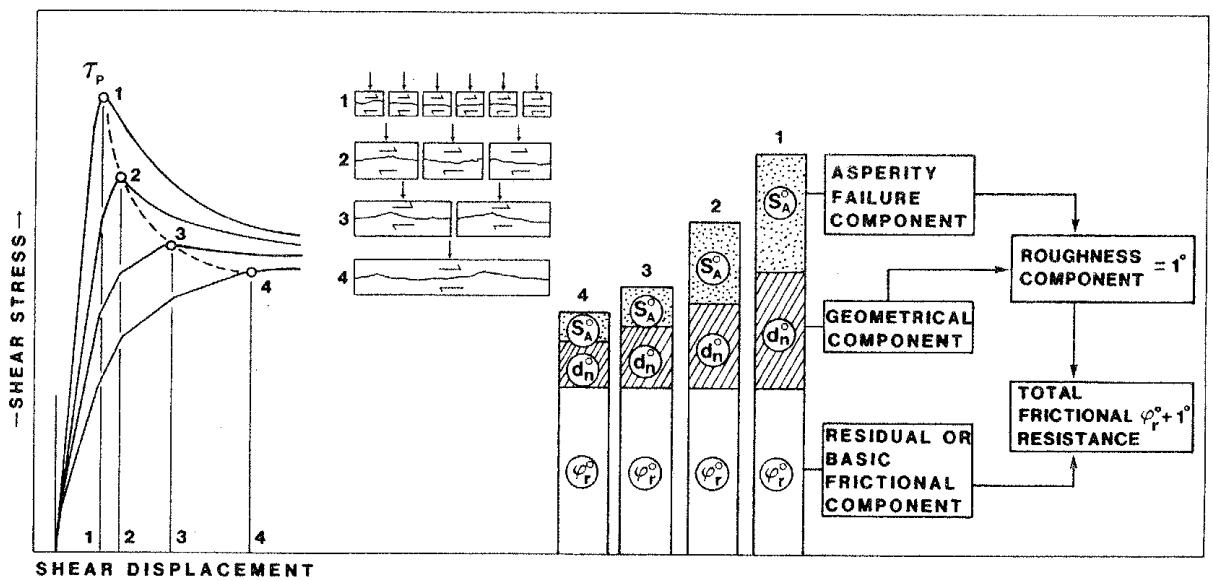

Figure 4.5. Size-dependence of shear strength components, after Bandis et al. (1981).

reduction to explain the even larger reduction of ϕ' with size. Since ϕ_r is unaffected, S_a must also reduce with increasing size. Evidence was therefore obtained that both JRC and JCS reduce with increasing size of sample, the latter caused by the lower effective compression strength of contacting asperities of larger size (Figure 4-1). Figure 4-5 summarizes the size-effects observed on the various components of shear strength.

A practical method of estimating the overall behavior of a joint sampled at different sizes is shown in Figure 4-6. It is assumed that only small joint specimens will initially be available, such as jointed core. Small-scale values of JRC and JCS could be extrapolated to larger size jointed blocks, prior to conducting larger size block tests and actually measuring the properties at realistic size. These dimensionsless reduction curves are based on the results of 378 shear tests on joint replicas of different size. In this comprehensive study, Bandis (1980) tested samples from eleven different joint morphologies, from very rough (JRC = 18.5) to smooth (JRC = 4). In practice, values of JRC_o and JCS_o could be obtained from tilt tests of jointed core (Figure 3-4 and 3-6) and Schmidt hammer tests, respectively. The reduction curves can be approximated by the following equations, for convenience of calculation.

$$JRC_n \simeq JRC_o\left(\frac{L_n}{L_o}\right)^{-0.02 JRC_o} \quad \text{---------- 4-4}$$

$$JCS_n \simeq JCS_o\left(\frac{L_n}{L_o}\right)^{-0.03 JRC_o} \quad \text{---------- 4-5}$$

Exmple: $JRC_o = 15$, $JCS_o = 150$ MPa, $L_o = 0.1$m (lab. scale tests)
The same joint sampled on a scale of $L_n = 2$m is likely to have the following approximate magnitudes of roughness and asperity strength:
$JRC_n \simeq 6$, $JCS_n \simeq 40$ MPa

Obviously greater reliability will be obtained by conducting some form of shear test on the larger sized block, and back-calculating values of JRC_n. Two inexpensive test methods are described later in this report.

4.3 SIZE-DEPENDENCE OF SHEAR STIFFNESS

The shear stiffness of a joint is defined as the slope of the shear stress-displacement curve obtained during a shear test under a given level of normal stress (Goodman, 1970). In recent years, the shear stiffness (K_s) and normal

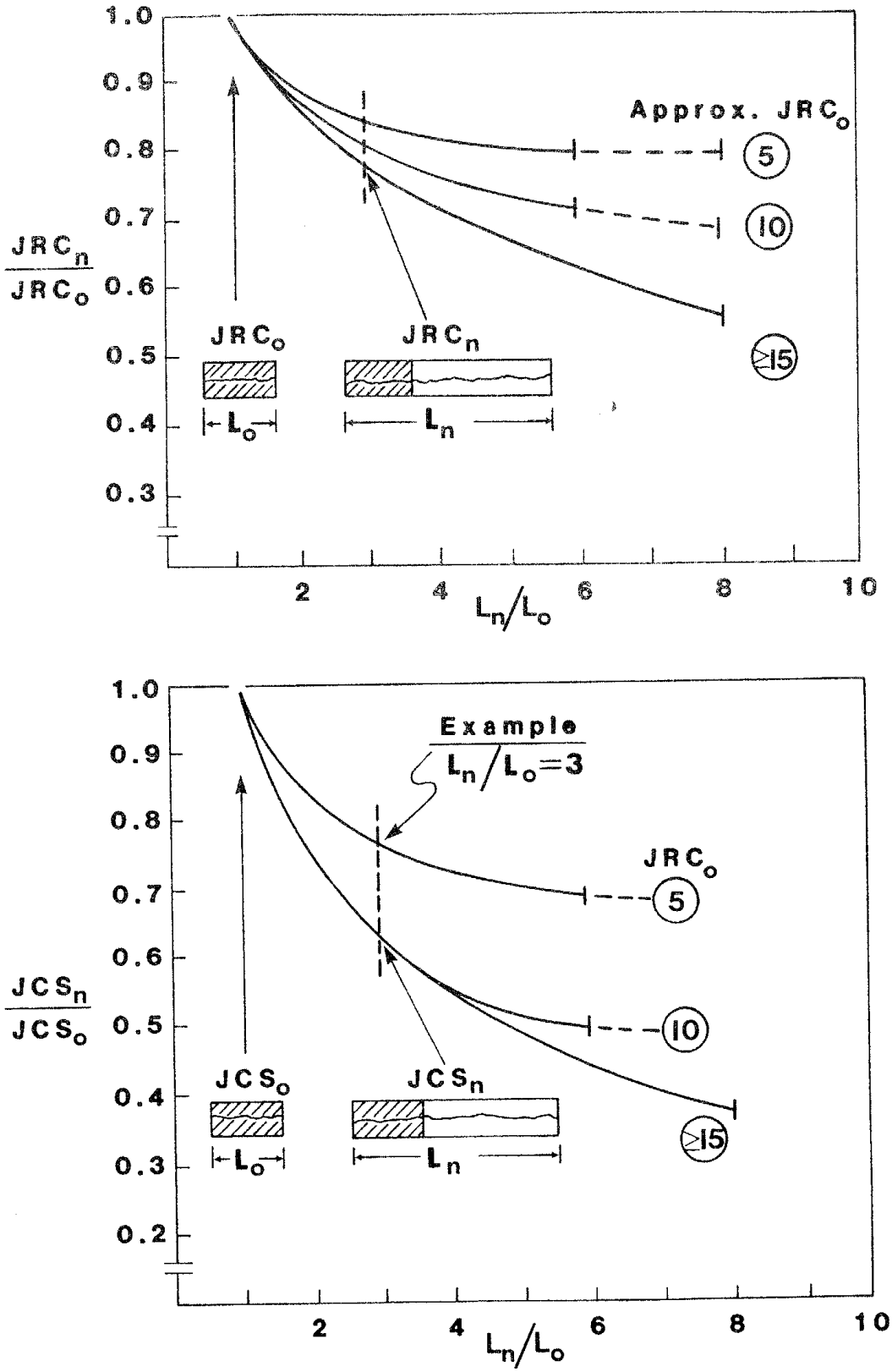

Figure 4.6. Method of estimating JRC and JCS values for larger sizes of rock joint, based on laboratory-size values (JRC and JCS) after Bandis et al. (1981).

stiffness (K_n) of a joint have been used to approximate the overall behavior of a joint, with special zero thickness, finite stiffness "joint elements". In many finite element analyses reported in the literature, joint behavior has been approximated to the extent that only two values of K_s and K_n are used. In reality, values of K_s are normal stress dependent and size-dependent. More realistic modelling is achieved by approximately simulating the complete stress-displacement curves, as described by Cundall et al. (1978) and Wahi et al. (1980).

Values of K_s reported in the literature have been reviewed, particular attention being paid to the effect of sample size and normal stress. The extensive data presented in Figure 4-7 suggests strong size-dependency, though care needs to be exercised in interpretation. The stippled lines representing normal stress levels were <u>located</u> using the mean values of JRC, JCS and ϕ_r obtained from the 137 shear tests on rock joints reported by Barton and Choubey (1977):

JRC = 8.9
JCS = 92 MPa L = 0.1m
ϕ_r = 27.5°

The most frequently measured value of δ(peak) was 0.6mm, giving a peak shear stiffness value of 1.7 MPa/mm under a normal stress of 1 MPa, according to equation 4-6 below:

$$K_s = \tau / \delta\,(\text{peak}) = \frac{\sigma_n'}{\delta(\text{peak})} \cdot \tan\left[\text{JRC} \log \frac{\text{JCS}}{\sigma_n'} + \phi_r\right] \quad \text{------ 4-6}$$

The values of K_s obtained at different levels of normal stress show close agreement with values measured in the laboratory. The <u>gradient</u> of the stippled normal stress lines in Figure 4-7 was based on extrapolated values of JRC_n, JCS_n and δ(peak) using equations 4-4, 4-5 and 4-2 respectively, and an assumed block size L_n of 1.0m. The following larger scale values are predicted:

JRC = 6
JCS = 50 MPa
ϕ_r = 27.5°
L = 1.0m
$\delta_{(peak)}$ = 3.6mm

Equation 4-6 gives K_s = 0.2 MPa/mm (for $_n'$ = 1.0 MPa)

Linear extrapolation of the above values of shear stiffness to larger block sizes and other normal stress levels provides the six stippled lines shown in Figure 4-7. The tentative extrapolation to the earthquake fault data (numbered points) of Nur (1974) is probably inaccurate, despite the apparently reasonable

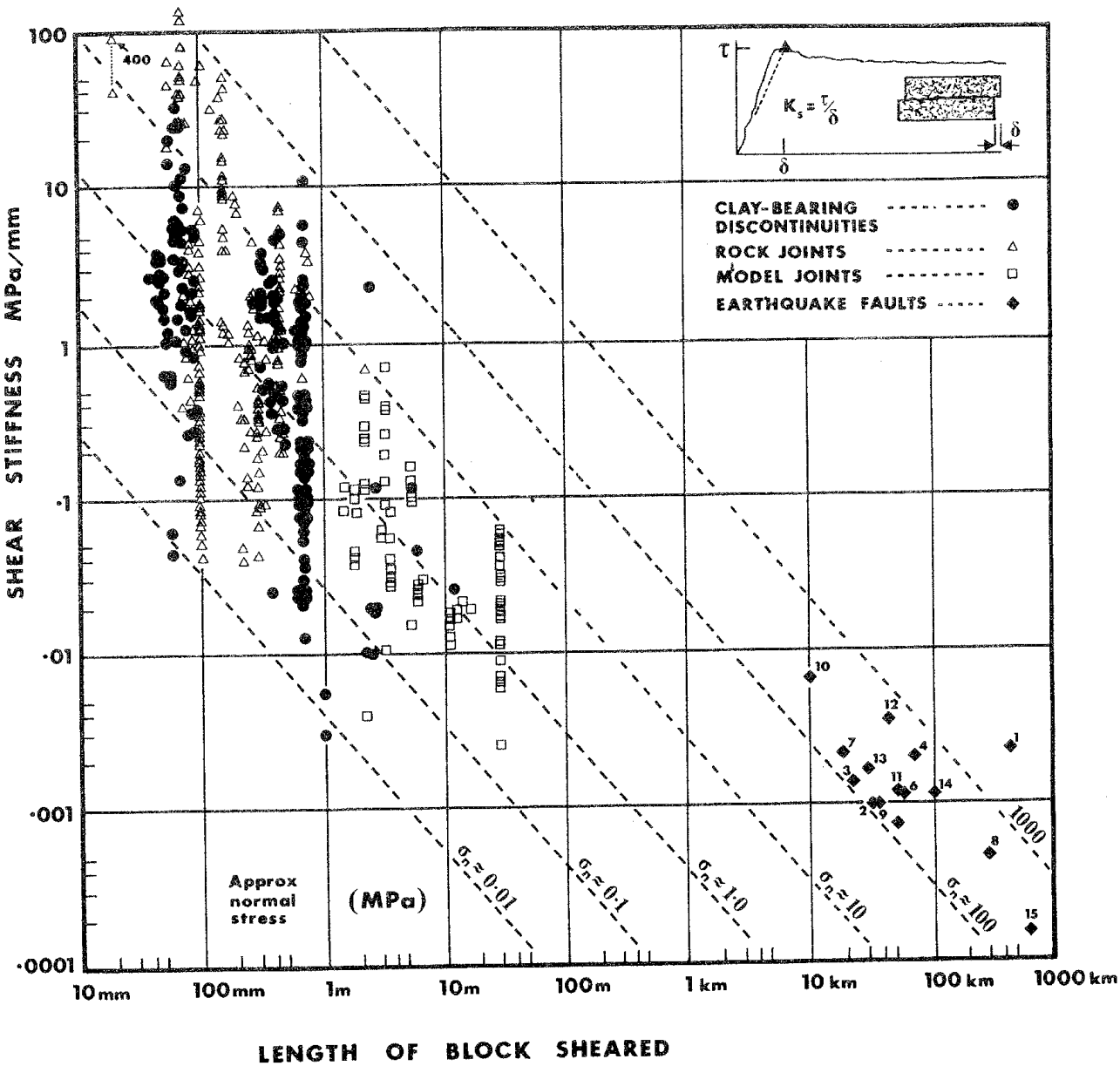

Figure 4.7. Size and stress dependence of shear stiffness, according to results collected from the literature. The normal stress diagonals are gross approximations.

levels of normal stress (100-1000 MPa) bracketing these earthquake events.

Applications of equations 4-2, 4-4, 4-5, and 4-6 over a range of block sizes from 100mm to 10m suggests that the normal stress diagonals probably flatten out as shown in Figure 4-8. In addition, it will be noticed that the stiffness of the rough, competent joint and that of the weaker, smooth joint converges when either the stress level, or block size is increased. The above method of estimating peak shear stiffness for rock joints is specifically directed at clay-free discontinuities. When clay is present, preventing (to) a greater or lesser extent) rock-to-rock contact, the peak shear stiffness tends not to be so size-dependent, and is also somewhat less stress dependent, due to the low shear strength. Laboratory and in situ shear tests of clay-filled discontinuities performed under a range of effective stresses from 0.5 to 2.5 MPa showed the following influence of clay-filling thickness on shear and normal stiffness:

TABLE 4-2

Dependence of Stiffness on Clay-Filling Thickness, After Infanti and Kanji (1978)

clay-filling thickness (mm)	K_s MPa/mm	K_n MPa/mm	ratio K_n/K_s
50 - 100mm	0.01 - 0.1	0.1 - 0.5	6
10 - 20	0.1 - 0.6	0.5 - 2.0	3.6
<1mm (1 case)	>1.0	>5.0	≈5

In contrast to the above, ratios of K_n/K_s may reach values of several hundred MPa/mm when large, clay-free rock joints are tested. The normal stiffness of rock joints will be discussed in detail in a later section of this report, in view of its importance to joint aperture and permeability.

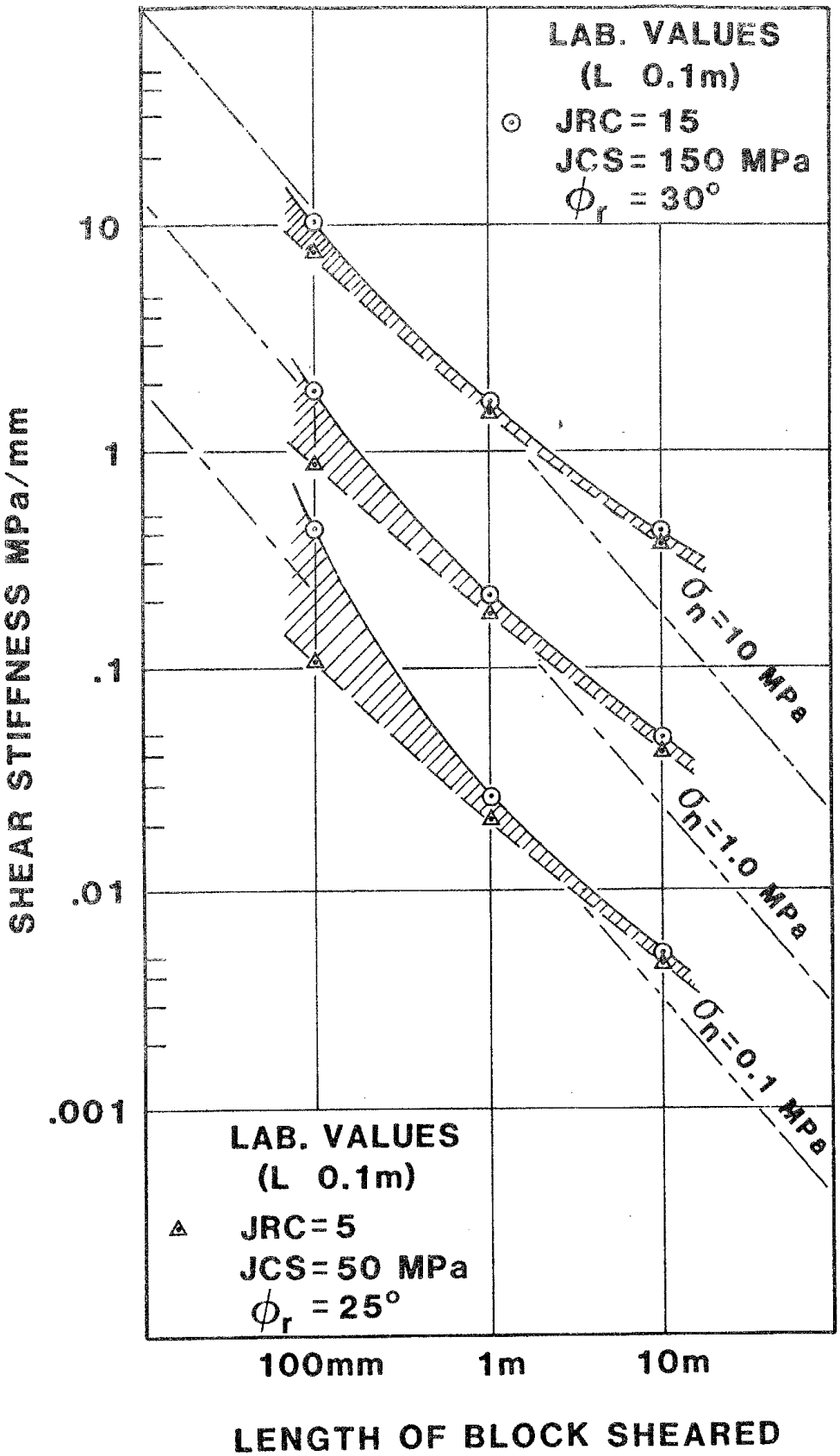

Figure 4.8. Application of the scaling equations 4.2, 4.4, 4.5 and 4.6 to two typical sets of laboratory data. The diagonal normal stress lines match those in Figure 4.7.

5 MODELLING SHEAR STRENGTH-DISPLACEMENT BEHAVIOR

Up to this stage, methods have been described for estimating only the peak strength and peak shear displacement points on the stress-displacement plot. Obviously the loading portion of this plot can be approximated by calculation of the appropriate peak shear stiffness (K_s) as just described. The important post-peak and pre-residual portions of the plot remain to be quantified. Unloading and reloading effects also have to be considered.

5.1 MOBILIZATION AND REDUCTION OF ROUGHNESS

The joint roughness coefficients (JRC) described up to this point have been peak values. By rearrangement of our peak strength equation we can also derive an expression for the mobilized shear strength (τ_m) pre- or post-peak, by using the concept of roughness mobilization; JRC (mobilized). This term will be defined as follows:

$$\text{JRC (mobilized)} = \frac{\arctan(\tau_m/\sigma_n')^\circ - \phi_r^\circ}{\log(\text{JCS}/\sigma_n')} \qquad \text{---------- 5-1}$$

With this form of equation, we can evaluate JRC (mobilized) along all points of a shear stress-displacement plot, and investigate how it varies. Figure 5-1 shows an example. Shear test data obtained from tests on model tension fractures have been normalized, and expressed in terms of two dimensionless ratios:

$$\text{JRC (mobilized)/JRC(peak)} \quad \text{and} \quad \delta/\delta(\text{peak})$$

It can be shown that:

$$\frac{\text{JRC(mobilized)}}{\text{JRC (peak)}} = \frac{\arctan(\tau_m/\sigma_n')^\circ - \phi_r^\circ}{\phi_p^\circ - \phi_r^\circ} \qquad \text{---------- 5-2}$$

where $\phi_p = \arctan(\tau_{peak}/\sigma_n')$.

When JRC (mob.)/JRC(peak) = 0.5, the shear strength mobilized is equal to $\frac{1}{2}(\phi_p + \phi_r)$. In other words, shear strength is midway between peak and residual. This point seems to occur at approximately 10 δ(peak) for the case of the rough model tension joints. (Smoother joints, or those under the influence of high normal stress, may apparently reach this point at smaller displacements).

The origin of Figure 5-1(B) is given by the simple expression $-(\phi_r/i)$ where $i = \text{JRC(peak)} \cdot \log(\text{JCS}/\sigma_n')$. Therefore, the model tests with JCS/σ_n'

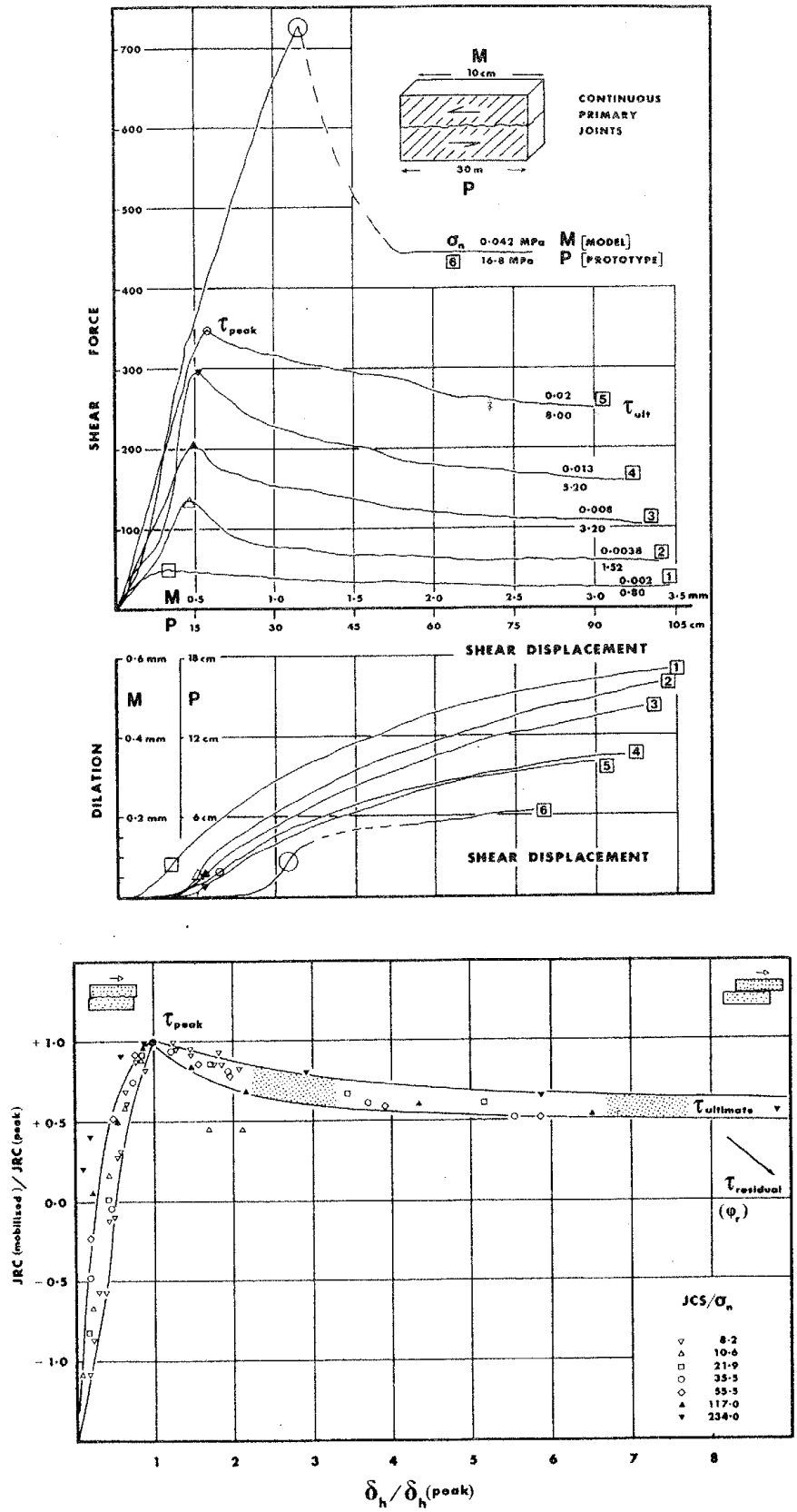

Figure 5.1. Normalization of stress-displacement data using the concept JRC (mobilized).

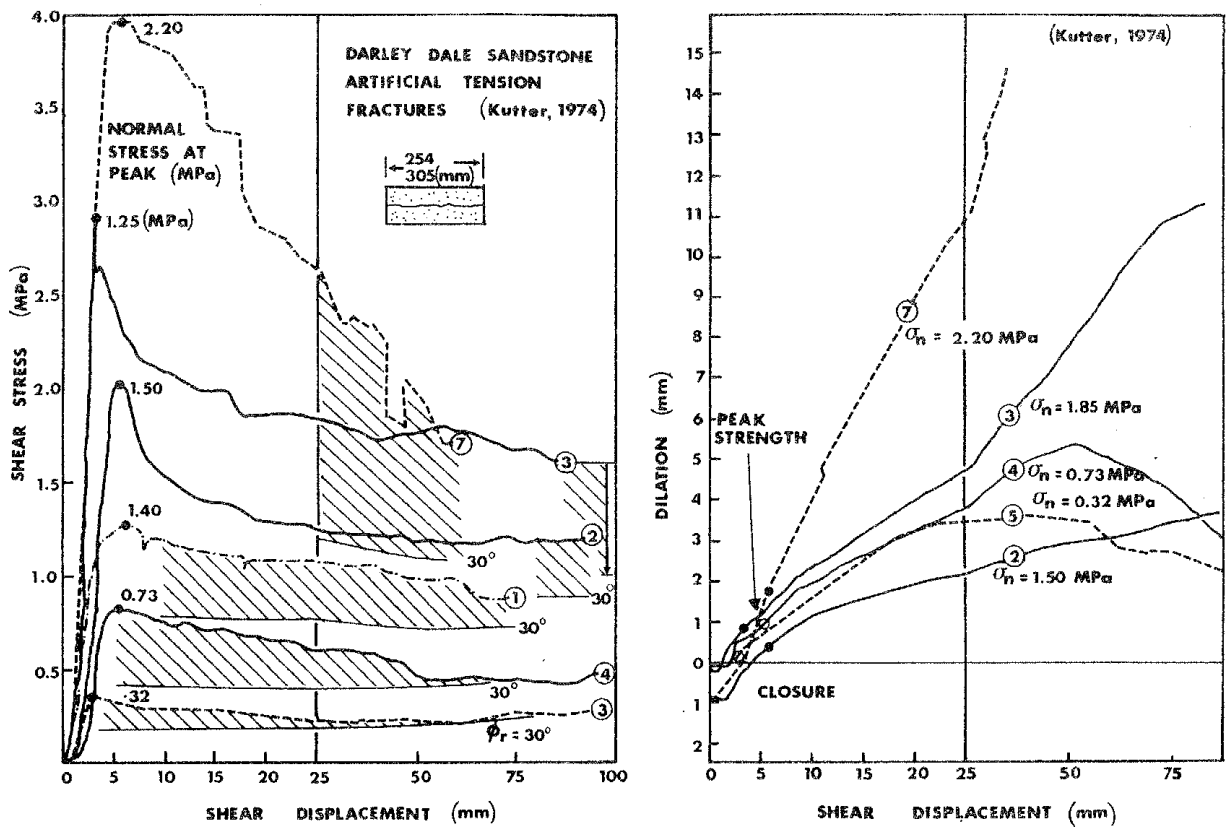

Figure 5.2. Large displacements are required to reach residual strength, here assumed to be represented by $\phi_r = 30°$. Data is from Kutter (1974).

varying from 8.2 to 234, and with $\phi_r = 30°$, have values of $-\phi_r/i$ in the range from -0.6 to -1.6 (approx). It is apparent from the measured dilation seen in the lower half of Figure 5.1(A) that roughness still contributes to shear strength, even after quite large shear displacements. The difficulty of reaching true residual strength is also indicated in the set of data shown in Figure 5-2. Samples that reach residual do so only when the dilation ceases (curves 4 and 5). The slow reduction towards residual strength found in practice suggests that it is more appropriate to use the term "ultimate" strength for the value measured at the end of a shear test. Several of the numerical techniques used to model "complete" stress-displacement behavior incorporate a far too conservative, abrupt fall-off to residual strength. A suitable model incorporating appropriate values of (JRC_m/JRC_p) and (δ/δ_{peak}) for general modelling of rock joint behavior is shown in Figure 5-3. This incorporates many of the features observed in shear tests, as will become apparent shortly.

The pairs of coordinates tabulated in the figure can of course be "smoothed" in a numerical analysis, or further coordinates added (i.e. $\delta/\delta_{peak} = 25$, $JRC_m/JRC_p = 0.4$ etc.) It should be noted that the origin or "start" position represented by $(-\phi_r/i)$ depends on the particular value of JRC(peak), JCS and σ_n'. In the example plot shown in the figure, these parameters give the origin at a value of -2. Other values of normal stress will give the characteristic varying shapes obtained from a set of shear tests. The value of δ(peak) required to define the coordinate (1,1) is estimated from equation 4-2. Its value depends on the length of sample and on the peak JRC value.

5.2 EXAMPLES OF STRESS-DISPLACEMENT MODELLING

The remarkable series of shear test experiments performed by Bandis (1980) and partially published in Bandis et al. (1981) provided the necessary data for validation of the present stress-displacement-dilation numerical modelling method. Bandis (1980) developed a brittle high density model material (unconfined compression strength = 2 MPa) and a rubber molding technique. He was thereby able to cast identical pairs of interlocking model joint specimens, matching the surface morphologies of a wide variety of joints, both weathered and fresh. Figure 5-4 illustrates an excellent degree of fit between experimental and numerical stress-displacement paths for four different joint morphologies, each tested at the same level of normal stress. The effect of different normal stress levels on three identical joint replicas is also modelled in a realistic manner, as shown in Figure 5-5.

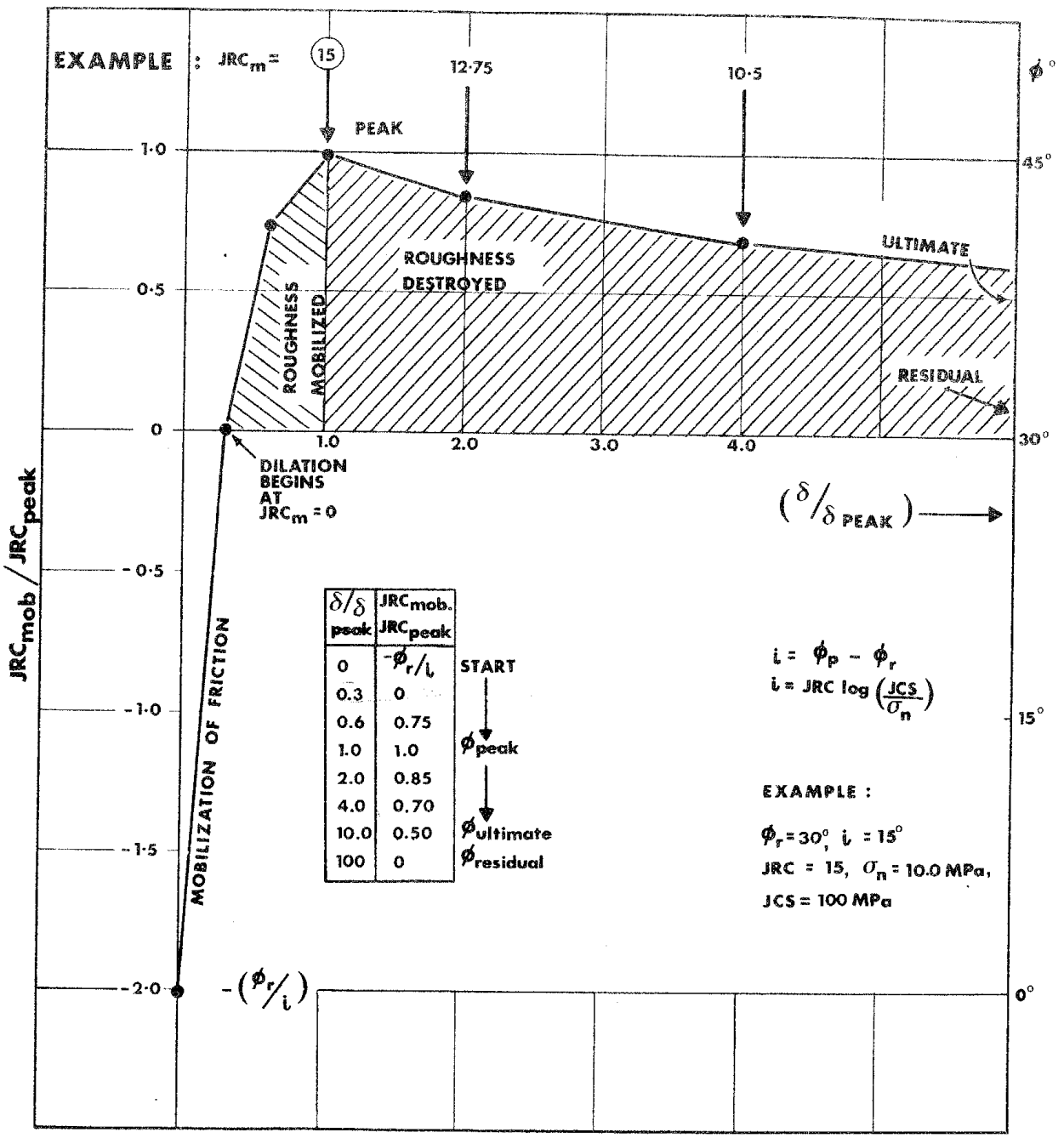

Figure 5.3. Recommended model for generating realistic shear stress-displacement plots for non-planar joints.

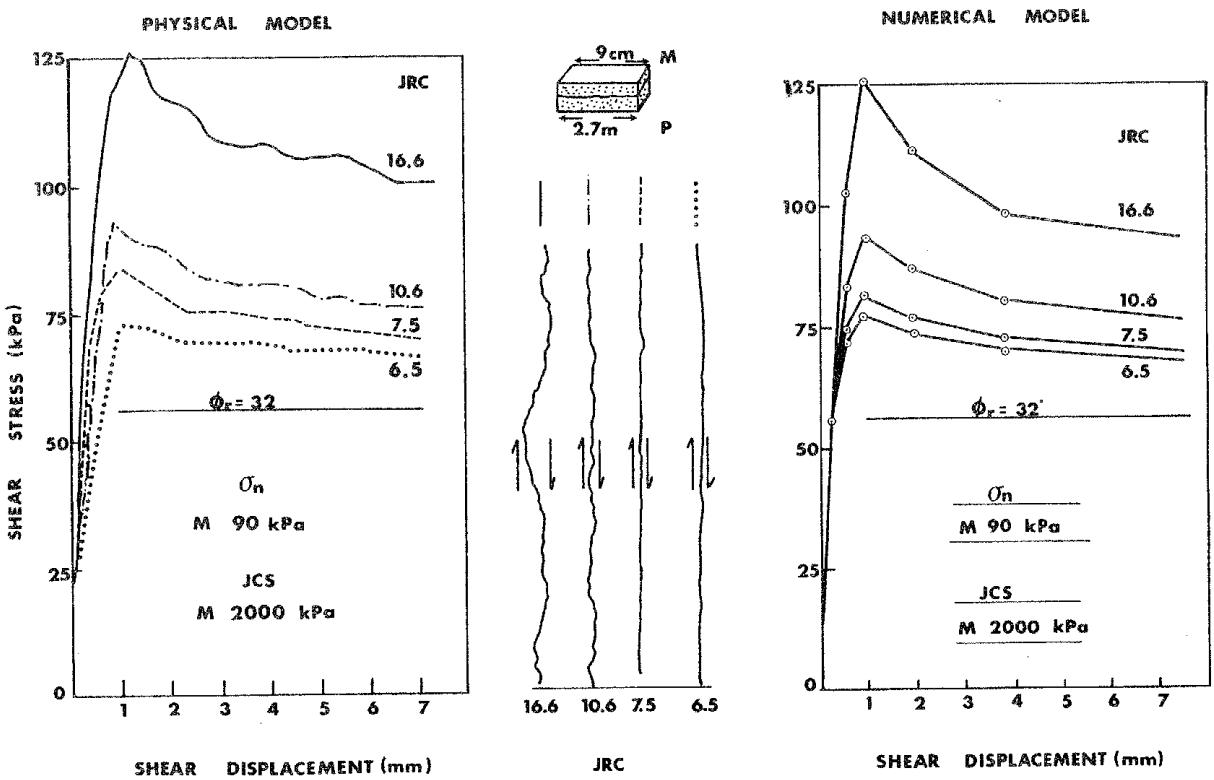

Figure 5.4. The numerical model for generating stress-displacement paths compares closely with experimental data reported by Bandis et al. (1981).

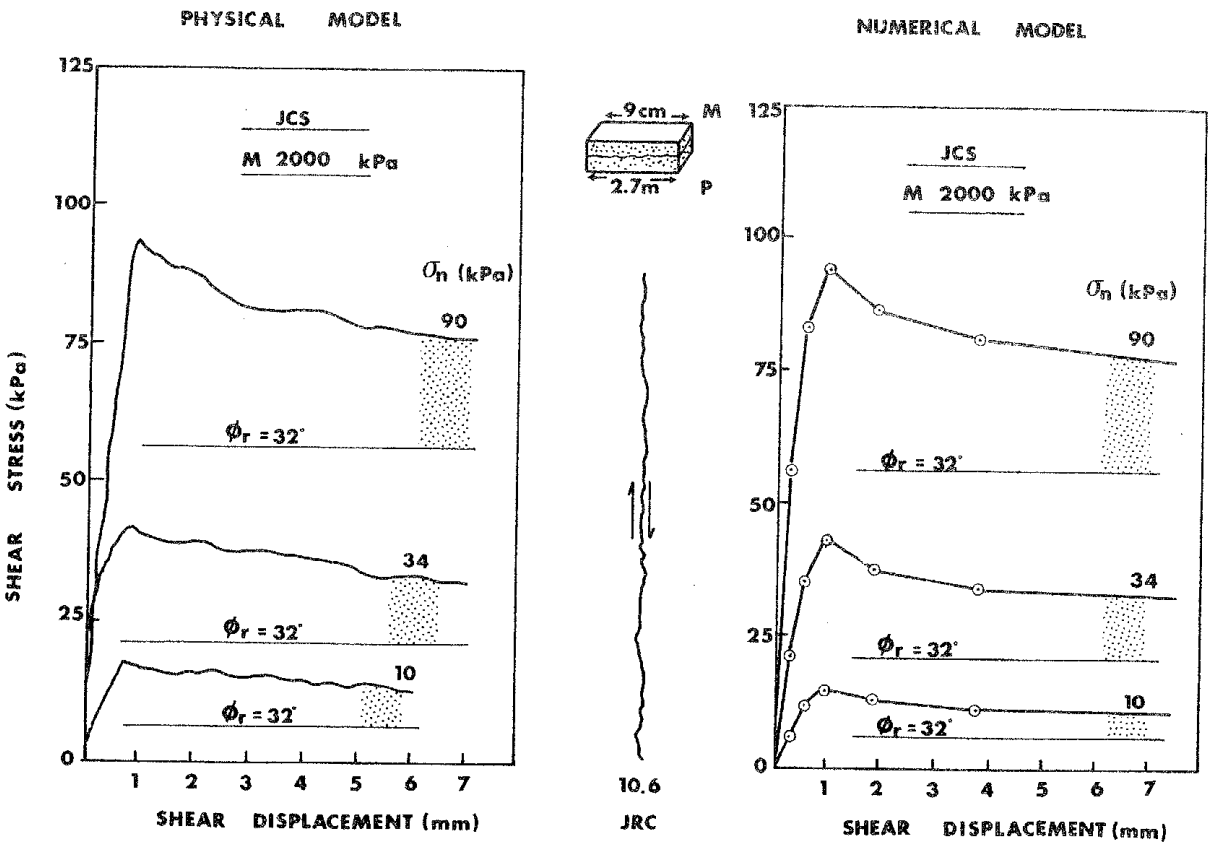

Figure 5.5. The joint modelling technique used by Bandis (1980) allows identical interlocking joint samples to be produced. Three identical samples tested under three levels of normal stress are quite closely modelled numerically.

When the size of sample is also a variable, a satisfactory degree of fit is obtained for the case of rough non-planar joints (Figure 5-6), but a poorer fit is evident for the case of planar joints (Figure 5-7). It is evident that the coordinates of the dimensionless JRC_m/JRC_p, δ/δ_p roughness mobilization model (Figure 5-3) need to be adjusted so that a reduced fall from peak strength is generated. Table 5-1 following indicates a suitable set of coordinates for the case of markedly planar joints (i.e. for $JRC_o \leq 5$ approx.).

Comparison with Figure 5-3 (non-planar joints) reveals that more rounded stress-displacement curves will be generated using the coordinates in Table 5-1. The values also emphasize the poorly defined peak observed in tests on planar joints, and the tendency for smaller δ(peak) values. These features are illustrated in a later example.

TABLE 5-1

Suggested Coordinates For Stress-Displacement Modelling of Planar Joints (see Figure 5-3 for comparison)

JRC (mobilized) / JRC (peak)	δ/δ (peak)
$-\phi_r/i$	0
0	0.3
0.75	0.6
0.95	1.0
1.0	2.0
0.9	4.0
0.7	10.0
0.5	25.0
0	100

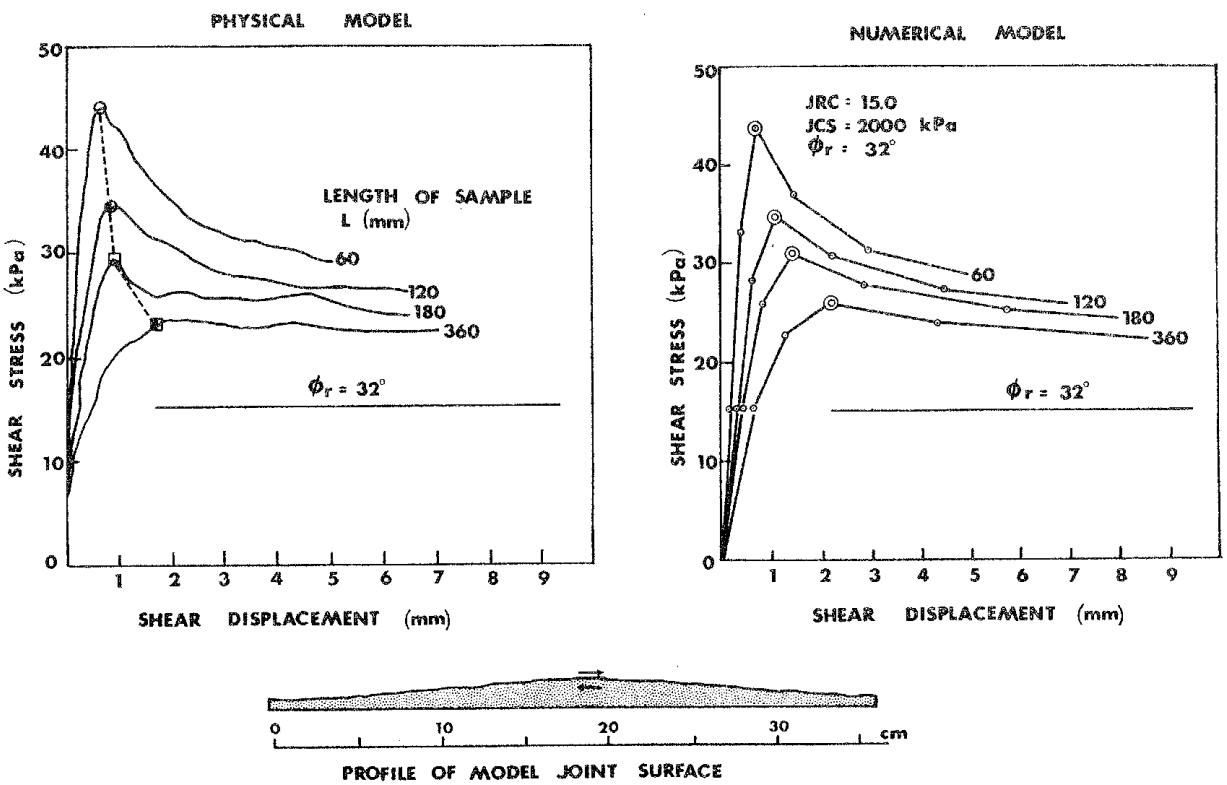

Figure 5.6. Data from shear tests on physical joint models of different size were obtained from Bandis (1980). The 60mm curve is the mean of 18 samples cut from the 360mm sample, the 120mm curve the mean of 9 samples, etc.

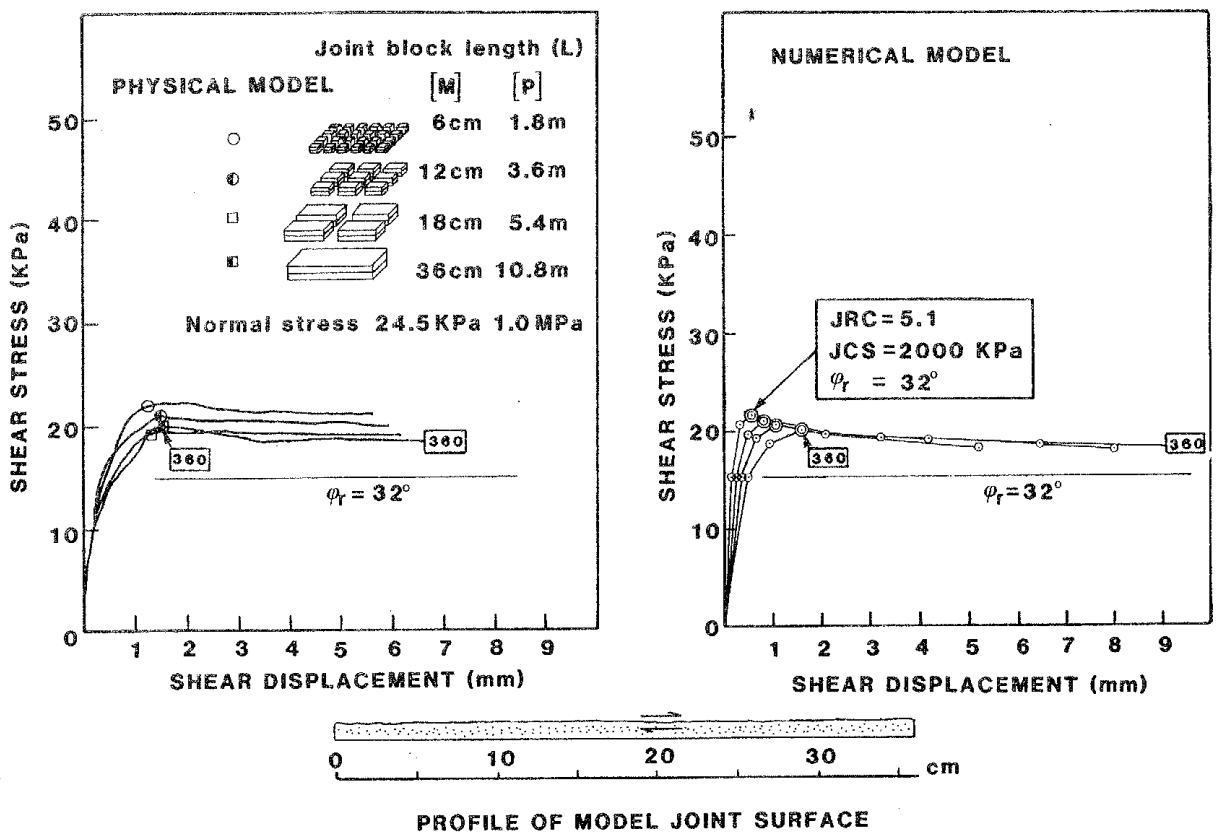

Figure 5.7. The physical model data (Bandis et al. 1981) obtained from tests on a very planar joint are poorly represented by the numerical models for rough joints except for the case of the full-size 360mm sample.

6 MODELLING DILATION BEHAVIOR

When rock joints are subjected to shearing stress while under normal load, the asperities on either side of the joint will tend to slide into contact at a few points along their opposed sloping faces, thereby changing the "at rest" contact positions. In fact, the mating joint walls offer relatively little shear resistance before this initial shear deformation, since dilation (displacement perpendicular to the joint) is virtually absent. However, when the opposed sloping faces of the major asperities make contact, the inherent shear characteristics begin to show; the shear strength rises and dilation against the normal load begins. The instant of peak strength is approaching.

In general, weak rough joint wall (low JCS, high JRC) will suffer more damage during shear than a strong smooth surface, though neither will dilate strongly. Only those surfaces with high JCS and high JRC will dilate strongly at the instant of peak strength.

In the case of an underground opening in rock, potential fall-out of an unstable block may be checked by the dilation of the relevant joints, if the latter are initially mated and non-planar. In this case, the confined boundaries will result in a corresponding increase in effective normal stress across the relevant joints, a stabilizing feature usually absent from rock slope stability problems. The increase in effective normal stress will result in a large increase in shear strength if the joints are dilatant rather than planar or clay-filled. It is this difference between dilatant and non-dilatant joints that causes some underground openings to stand permanently unsupported with spans of up to 100 meters, even in jointed rock, while some small adits are unstable even with a span of only 1 meter, if the joints are clay-filled (Barton, 1976). Aside from stability considerations, the dilation accompanying shear displacement of non-planar joints may be expected to have a marked influence on the permeability of the relevant joints. If the dilation path can be successfully modelled, the goal of coupled hydro-mechanical joint modelling may be achieved.

6.1 THE PEAK DILATION ANGLE

The peak dilation angle, d_n, is the maximum dilation angle which occurs more or less simultaneously with peak shear resistance. It is difficult to measure consistently because the angle will depend on the shear displacement increment considered.

Figure 6-1, reproduced from Barton and Choubey (1977), indicates the wide range of values that may be measured in a suite of tests. The majority of peak dilation angles fell between the following limits:

$$0.5\ JRC \cdot \log\ (JCS/\sigma_n) < d_n < 2\ JRC \cdot \log\ (JCS/\sigma_n)$$

Line number 2 appears to be a good lower bound to the great majority of the data; i.e.

$$d_n \simeq \tfrac{1}{2}\ JRC \cdot \log\ (JCS/\sigma_n) \qquad \text{6-1}$$

However, the middle envelope (line 1) is a close approximation to the mean performance of the 136 joint samples tested. The overall mean value of $d_n°$ for the 136 samples was 20.0°, compared to 21.1° for the asperity component. In other words, where asperity damage is slight (due to relatively high JCS values, or low σ_n' values, and/or small JRC values) the dilation angle is well approximated by the asperity component (i).

A series of direct shear tests on rough model tension fractures that were reported by Barton (1971), were performed at normal stress levels that resulted in considerably greater asperity damage than that encountered in the tests shown in Figure 6-1. In fact, JCS/σ_n' ranged from about 4.1 to 125 (mean of 29 for 130 artificial fractures). In the series of shear box tests on 136 natural joints, the mean value of JCS/σ_n' was 440 (range 15.5 to 5550).

Equation 6-1 (the lower bound) gives an extremely good fit to the test data obtained from these 130 model fractures. In fact, the mean measured peak dilation angle for the 130 fractures was 13.15°, while the mean asperity component ($JRC \cdot \log\ JCS/\sigma_n$) was 26.34°. This close agreement led to the following relationship being suggested for the peak shear strength of rough undulating joints (Barton, 1971):

$$\tau = \sigma_n' \tan\ (2d_n + 30°) \qquad \text{6-2}$$

where 30° represented the basic friction angle (ϕ_b) of the unweathered material.

In summary, a conservative estimate of the peak dilation angle will be given by one half of the asperity component ($\frac{1}{2}i$), and is relevant to cases where significant asperity damage occurs. For near-surface problems, the approximation $d_n \simeq i$ will be more appropriate.

6.2 MOBILIZATION OF DILATION

In Figure 5-3, it is indicated that dilation will begin at the instant that JRC(mobilized) exceeds zero. In other words, friction is mobilized up to the value ϕ_r, following which dilation begins.

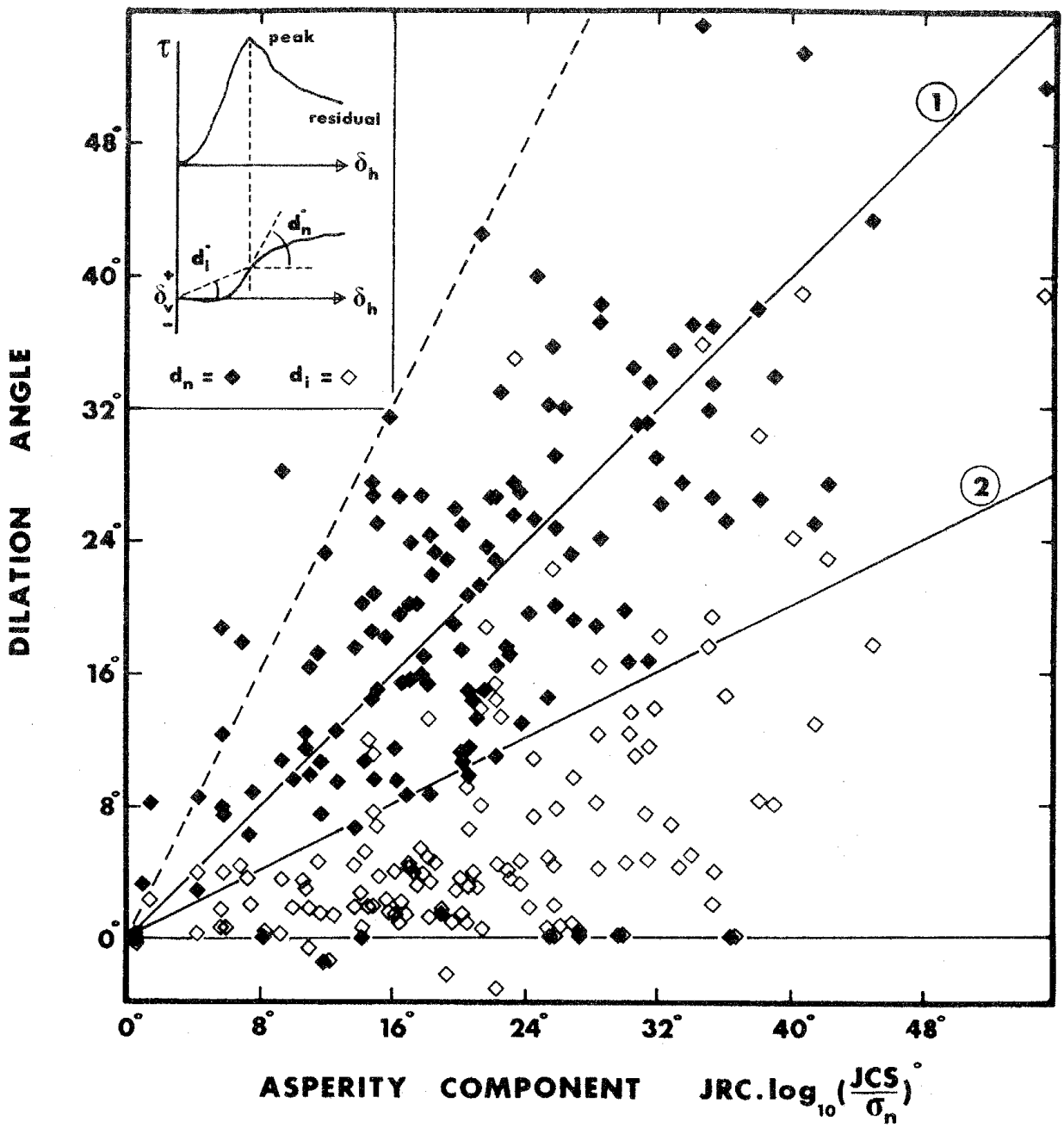

Figure 6.1. The peak dilation angle can be crudely approximated to the asperity component (i), or to a simple function of (i). After Barton and Choubey (1977).

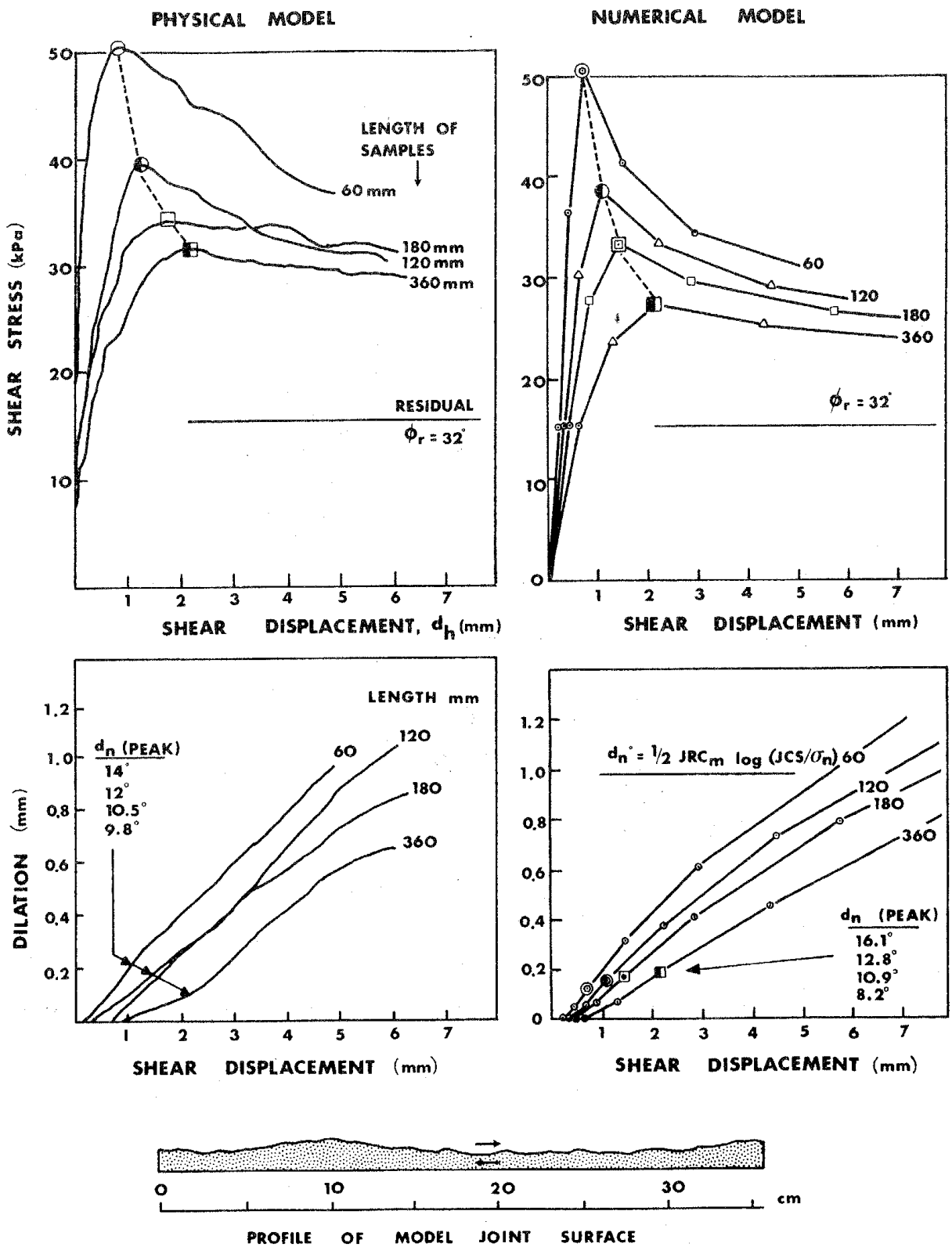

Figure 6.2. Experimental and predicted data show the potential for modelling the size-dependent dilation that occurs when samples of different size are sheared.

While this is essentially a thereotical concept, there is strong evidence that it is qualitatively correct. It will be noted that the value of δ/δ_{peak} at which dilation is supposed to begin is 0.3, both for non-planar and planar joints (Table 5-1). This implies that the onset of dilation will be delayed by an increase in sample size. This phenomenon is in fact consistently observed in the data presented by Bandis et al. (1981), both for planar and non-planar joints.

An example of experimental, size-dependent dilation data for a rough, non-planar joint surface is shown in Figure 6-2 (data on left-hand side of figure). The stress-displacement modelling shown on the right-hand side of the figure shows moderately realistic behavior. The dilation modelling below this is based on a modification of equation 6-1:

$$d_n(\text{mobilized}) \simeq \tfrac{1}{2}\, JRC(\text{mobilized}) \cdot \log\,(JCS/\sigma_n') \quad \text{--------} \quad 6\text{-}2$$

It is seen that good agreement is achieved with this "mobilized dilation" form of the equation. The delayed dilation that occurs with increasing size is also quite closely modelled. It thus appears that the relationships between dilation angle, asperity component (i), and peak shear strength ($\phi_r + i$) are mutually consistent. This is important, as it suggests that the effects of normal unloading and reloading, and shear reversals on shear strength and dilation can be correctly modelled, if the appropriate paths for JRC (mobilized) can be predicted.

7 REVERSALS AND UNLOADING

There is relatively little data in the literature giving complete reversal and unloading force-displacement and dilation records. Before reviewing the small number of available records, it may be of value to mention a standard test technique which provides a part of the required data.

7.1 MULTI-STAGE TESTING

Due to the expense of sample preparation, direct shear testing is frequently performed using a multi-stage sequence. It is widely believed that an approximation to the peak strength envelope can be obtained from one sample, by first shearing at low normal stress, then at successively higher stress levels. In the case of laboratory testing, where the sample is of manageable proportions, the sample is replace to its zero shear displacement position before each increase in normal stress.

Force displacement records obtained from the second and subsequent load sequences are clearly unrepresentative of real shear histories. A more realistic loading sequence, frequently used in large-scale in situ testing, consists of continued shearing at successively higher loads, without replacement of the sample to the zero displacement position before changing load. Examples of typical shear force-displacement records are given by Krsmanovic and Popovic (1966) and Link (1969).

A non-exhaustive review of seven sets of data reported in the literature indicates that shear stiffness measured during the second and subsequent load sequences averages approximately 1.5 times the initial shear stiffness. This level of increased stiffness is also evident in repeated loading and unloading tests. Initial stiffness is invariably the lowest, as shown for example in ultra-large scale in situ tests reported by Evdokimov and Sapegin (1970). Well-controlled large-scale laboratory tests reported by Kutter (1974) also indicate similarly increased stiffness when normal load is increased during a shear test.

7.2 SHEAR REVERSAL

Three sets of data that include reversal are shown in Figures 7-1, 7-2, and 7-3. The initial shear stress, displacement and dilation record shown in Figure 7-1 indicates that dilation is incomplete after 7mm of shear. Reversal of the shear direction at this point causes contraction and a markedly slow

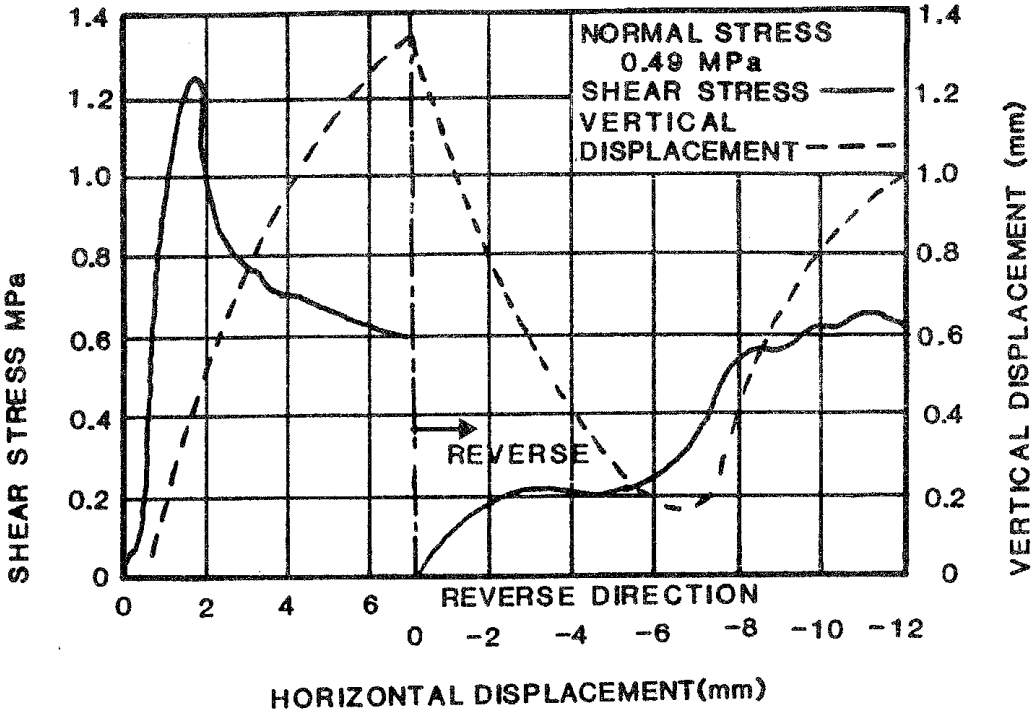

Figure 7.1. Direct shear data on weathered greywacke, after Martin and Millar (1974). Note contraction on reversal, and remobilization when passing "origin".

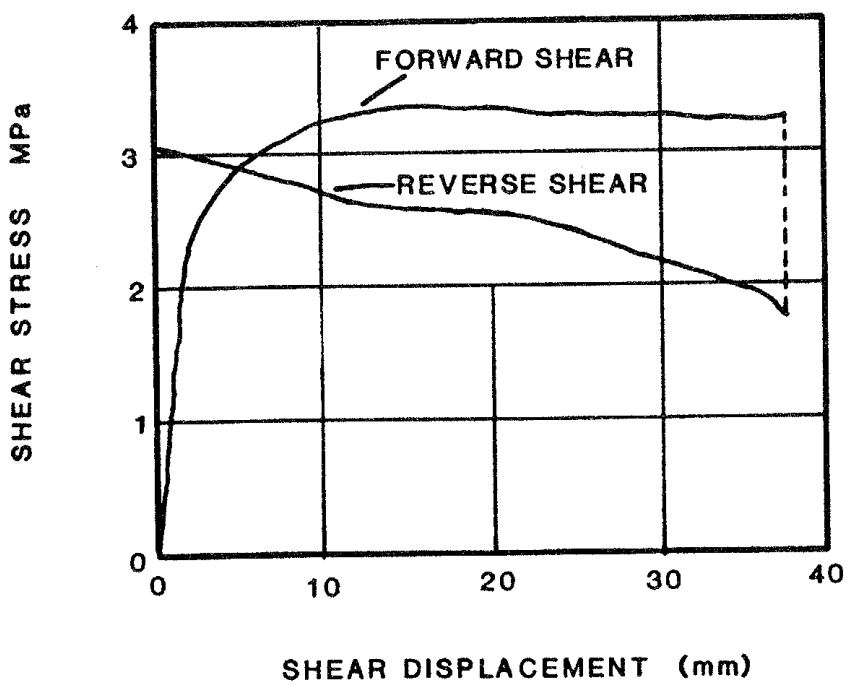

Figure 7.2. Reduction of shear strength upon reversal is caused by the negative dilation (ϕ_r - i) effect. Normal stress level = 4.1 MPa, Weissbach and Kutter (1978).

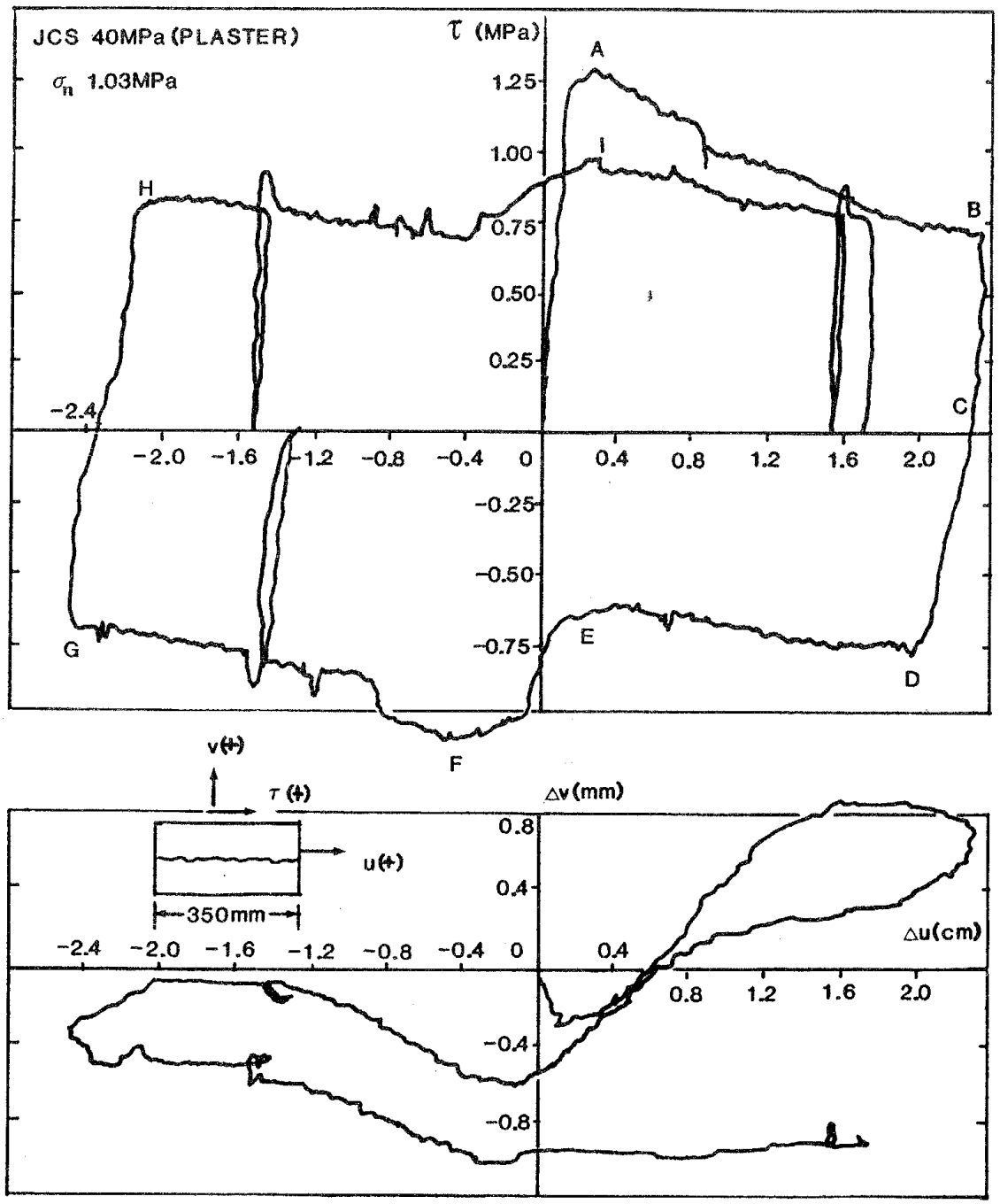

Figure 7.3. Multiple reversal shear test showing shear stress-displacement and dilation records for a plaster replica of a joint in sandstone after Celestino and Goodman (1979).

mobilization of shear strength in the reverse direction (due to ϕ_r - i effect). However, on passing the "origin" after 7mm of reversed shear, dilation increases, and shear strength is mobilized, but to little higher than the original ultimate level.

Figure 7-2 indicates a similar (ϕ_r - i) effect, caused by contraction upon reversal. Weissbach and Kutter (1978) suggested that the midpoint of the stress drop should give an accurate value of ϕ_r, in this case approximately 31°(arctan 2.5/4.1).

The most complete shear reversal record available in the literature is reproduced in Figure 7-3, from Celestino and Goodman (1979). The test parameters reported by these authors indicate that the values of ($-\phi_r/i$) will be approximately -2, giving a convenient initiation point for converting the data to the form JRC (mobilized/JRC(peak) and δ/δ(peak)(see Figure 5-3).

Pending additional data, the record shown in Figure 7-3 will be used as primary input since it shows several of the features discussed above. Figure 7-4 indicates how the shear stress-displacement performance could be simulated using the JRC(mobilized) concept. For convenience, the gradients of the various loading, unloading and reversal curves are defined in units of (m) which is given by the following empirical relation:

$$m = \frac{\phi_r/i}{0.3}$$

The denominator 0.3 is the value of δ/δ(peak) reached when dilation begins as shown in Figure 5-3. Curve a.b.c.d.u in Figure 7-4 follows the form of this figure. The unloading, reloading and reversal curves should be treated as guidelines only. Celestino and Goodman's (1979) data were not obtained directly from rock joints, there was no weathering effect to stimulate gouge production, and the roughness of the surfaces was unusual, consisting of interlocking ripple marks molded from joints in sandstone. The proposed method should be validated against the dilation record shown in Figure 7-3, using the mobilized-dilation concept (equation 6-2), and appropriate positive or negative values of JRC (mobilized) as obtained from Figure 7-4.

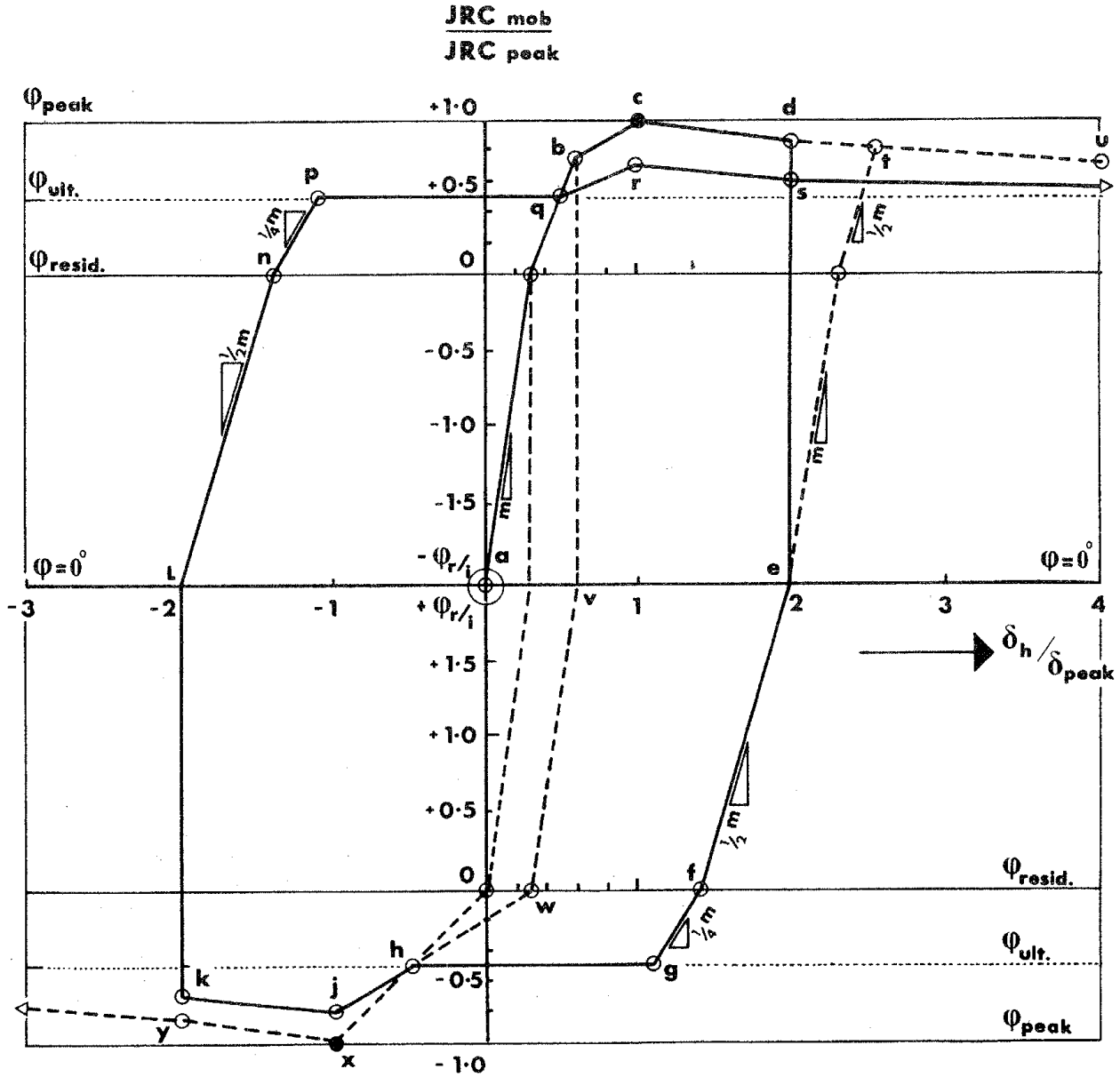

Figure 7.4. A preliminary model for simulating the effects of shear reversal and unloading of rock joints.

8 JOINT CLOSURE AND NORMAL STIFFNESS

The most comprehensive data concerning normal stress-closure behavior of natural rock joints are those reported by Bandis (1980). More than 60 joints were tested, representing a range of weathering grades, five different rock types, and correspondingly wide ranges of JCS and JRC, all of which were measured.

Bandis found that the maximum closure (V_m) of joints with similar average aperture thickness (a_j) depended primarily on the strength (JCS) of the joint walls. Variations in the maximum closure of joints with similar wall strength and aperture were related to differences in the joint roughness (JRC). Large values of maximum closure were recorded for certain weathered joints, due to the combined effect of wider initial apertures and low wall strength. The ratio JCS/a_j was found to be a sensitive indicator of this behavior, low ratios giving large values of V_m and vice versa.

Examples of normal closure tests on joints in limestone and dolerite are given in Figures 8-1 and 8-2. The most important feature is the stiffer behavior on the second and third load cycles. The first cycles are essentially tests on disturbed specimens, and the low values of stiffness obtained should not be misinterpreted. Approximately similar behavior is exhibited by normal loading tests on artificial tension fractures in granite, basalt and marble, as reported by Iwai (1976).

As expected, the slope of the stress-closure curves for the joints approaches that of the intact blocks, at the highest levels of normal stress. Most of Bandis (1980) tests were run up to maximum stress levels in the range of 30-50 MPa, roughly one third to one half of the JCS_o values.

8.1 JOINT APERTURES

The aperture of joints can be indirectly estimated from in situ measurements of water conducting capacity (see later section) or crudely in the laboratory from tapered feeler gauge surveys of jointed blocks that have been diamond sawn to give a good plane cross-section of the joint in question.

Feeler gauge measurements reported by Bandis (1980) indicated that the apparent joint apertures were larger when the joint was weathered (low JCS_o value) and had a weak dependence on the JRC_o value - apertures in general tended to be smaller for the more planar joints. Bandis measured apertures ranging from less than 0.1mm (unweathered joints in slate) to 0.6mm (weathered

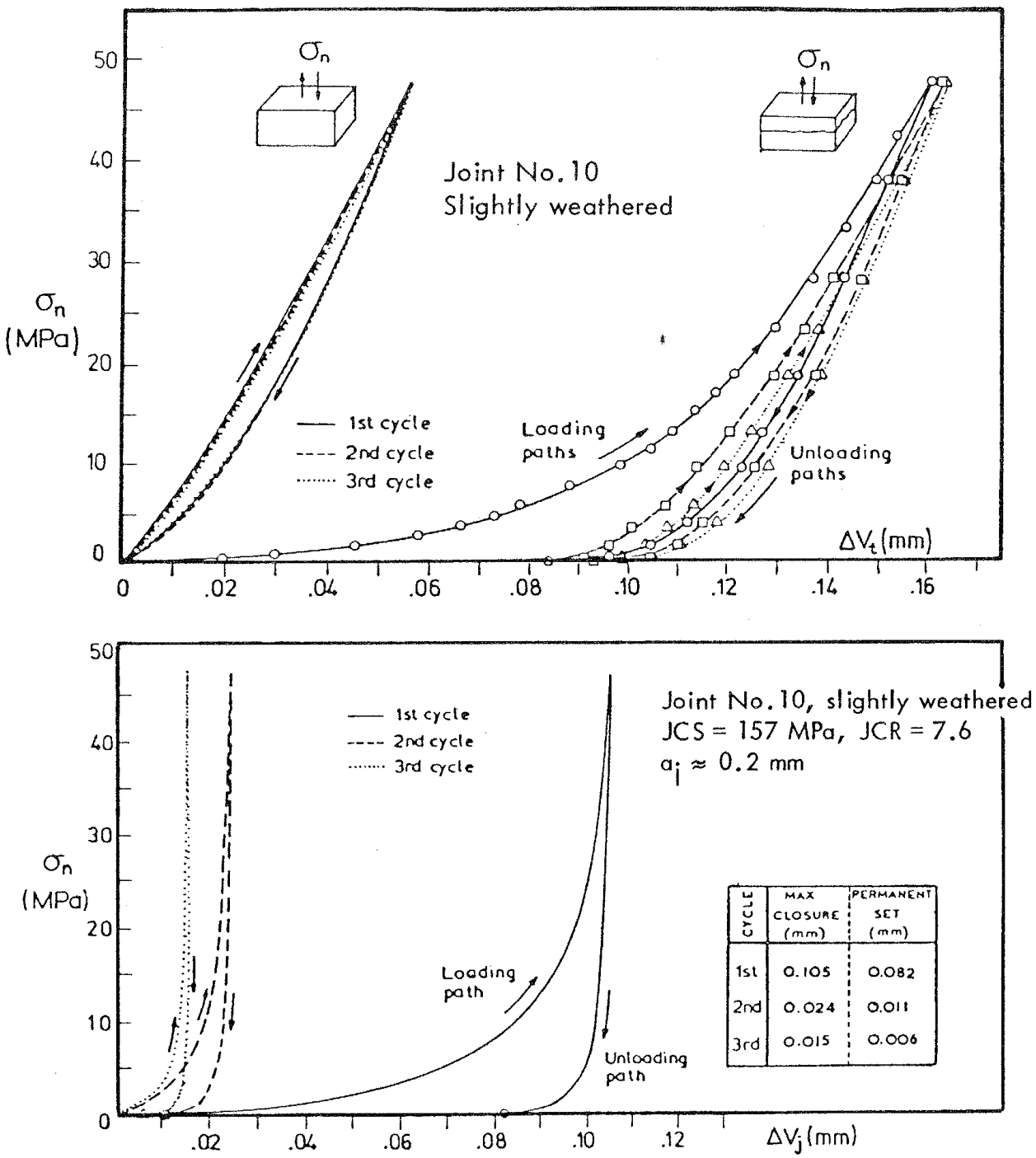

Figure 8.1. Normal load tests on solid and jointed samples of slightly weathered limestone, after Bandis (1980).

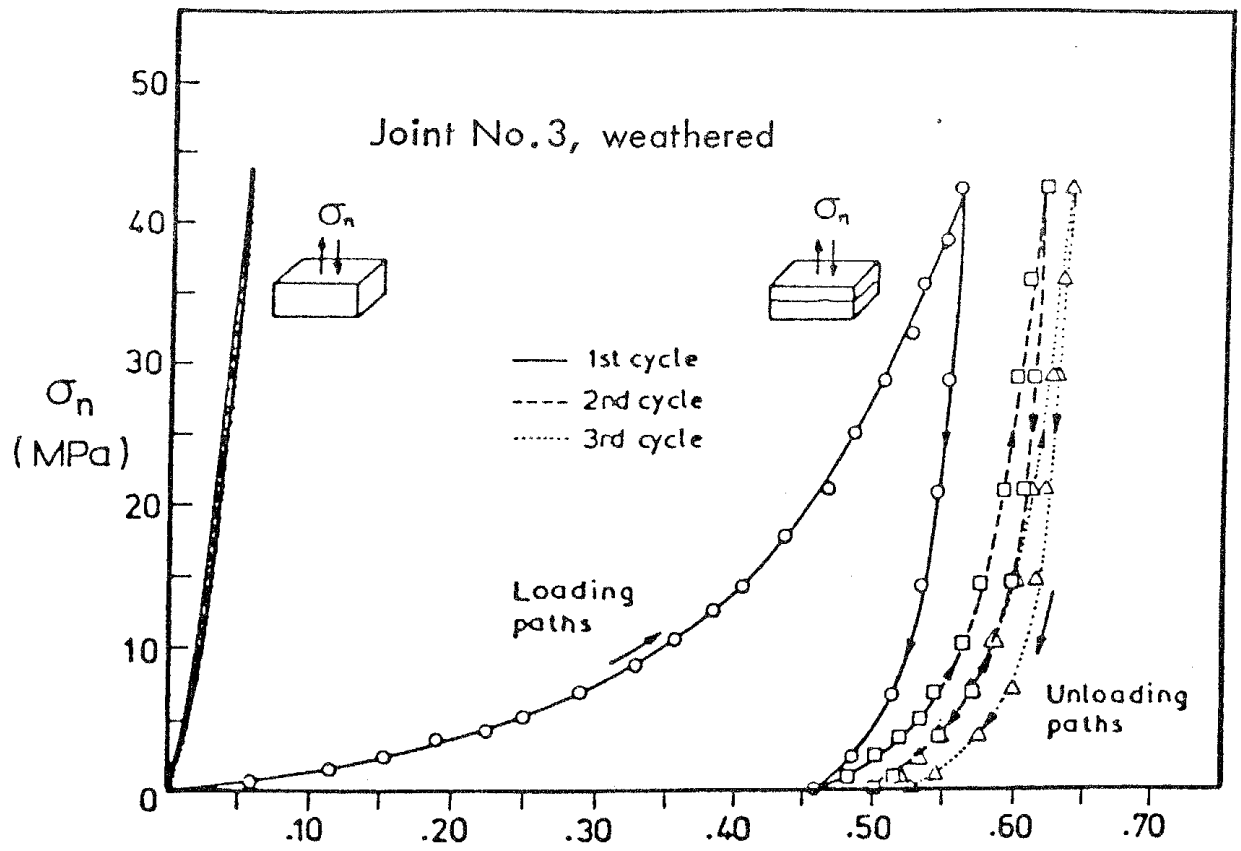

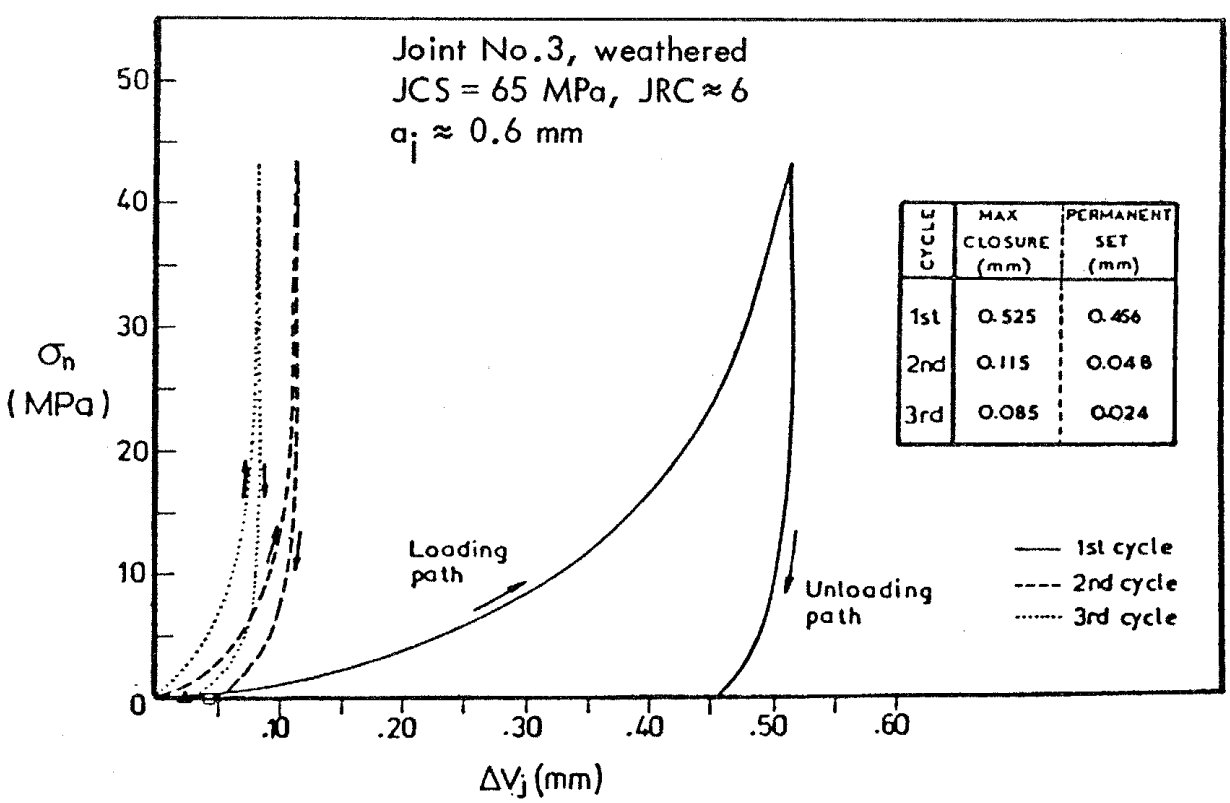

Figure 8.2. Normal load tests on solid and jointed samples of weathered dolerite, after Bandis (1980).

joints in siltstone, dolerite, limestone and slate). The samples were under self weight loading.

A convenient method of describing the degree of joint weathering is the relative alteration factor defined by Barton and Choubey (1977) as the ratio of unconfined compression strength (σ_c) of the intact rock and the joint wall compression strength (JCS). Both can be estimated from Schmidt hammer tests. Analysis of Bandis's comprehensive data indicates that the following simplified empirical relation gives a fair approximation to the initial aperture of a joint:

$$a_j \simeq \frac{JRC_o}{5} \cdot \left(0.2 \frac{\sigma_c}{JCS_o} - 0.1\right) \quad \text{----------} \quad 8\text{-}1$$

where a_j = initial joint aperture expressed in mm. under self-weight stress (approximately 0.001 MPa)

JRC_o = joint roughness coefficient of laboratory scale samples (i.e. L ≃ 100mm).

Example: medium-weathered joint

relative alteration (σ_c/JCS_o) = 120 MPa/80 MPa = 2

JRC_o = 7.5

Equation 8-1 gives $a_j \simeq 0.3$mm

8.2 JOINT CLOSURE AND NORMAL STIFFNESS

The above initial aperture is dramatically reduced on first loading (see Figures 8-1 and 8-2) but on the second and third load cycles appears to close very little above a normal stress level of about 20 - 30 MPa. This is essentially the same "threshold stress" reported by Pratt et al. (1977) for field tests on weathered joints in granite, based on the unchanged joint conductivity observed at normal stress levels above 30 MPa.

Bandis' analysis of 64 sets of experimental joint closure curves has shown that the behavior of natural, unfilled, interlocked joints can be adequately described by a hyperbolic relationship, irrespective of joint type, stress history and loading mode. The normal stiffness (K_n) of a joint cannot therefore be defined by a single value; for each increment of σ_n, the corresponding K_n value must be obtained from the derivitive of the hyperbolic function.

The hyperbolic function given in equation 8-2 (Bandis, 1980) was found to give an improved fit to experimental data when compared to the two functions suggested by Goodman (1974, 1976), which have frequently been used in numerical analyses of joint behavior in the past:

$$\sigma_n = \frac{\Delta V_j}{a - b\,\Delta V_j} \quad \text{----------} \quad 8\text{-}2$$

where ΔV_j = joint closure

a, b = constants

The straight line form of equation 8-2 given below:

$$\frac{\Delta V_j}{\sigma_n} = a - b\Delta V_j \qquad \text{8-3}$$

gave an excellent fit to the extensive experimental data (Bandis, 1980).

It can be shown that the asymtote to the hyperbola (a/b) is equal to the maximum joint closure (V_m). The constant (a) is equal to the reciprocal of the inital normal stiffness (K_{ni}). Expressions for K_{ni} and V_m would therefore define the complete stress-closure behavior.

Table 8-1 indicates the range and mean values of K_{ni} and V_m measured on 64 specimens, during the first, second and third load cycles:

TABLE 8-1

Values of Initial Normal Stiffness

and Maximum Closure for 64 Joint Specimens After Bandis (1980)

first load cycle		second load cycle		third load cycle	
K_{ni} (MPa/mm)	V_m (mm)	K_{ni} (MPa/mm	V_m (mm)	K_{ni} (MPa/mm)	V_m (mm)
(15.33)	(0.227)	(51.23)	(0.083)	(78.90)	(0.067)
2.54 - 34.51	.040 - .525	8.80 - 344.3	.015 - .238	11.33 - 424.4	.015 - .175

(mean values given in parentheses)

As indicated earlier, measured values of maximum joint closure (V_m) and normal stiffness (K_n) are found to be dependent on a_j, JCS_o and JRC_o, roughly in this order of influence. Experimental values of V_m plotted against the ratio JCS_o/a_j produced distinctly non-linear relationships of high correlation. The separate influence of JCS_o and JRC_o on maximum closure is clearly illustrated in Figure 8-3. Corresponding data for the second and third loading cycles was not so well defined, though a similar trend was apparent. As expected, normal stiffness increased with increasing joint roughness, due to the effect of reduced closure seen in Figure 8-3.

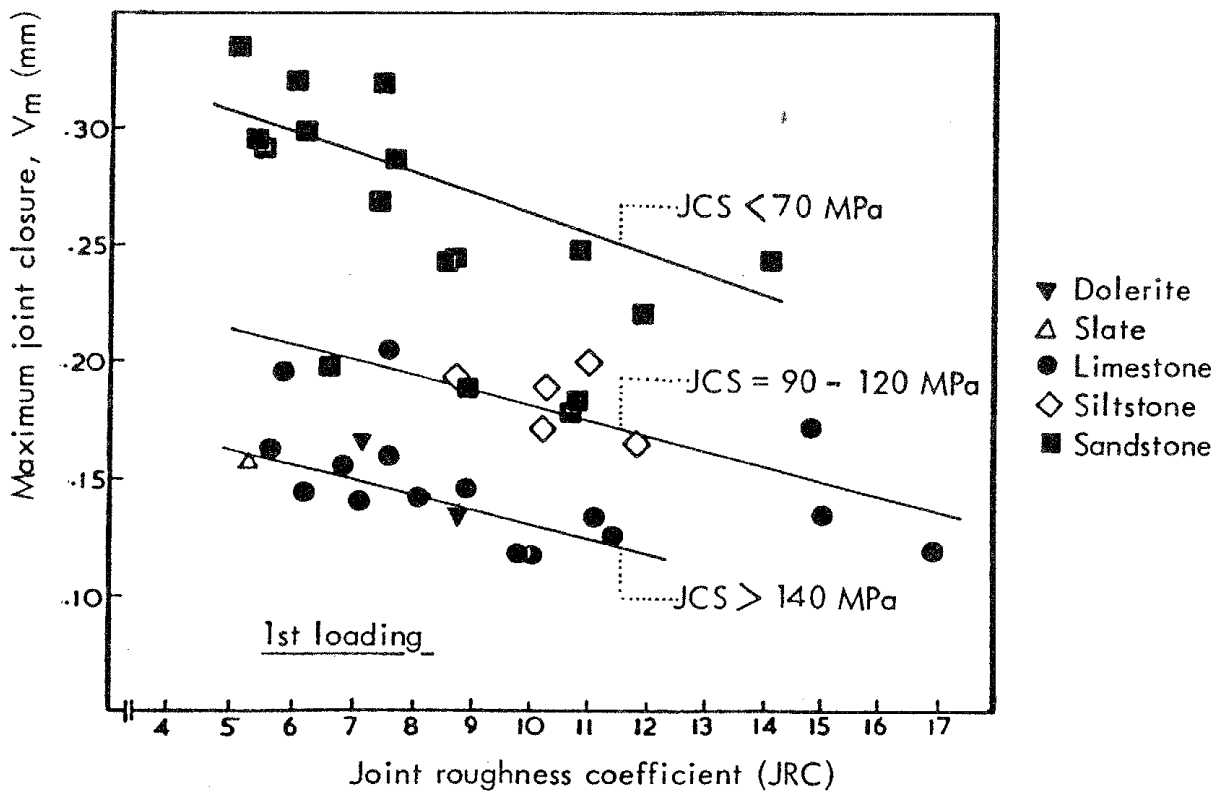

Figure 8.3. Influence of laboratory scale joint wall compression strength (JCS_o) and joint roughness coefficient (JRC_o) on the maximum joint closure (V_m) measured under first loading, after Bandis (1980).

Bandis (1980) succeeded in fitting the wide range of experimental data for maximum closure, with the following empirical relationship:

$$V_m = A + B\ (JRC\ ) + C \left(\frac{JCS_o}{a_j}\right)^D \text{---------- 8-4}$$

where JCS_o is in (MPa)

a_j is in (mm)

V_m is in (mm)

Multiple regression of all sets of data yielded the following values for the constants A, B, C and D (subscripts 1, 2 and 3 below correspond to the cycle number. The values below have been simplified from Bandis, 1980).

$A_1 = -0.30$	$A_2 = -0.10$	$A_3 = -0.10$
$B_1 = -0.006$	$B_2 = -0.007$	$B_3 = -0.007$
$C_1 = 2.24$	$C_2 = 1.01$	$C_3 = 1.14$
$D_1 = -0.25$	$D_2 = -0.23$	$D_3 = -0.25$

Equation 8-4 represents a simple constitutive relationship describing the variations in the maximum closure of unfilled interlocked joint types displaying the following range of wall strength and geometry indices: JRC_o = 5-15; JCS_o = 22-182 MPa; $a_j \simeq 0.10 - 0.60$ mm, and provided that the initial stress condition does not exceed a level of 1×10^{-3} MPa. Note that values of (a_j) for the second and third cycles are based on the initial aperture minus the permanent set at the end of the first and second cycles respectively.

Example: σ_c = 120 MPa, JCS_o = 80 MPa, JRC_o = 7.5

a_j = 0.3mm (equation 8-1) =

V_m (from first loading) = 0.23mm (equation 8-4)

The ability to predict values of V_m means that values of the asymptote (a/b) to the hyperbola (equation 8-2) can also be predicted. The value of the constant (a) in this equation is equal to the reciprocal of the inital normal stiffness (K_{ni}), and is obtained from the following relationship: (simplified from Bandis, 1980)

$$K_{ni} = 0.02\ (JCS_o/a_j) + 2\ JRC_o - 10 \text{ ---------- 8-5}$$

where K_{ni} = initial normal stiffness (MPa/mm)

Thus, a complete hyperbolic stress-closure curve for a given joint can be predicted, using equations 8-4 and 8-5 to obtain the appropriate constants for evaluating equation 8-2.

Example : σ_c = 120 MPa $a_j \simeq 0.3$ mm (equation 8-1)

JCS_o = 80 MPa $V_m \simeq 0.23$mm (equation 8-4)

JRC_o = 7.5 MPa $K_{ni} \simeq 10.3$ MPa/mm (equation 8-5)

Thus $a/b = 0.23$ (mm)

$a = 0.047$ mm/MPa

Figure 8-4 illustrates the predicted stress-closure curve, (No. II) using the hyperbolic relationship of equation 8-2. An example of closure prediction for a smoother and less weathered joint is also given for comparison (curve No. I).

Values of normal stiffness (K_n) at different levels of normal stress can be calculated from the following equation which Bandis (1980) derived from the derivate of the hyperbolic equation 8-2.

$$K_n = K_{ni}\left(1 - \frac{\sigma_n}{V_m K_{ni} + \sigma_n}\right)^{-2} \qquad \text{8-6}$$

The two examples shown in Figure 8-4 have the following values of normal stiffness (K_n) at normal stress levels of 1 and 10 MPa respectively:

σ_n = 1.0 MPa: I. K_n = 39.3 MPa/mm; II. K_n = 20.8 MPa/mm

σ_n = 10 MPa: I. K_n = 714 MPa/mm; II. K_n = 281 MPa/mm

8.3 STRESS-CLOSURE BEHAVIOR OF DISPLACED JOINTS

The closure and normal stiffness characteristics of perfectly interlocked joints as just described do not correctly represent the behavior of joints that are in the process of shear deformation, The recent joint compressibility theory of Walsh and Grosenbaugh (1979) was in fact based on the simplifying (though incorrect) assumption that the opposing surfaces of a joint are topographically uncorrelated with one another. Based on this theory, they predict that normal stiffness will be proportional to normal stress. Equation 8-6 indicates that this is not consistent with the majority of observed closure behavior.

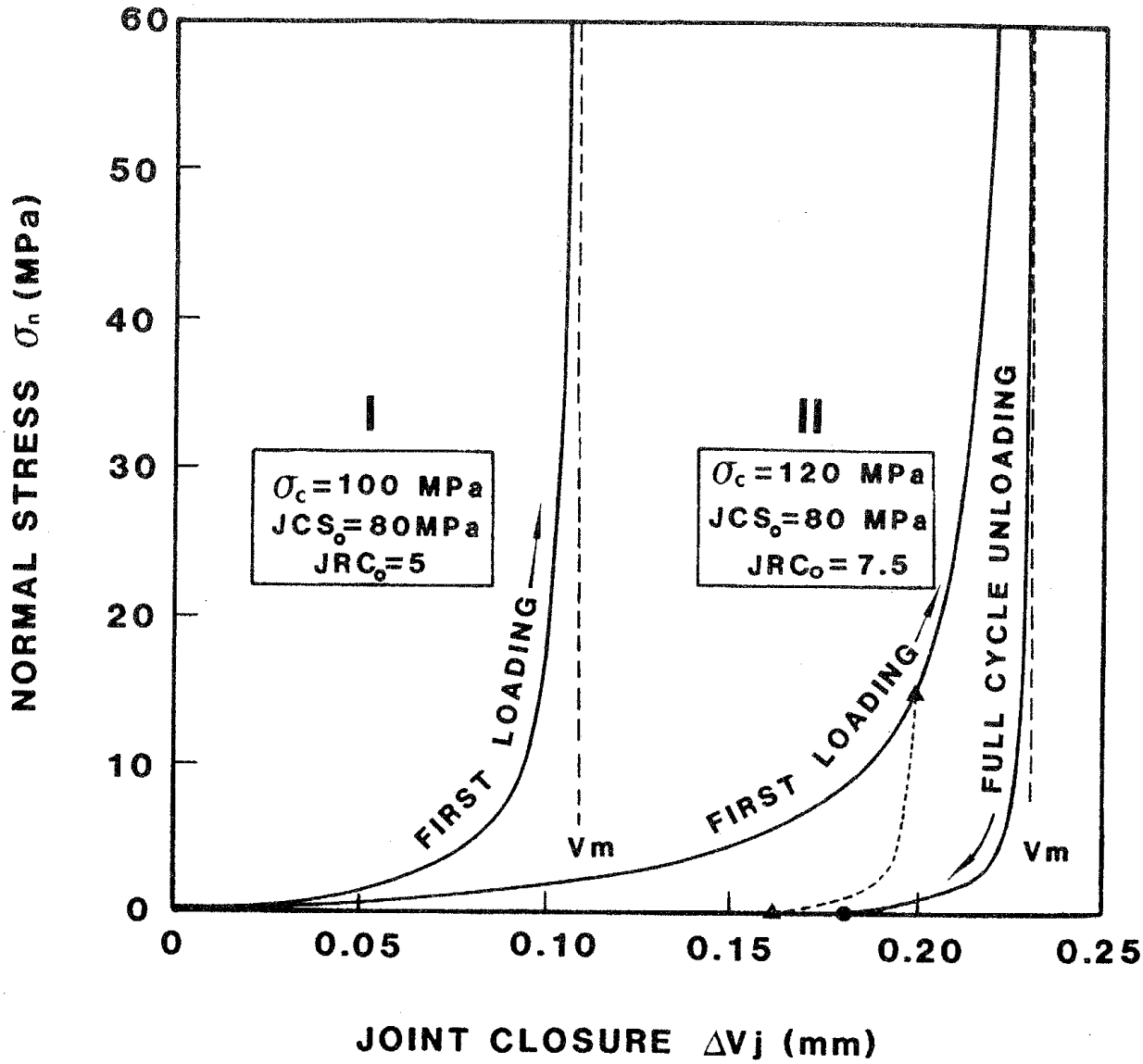

Figure 8.4. Examples of estimated stress-closure curves for two hypothetical joints, one slightly weathered and planar, the other medium weathered and medium rough. Derivation of the unloading curves is explained later in the text.

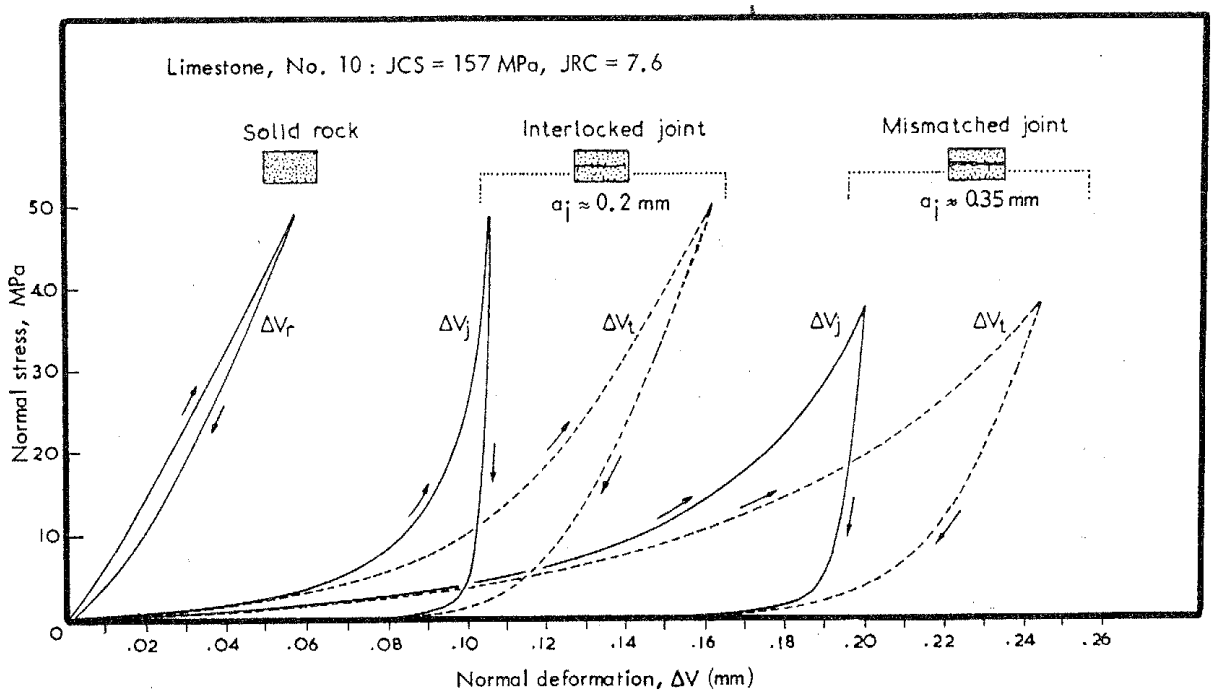

Figure 8.5. Comparison of total deformation (ΔV_t) and net closure curves ($\Delta V_j = \Delta V_t - \Delta V_r$) from the first loading cycle of the same joint tested in fully interlocked and mismatched positions, after Bandis (1980).

Twenty-four tests of mismatched (displaced) joints are reported by Bandis (1980). Displacements of 0.5 - 2.5 mm were studied, and five rock types were represented; limestone, sandstone, millstone grit, siltstone and slate. Apertures were first recorded when a small normal load was applied (0.15 MPa), and averaged 0.15 - 1.3 mm, depending on roughness. Comparison of the interlocked and mismatched stress-closure records for the same joints indicated that the interlocked joints were several times stiffer. A similar observation was made by Goodman (1976). An illustrative example is shown in Figure 8-5. Note in particular the large permanent closure of the mismatched joint, due presumeably to crushing of contacting points.

The maximum closure condition evident in tests on interlocked joints could not be achieved with mismatched joints, even when σ_n was raised as high as 0.5 JCS, and when the loading was performed three times (as in Figure 8-1 and 8-2). Significantly, the data for mismatched joints did not show linear behavior when plotted in terms of $\Delta V_j/\sigma_n$ versus ΔV_j (equation 8-3). In other words, it did not show the classic hyperbolic form of stress-closure common to interlocked joints. The best approximation was obtained from a semi-logarithmic equation of the following form:

$$\log \sigma_n = p + q\ \Delta V_j \qquad \text{8-7}$$

Typically (q) ranged from 8 - 24, and (p) ranged from -0.57 to -0.76. Normal stiffness (K_n) at a given level of normal stress can be estimated from the derivative of equation 8.7. Thus:

$$K_n = \frac{q \cdot \sigma_n}{\log_{10} e} = \frac{q \cdot \sigma_n}{0.434}$$

Table 8-2 summarizes measured values of K_n (interlocked)/K_n(mismatched) for a variety of joints, at three levels of normal stress.

The markedly stiffer behavior of the interlocked joints is due to the larger, and more uniformly distributed areas of asperities in contact. Highest ratios of K_n (intl.)/K_n(mism.) were, as expected, obtained from joints with high JRC and JCS values. The following empirical relationship indicates how the data presented in Table 8-2 can be used to modify the K_n(interlocked) data obtained from equation 8-6, to allow for the changes induced by shearing (mismatching):

$$\frac{K_n \text{ (interlocked)}}{K_n \text{ (mismatched)}} \simeq 2 + \frac{JRC_o \cdot JCS_o \cdot \sigma_n}{2500} \qquad \text{8-8}$$

Example: JRC_o = 10, JCS_o= 100 MPa, σ_n = 1 MPa, 10 MPa

Equation 8-8 predicts K_n(int.)/K_n(mism.) ≃ 2.4 and 6 respectively

TABLE 8-2

Summary of Interlocked and Mismatched
Normal Stiffness Ratio Values, After Bandis (1980)

NORMAL STRESS (MPa)		0.5	5.0	15.0
		K_n (interlocked)/K_n(mismatched)		
HIGH JRC	HIGH JCS: (4 spec.)	7.5 (4.5-10)	6.5 (4.5-10)	12.1 (7.7-20)
	LOW JCS: (6 spec.)	3.7 (1.4-5.6)	3.3 (2.1-7.7)	4.3 (3.0-6.6)
LOW JRC	HIGH JCS: (5 spec.)	3.1 (2.0-7.7)	3.7 (2.9-11.8)	7.1 (5.3-12.5)
	LOW JCS: (8 spec.)	1.9 (1.1-2.9)	2.0 (1.4-2.4)	3.3 (2.8-4)

Note: HIGH JCS: 120-175 MPa (mean = 156 MPa)
LOW JCS: 44-105 MPa (mean = 70 MPa)
HIGH JRC: 9.5-15 (mean = 11.0)
LOW JRC: 4.0-7.6 (mean = 6.4)

For purposes of numerical simulation of the complete shearing process of a joint, it is important to know how rapidly normal stiffness falls with shear displacement to the values represented in Table 8-2. Test results given by Bandis (1980) indicate that an assumption of a linear increase in K_n(intl.)/K_n(mism.) with shear displacement from zero to δ(peak) will be sufficiently accurate at this stage in our knowledge of joint behavior.

Post-peak, at displacements of more than 1mm for laboratory samples, the change of K_n(intl.)/K_n(mism.) is apparently slight. This suggests that the ratio of real/assumed contact area for a joint changes rapidly up to the point of peak shear strength (where $A_1/A_0 \simeq \sigma_n/JCS$ according to Barton and Choubey, 1977). Thereafter, the real area of asperities in contact changes only slightly.

8.4 UNLOADING AND IRRECOVERABLE CLOSURE

Goodman (1976) has suggested that the unloading curves for joints will

follow essentially the same path as for the intact rock. A cursory glance at the examples shown in Figure 8-1 and 8-2, and numerous other examples presented by Bandis (1980) indicate that joint behavior is not so simple as this. An important fact that emerges from Bandis' work is that the unloading stress-opening curves for joints are also hyperbolic. Behavior is governed by equation 8-2 as for loading, and linear relationships are obtained when data is plotted in the form of equation 8-3.

An examination of available data suggests that when the loading stages are taken to the maximum closure condition (to stress levels in the 40 - 50 MPa range) the hyperbolic unloading curves obtained from the first, second, and third cycles are each of similar shape. However, this common shape is dissimilar to the unloading curve for the solid rock. This is to be expected in view of the different sample thickness and "areas of contact" involved. Joints exhibit much higher unloading stiffnesses than the solid rock, though if a sufficiently thin "slice" of solid rock were unloaded, behaviors would possibly converge somewhat.

There are several as yet unresolved problems concerning loading and unloading behavior of rock joints. It is difficult to predict the ratio of maximum closure (V_m) to initial aperture (a_j), values for the first load cycle range from 0.3 - 0.9, though generally average about 0.7. The ratio of irrecoverable closure (V_i) to maximum closure (V_m) for a given load cycle is also difficult to predict. An analysis of available data shown in Figure 8-6 indicates considerable scatter, though consistent trends are apparent. For example, the irrecoverable closures for the two calculated loading curves shown in Figure 8-4 can be estimated as follows:

Case I	Case II	
$a_j \simeq 0.15$mm	$a_j \simeq 0.3$mm	equation 8-1
$JCS/a_j \simeq 530$ MPa/mm	$JCS/a_j \simeq 265$ MPa/mm	
$V_m = 0.11$mm	$V_m = 0.23$mm	equation 8-4
$V_i/V_m \simeq 75\%$	$V_i/V_m \simeq 80\%$	Figure 8-6
$V_i \simeq 0.08$mm	$V_i \simeq 0.18$mm	

These irrecoverable closures are shown by circles on the axis of Figure 8-4. The constants (a) and (b) required to define the unloading hyperbola for a given load cycle can be estimated from the following:

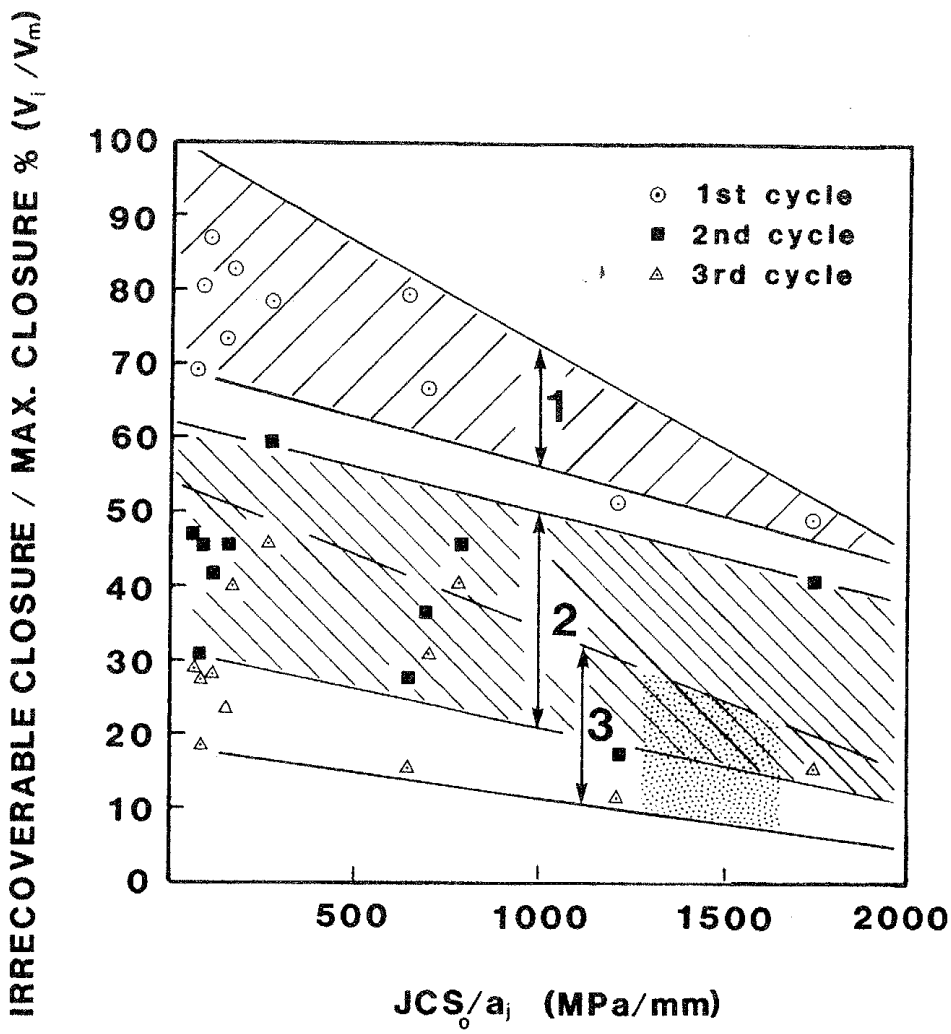

Figure 8.6. Irrecoverable joint closure reduces with number of load cycles, with JCS_o value, and with the smallness of the initial joint aperture (a_j).

$$a/b \simeq V_m - \Sigma V_i$$

$$a = 1/K_{ni}$$

where K_{ni} is estimated from equation 8-5 with a_j replaced by $(a_j - \Sigma V_i)$

An example calculation for a "full cycle unloading" curve, using the above method, is illustrated in Figure 8-4. It is apparent that the "complete" load-unload cycle to infinitely high applied stress is simulated by this method. Intuitively, it would seem likely that unloading curves from intermediate stress levels could be simulated with acceptable accuracy by replacing the term maximum closure (V_m) with current closure V_c.

An example will now be given showing an intermediate unloading curve from a stress level of 15 MPa, where the current closure (V_c) on first loading is approximately 0.20mm (see Figure 8-4, example II). The assumption will be made that V_m can be replaced by V_c in Figure 8-6. Thus, the irrecoverable closure V_i will now be ≃80% of 0.20mm = 0.16mm (in place of 0.18mm for a complete cycle). The initial stiffness K_{ni} is calculated with (a_j) replaced by $(a_j - V_i)$. The dotted curve in Figure 8-4 illustrates the intermediate unloading curve which is readily estimated by this method. In a numerical analysis, it will merely be necessary to keep track of the current closure V_c during a given cycle, to be able to estimate an appropriate unloading hyperbola. Reloading will be handled in a similar manner, with aperture a_j in equations 8-4 and 8-5 replaced by $(a_j - V_c)$. The relevant reloading hyperbola is thereby defined by the newly calculated values of V_m and K_{ni}.

9. COUPLING JOINT WATER FLOW WITH DILATION AND CLOSURE

The mechanical and hydraulic behavior of rock joints when subject to stress change cannot be accurately modelled, unless an accurate method can be derived for measuring real joint apertures in situ, prior to stress perturbation. The unknown stress history of joints in situ means that the techniques developed in Section 8 would only provide a crude approximation to apertures in situ, even if the present stress distribution was known. An alternative method for estimating apertures in situ is presented by water flow tests.

The flow of water through rock joints can be represented by adopting the analogy of laminar flow between smooth parallel plates. The equivalent smooth wall aperture (e) and permeability ($e^2/12$) can be derived from the following modified form of Darcy's law relating flow rate (q) and gradient (dP/dy):

$$q = \frac{w \cdot e^3}{12\mu} \cdot \frac{dP}{dy} \qquad \text{---------- 9.1}$$

where w = width of flow path (lateral dimension)

μ = absolute viscosity (1.2×10^{-5} gm.sec/cm^2 at 10°C)

Analysis of linear and radial flow tests through artificial tension fractures in granite, basalt and marble led Witherspoon et al. (1979) to conclude that this so-called "cubic" law was valid whether the fracture surfaces were open to 250 m, or closed to 4 m by application of normal stresses as high as 20 MPa. However, they did note slight deviations (reduced flow) and indicated that (q) ranged from 60 - 96% of the above theoretical flow rate due to roughness effects.

However, analysis of Witherspoon et al. (1979) indicates that the absolute apertures of the fractures were not recorded, only changes in aperture (Δe). The reported analyses were based on estimates of the residual apertures - the apertures remaining when the normal stress was as high as 20 MPa.

Analysis of other data reported in the literature suggests that tortuosity and roughness causes much larger flow losses than indicated above. In fact, Kranz et al. (1979) and Walsh (1981) went so far as to suggest that the law of effective stress may not apply to flow through jointed rocks.

9.1 REAL APERTURE AND CONDUCTING APERTURE

In a recent article, Tsang and Witherspoon (1981) have also questioned the exactness of equation 9.1, and have proposed that the roughness of the fracture walls be taken into account to modify the true aperture. In fact, the concept of discrete values of real aperture (E) and conducting aperture (e)

(with E>e) was used several years ago by Heimli (1972) and Barton (1972) to explain the observed discrepancy between (E) and (e) in fracture flow tests conducted in Norway and elsewhere.

Recent analysis of fracture flow data, and comparison with data obtained from Terra Tek's heated block test (Terra Tek, 1981) is illustrated in Figure 9.1. It is apparent that the cubic law with E=e, may only be valid when joints are exceptionally smooth, or when apertures are very wide. These observations of the dependence of (E/e) on the joint roughness and aperture have lead to the formulation proposed in Figure 9.2. It will be seen that divergence from the cubic law (e=E) is modelled for rough joints of very wide aperture (≥1mm). No divergence is modelled for the smoothest joints unless conducting apertures are very small (i.e. <10μm). These features of the model broadly correspond with observed behavior. The following equation represents the curves in Figure 9.2.

$$e = \frac{JRC_o^{2.5}}{(E/e)^2} \qquad \text{---------- 9.2}$$

where e is expressed in microns (μm)

The equation is only valid for values of E/e≥1. An alternative form of this equation is given below:

$$e = E^2/JRC_o^{2.5} \qquad \text{---------- 9.3}$$

During site selection and preliminary site characterization studies, estimates of the variation in conducting aperture (e) for the different joint sets may be back-calculated from flow tests, using closely spaced double-packers coupled with a method for accurately locating the packers across joints. The estimates of (e) obtained from these tests could also be based on the statistical method proposed by Snow (1968), which provides a useful estimate of not only the conducting aperture (e), but also the mean spacing of the water conducting joints (S), assuming the rock mass can be idealized by a cubic network of joints. In each case, the estimated apertures will reflect the effective normal stress levels operating across the joints at the various test levels. Care will need to be taken to use very low injection water pressures, so as not to reduce this stress level and cause opening of the joints, close to the borehole walls. Since it would be difficult to monitor such changes in aperture, the borehole pump-in test should essentially be an investigation of "fixed" apertures, with a degree of built-in uncertainty.

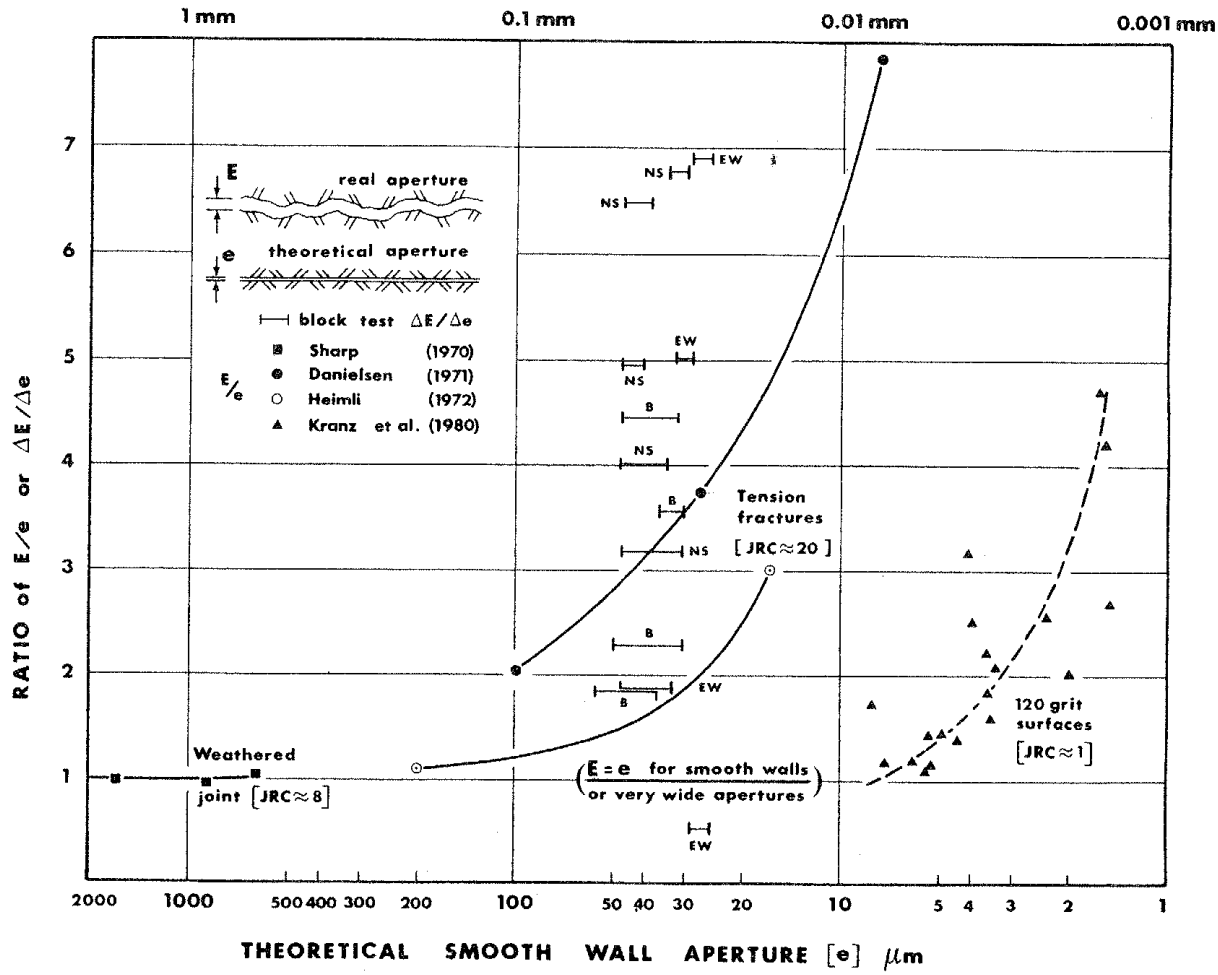

Figure 9.1. Comparison of real apertures and conducting apertures in fracture flow tests, and in Terra Tek's heated block test (Voegele et al, 1981).

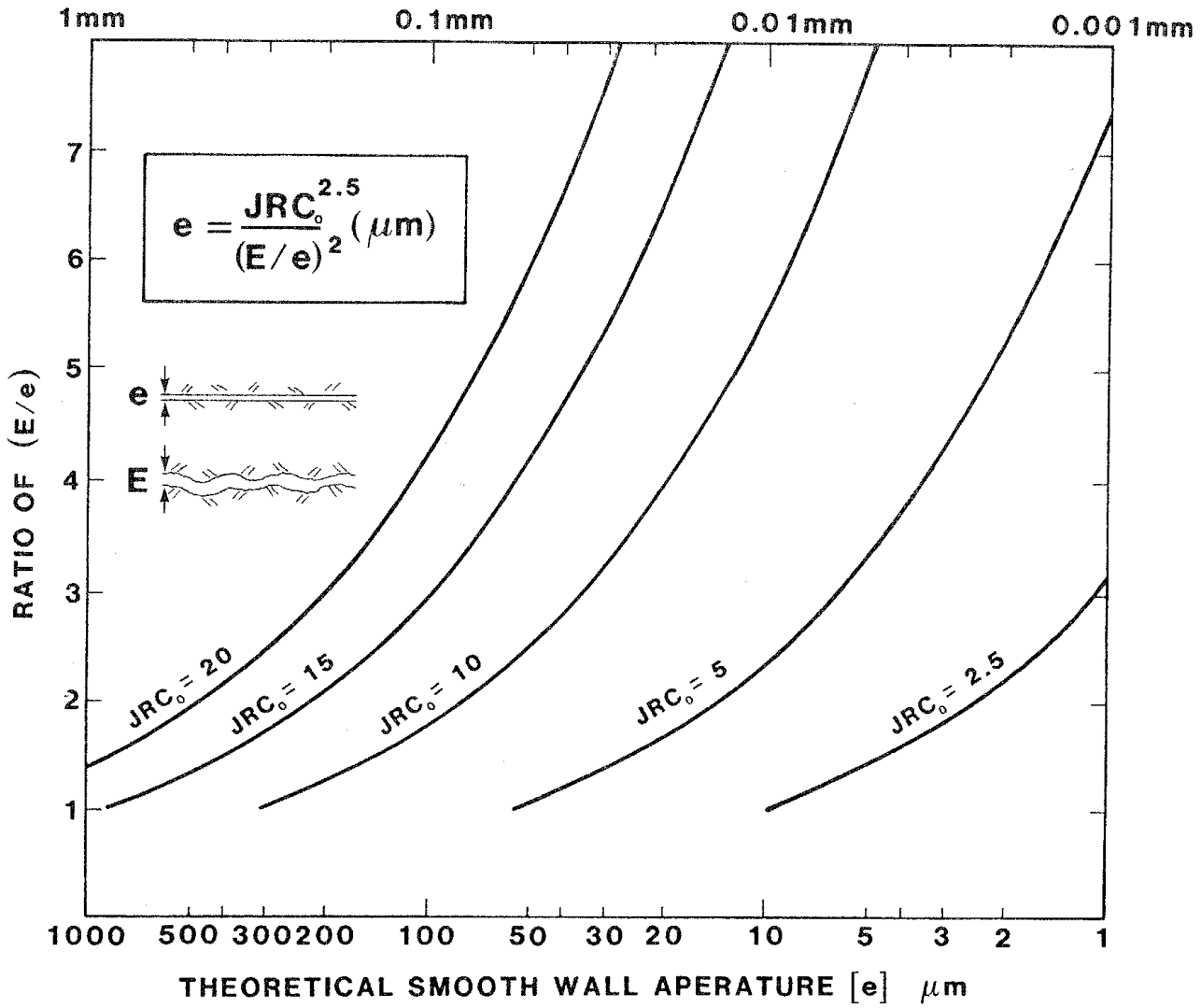

Figure 9.2. A constitutive model relating conducting aperture with real aperture and joint roughness.

Once the distribution of conducting apertures (e) has been obtained from carefully planned flow tests, estimates of real in situ apertures (E) can be obtained from equation 9.3. Example:

(i) from flow test data: e = 50μm

(ii) from tilt tests of jointed core: JRC_o = 10

(iii) real aperture E≈126μm (equation 9.3)

This value would then be the starting point for calculations of mechanical and hydraulic response to future stress perturbation.

9.2 COUPLING FLOW WITH SHEAR DISPLACEMENT

The potential for greatly increased conducting aperture when a non-planar joint is made to shear up to, or past, peak strength is illustrated in Figure 9.3. The overlapped asperity tips shown by these plastic replicas of measured roughness profiles, will in reality be sheared material, partially filling some of the voids shown in the figure. The ratio of JCS/σ_n represented by these tests was 10.7, giving a degree of asperity damage roughly equivalent to that for rough joints in competent granite (JCS = 150 MPa) at 600 meters depth.

When shearing is accompanied by dilation, the initial aperture (E_0) will be increased by the vertical component of dilation (E_1), giving a total aperture (E_2) of (E_0+E_1). The initial smooth wall conducting aperture (e_0) will also increase, but at a reduced rate, according to the empirical relationship given by equation 9.3. Since it is known that the true area of contact of interlocked joints is of similar magnitude to that of joints under shear (both are very small), it will be assumed that our relationship between (e) and (E) also holds for shearing events. (Data marked NS, EW in Figure 9.1 was in fact obtained from shear tests.)

The technique for modelling the shear strength-displacement and dilation of joints of different size, which was developed in Sections 5 and 6, can now be extended to include water flow. For simplicity it will first be assumed that the joint water does not change the effective normal stress. In a fully-coupled numerical model, the changing permeability will alter the water pressure distribution, and the effective normal stress will be recalculated, again changing the aperture in an interactive cycle, using the techniques developed in Sections 7 and 8.

Figure 9.4 illustrates the stress-displacement modelling capabilities developed in Section 5. Realistic laboratory scale data:

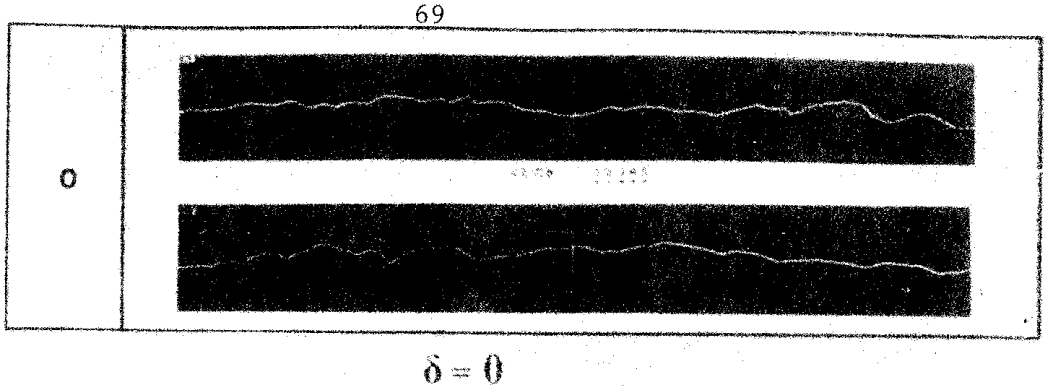

$\delta = 0$

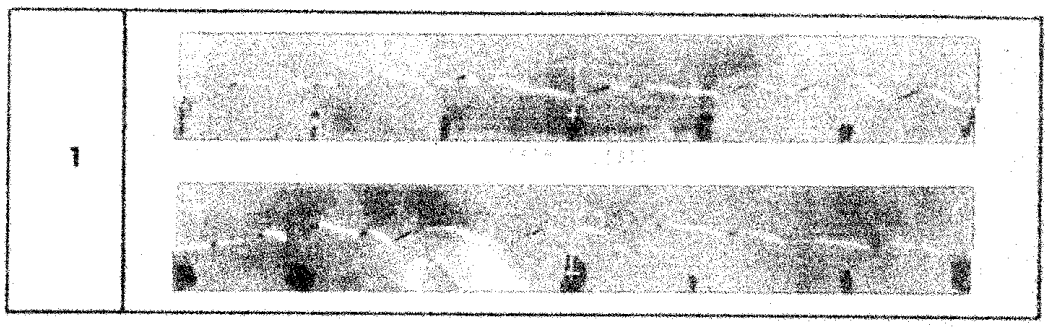

$\delta \simeq {}^{1}/_{2}\,\delta\,(\text{peak})$

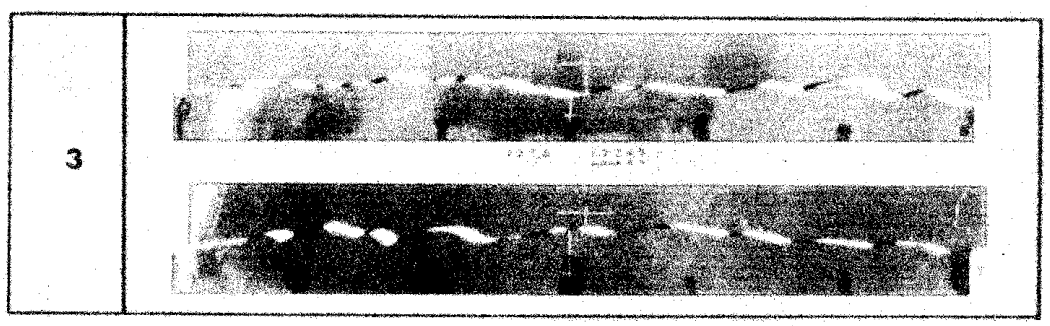

$\delta \simeq 2\,\delta\,(\text{peak})$

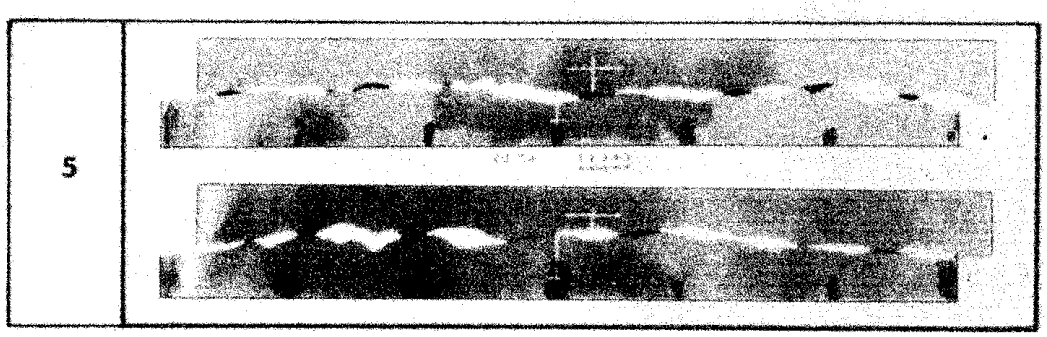

$\delta \simeq 5\,\delta\,(\text{peak})$

Figure 9.3. Reconstructed shearing events for a rough model tension joint, after Barton, 1971).

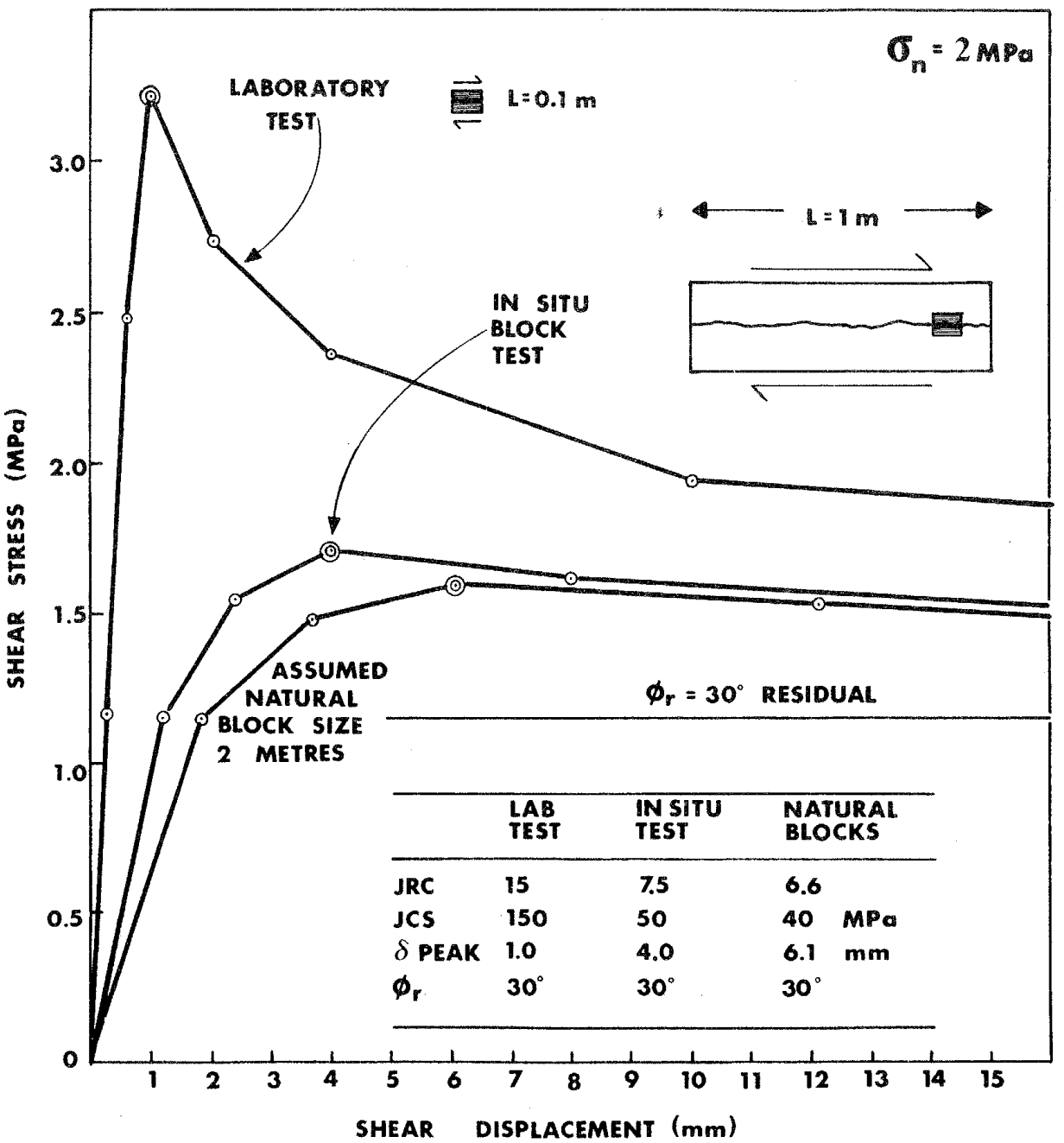

Figure 9.4. Stress-displacement modelling of shear tests on three different sizes of joint sample.

$JRC_o = 15$, $JCS_o = 150$ MPa, $\phi_r = 30$

has been extrapolated to larger sample sizes, representing typical in situ block sizes.

Figure 9.5 illustrates the corresponding dilation paths predicted by the techniques described in Section 6. Note the delayed dilation of larger samples, as discussed earlier. We will now use two of these dilation paths (L = 0.1 m, L = 2.0 m) to predict changes of joint permeability ($e^2/12$). As noted earlier, an initial aperture (E_o) is required before the calculations can be performed.

Recent large-scale block tests (Pratt et al. 1977, Voegele et al. 1981) have indicated a joint permeability of approximately 10^{-3} m/sec under the effective normal stress of 2 MPa chosen for these example calculations. This corresponds to a conducting aperture (e_o) of 35μm. If we assume a laboratory scale roughness (JRC_o) of 15, an initial real aperture (E_o) of 174μm is obtained from equation 9.3. (Although we are interested in the behavior of large size blocks, it is believed that the laboratory scale roughness (JRC_o) will be the most representative value for estimating aperture closure under normal stress. It is unlikely that normal closure is size-dependent.)

The vertical increments of dilation (E_1) are added to (E_0) to obtain the estimate of conducting aperture from equation 9.3. As an example, the following apertures were calculated for the instant of peak strength in two of the examples illustrated in Figure 9.4 and 9.5.

1. L = 0.1m
   δ(peak) = 1mm
   E_0= 174μm e_0= 35μm
   E_1= 156μm
   E_2= 330μm e_2= 125μm

2. L = 2.0m
   δ(peak) = 6mm
   E_0= 174μm e_0= 35μm
   E_1= 260μm
   E_2= 434μm e_2= 220μm

Figure 9.6 (A curves) indicates how the permeability increases by at least an order of magnitude when the 0.1m and 2.0m long joint samples are sheared up to peak strength. Three orders of magnitude increase are possible if shearing is unchecked. A hypothetical normal stress of 20 MPa was also investigated (B curves). However, the same initial permeability of 10^{-3}m/sec was assumed for both cases, for simplicity.

Unfortunately, there is at present an almost non-existent data base against which to validate these important modelling techniques. Coupled

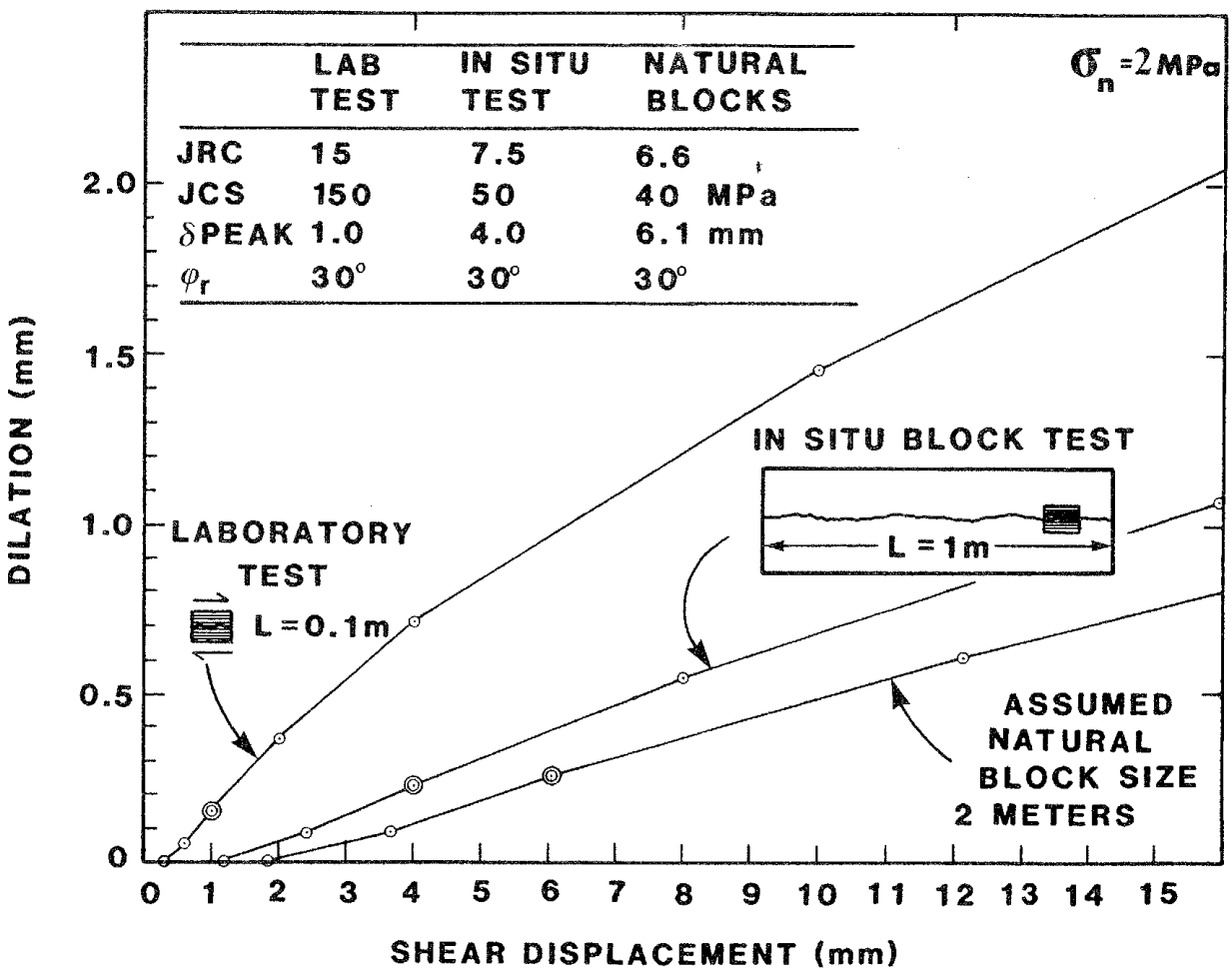

Figure 9.5. Dilation modelling for the shear tests on the three different sizes of sample shown in Figure 9.4.

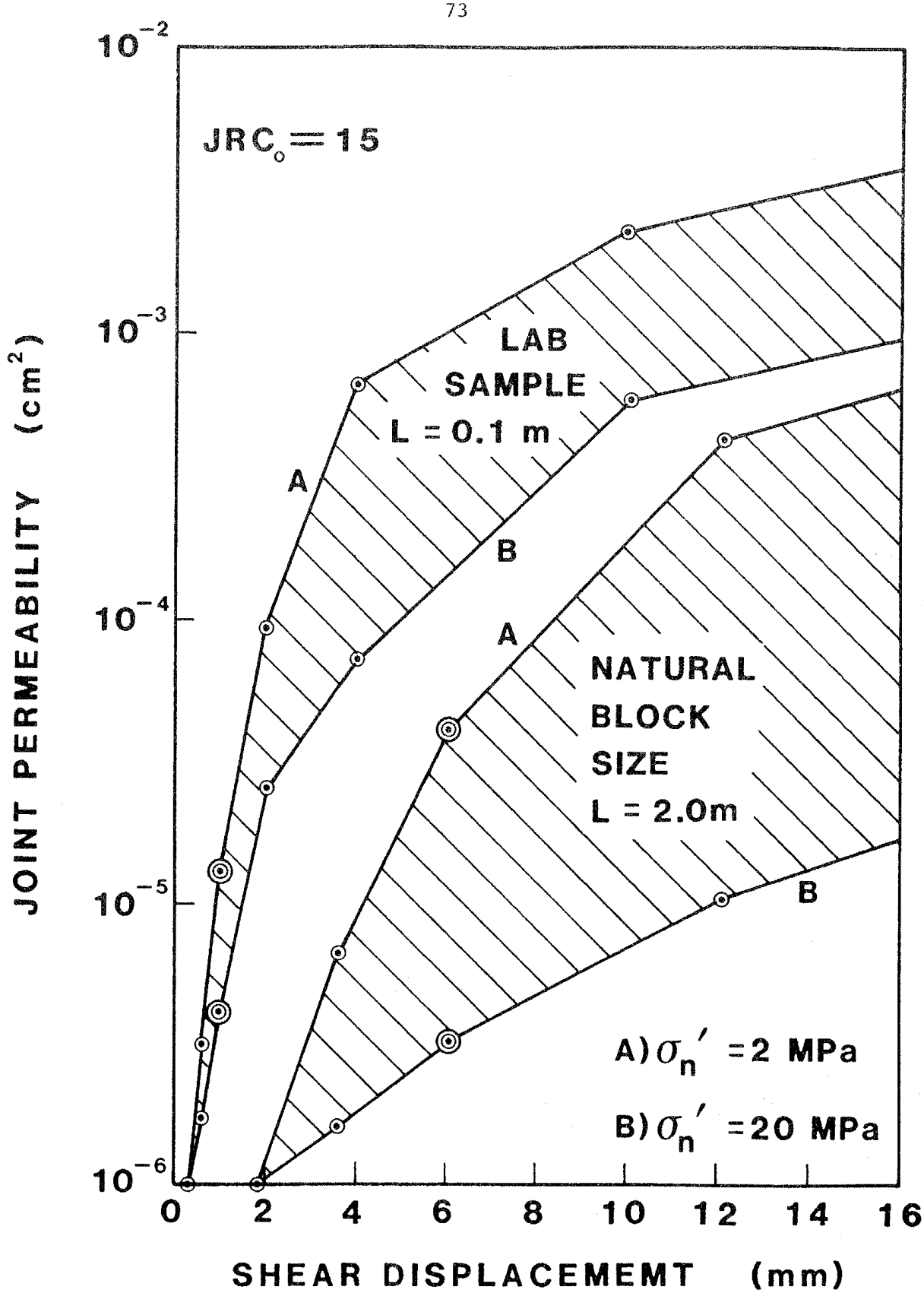

Figure 9.6. Estimated change in permeability for two different sizes of joint sample when sheared up to, and beyond peak strength (double circles).

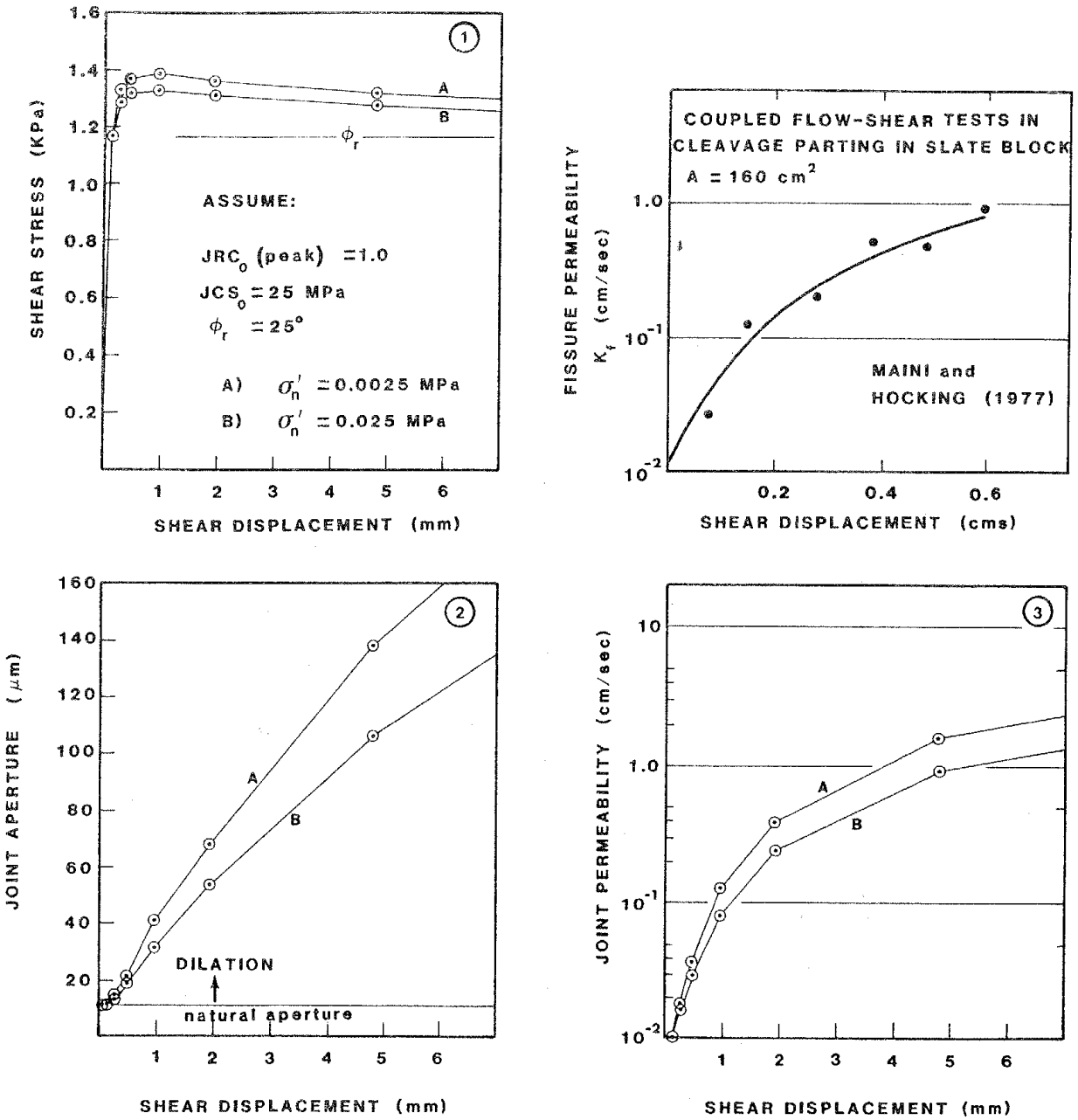

Figure 9.7. Example validation of coupled flow-shear modelling with Maini's (1971) coupled flow-shear test on a cleavage parting in slate.

water flow and joint shear was reported by Maini (1971), and Maini and Hocking (1977). Maini's sample was a 25 in^2 cleavage joint in a block of slate. The sample was sheared under self-weight loading. Permeability was found to change from 10^{-2} to 10^{-1} cm/sec in the first 2mm of shear displacement, and a further order of magnitude in the next 4mm. The very low normal stress was considered responsible for the large increase in permeability. On the other hand, a cleavage joint in slate is generally a very planar feature which would be expected to dilate only a minimal amount, even under vanishingly small stress levels.

Figure 9.7 illustrates three stages of validation, using our numerical model to generate shear stress-displacement, dilation and displacement-permeability curves, for comparison with Maini's results (top right hand graph). Two possible normal stress levels have been investigated, representing the self-weight loading from 10cm and 100cm depths of block respectively. Agreement appears to be good with the realistic set of assumptions adopted.

9.3 COUPLING FLOW WITH NORMAL CLOSURE

A recent attempt by Tsang and Witherspoon (1981) to model the effect of normal stress on flow rate, utilizes a concept of void deformation to explain the closure under normal stress, and utilizes the concept of increasing asperity contact to explain reduction in flow. Tsang and Witherspoon obtained good agreement with measured flow rates when they assumed arbitrary contact area ratios (real/apparent: A_1/A_0) in the range 0.10 - 0.20. The salient feature of their method is the use of measured normal stress-closure records for solid and jointed rock to define the relevant joint"roughness profile", which in turn is used to predict flow as a function of normal stress. Shearing is not considered.

In the present modelling technique, we make the assumption that all the input data should be obtainable from relatively inexpensive tests such as tilt tests and Schmidt hammer tests on recovered core, and from in situ pumping tests in exploratory boreholes. The opportunities to perform normal loading tests will necessarily be limited in practice, until a repository is under the early stages of excavation.

An example of joint closure-permeability-normal stress prediction using the techniques developed in Section 8 is shown in Figures 9.8 and 9.9. Data obtained from joint characterization of Terra Tek's heated block facility are utilized. Only three parameters are required for complete prediction, and these would initially be obtained from tilt tests and Schmidt hammer tests of jointed core, together with results of borehole pumping tests to obtain a

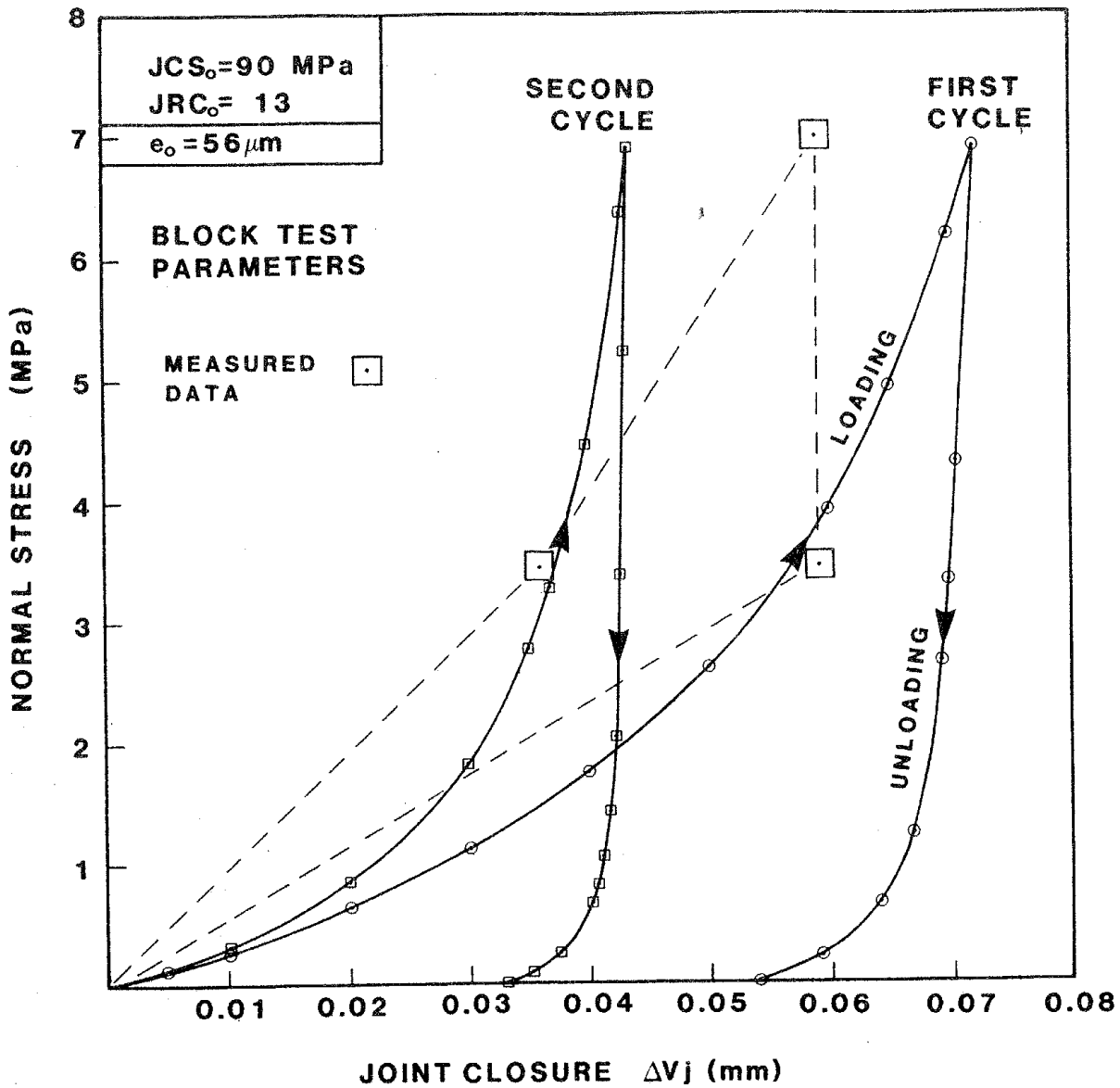

Figure 9.8. Examples of normal stress-closure prediction for first and second load cycles, utilizing data from Terra Tek's heated block test.

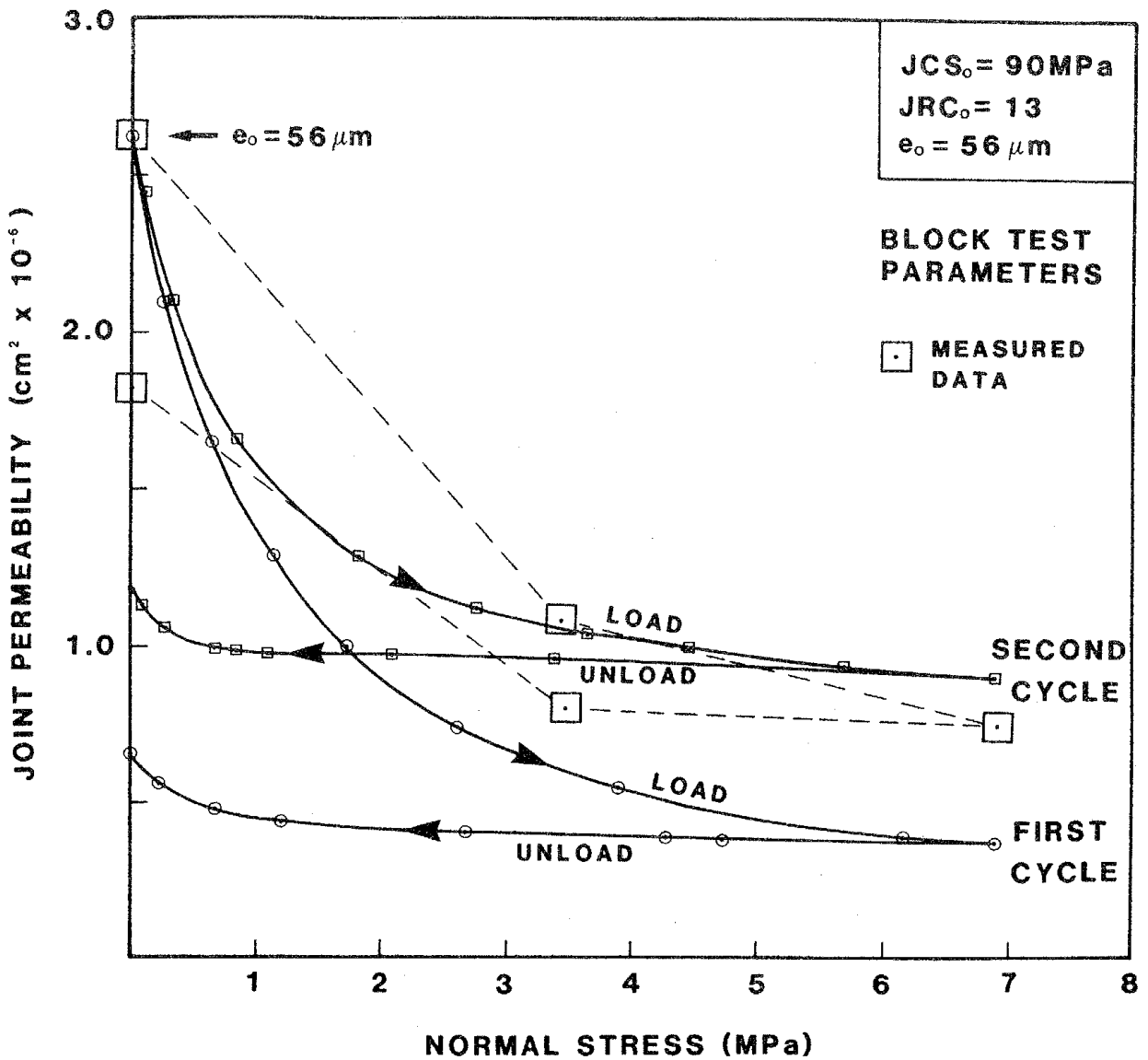

Figure 9.9. Examples of normal stress-joint permeability prediction for first and second load cycles, utilizing data from Terra Tek's heated block test.

representative value for the initial conducting aperture (e_o). The following values were obtained at the heated block test facility:

JRC_o = 13

JCS_o = 90 MPa (weathered diagonal joints)

e_o = 56μm (σ_n = 0, prior to biaxial load cycle to 6.9 MPa)

Equation 9.3 indicates that the real initial aperture approximates 185μm. Equation 8.4 indicates maximum closures on first and second loading of 99μm and 52μm respectively. Equation 8.5 is evaluated to determine the inital normal stiffness K_{ni} = 25.7 MPa/mm. The hyperbolae (equation 8.2) defining the first and second loading cycles are thereby defined (see Figure 9.8). Unloading hyperbolae are calculated from the two values of current closure (V_c) at the maximum stress level of 6.9 MPa. Irrecoverable closure points are estimated from Figure 8.6 as before. Permeability ($e^2/12$) is calculated from the values of real aperture (E) which are successively reduced by closure, then converted to approximate conducting apertures (e), utilizing equation 9.3.

Also shown in Figure 9.8 and 9.9 are measured data from the main biaxial load cycle conducted on the $16m^3$ jointed block of gneiss. The data is roughly bracketed by predictions of first and second loading cycles. In reality, the test joint has undergone a complex history of loading and unloading prior to this test:

1. excavation of test adit
2. slot drilling for flatjacks
3. test cycle to σ_n = 3.5 MPa
4. Test: 0-3.5-6.9-3.5-0.

Another cause of discrepancy is the finite injection pressures (0.14-0.34 MPa) used to measure conducting aperture. When the diagonal joint is under zero stress, these water pressures can be expected to have prised the joint open slightly, thereby causing poor agreement with the predicted residual permeabilities.

10. THERMAL AND TIME EFFECTS

A slow, near-field thermal stress perturbation will be experienced by the rock mass surrounding a waste repository. Being so slow in relation to excavation-induced stress changes, it is probable that joints will react in a stick-slip mode, with relatively long periods of stick. The evaluation of both temperature and length of stick on joint properties is therefore a necessary step in developing an all-encompassing constitutive model.

10.1 THERMAL EFFECTS ON THE SHEAR STRENGTH OF JOINTS

Experience has shown that factors which reduce the unconfined compression strength of rock, such as weathering along the joints, also reduce the shear strength, due in part to the reduced values of JCS. A similar though usually smaller reduction in σ_c or JCS due to water saturation also causes a slight reduction in friction angle, particularly for layer lattice minerals which suffer a disproportionate reduction in compression strength with saturation.

Triaxial tests of rocks at elevated temperature, such as those performed by Heard (1970) and Enniss et al. (1979) indicate an accelerating reduction in differential stress $(\sigma_1-\sigma_3)$ at failure as temperature increases. Tests on Westerly granite and basalt indicate approximately 25% reduction in $(\sigma_1-\sigma_3)$ over the temperature range 25-300°C, though only a few percent reduction in the range 25-100°C. In view of the logarithmic relationship between compression strength and peak friction angle, it is therefore to be expected that frictional strength will reduce imperceptably in the range 25-100°C. Elevated temperature triaxial tests on fractures in Westerly granite reported by Stetsky (1977) in fact show little dispersion in strength in the range 25-300°C. Significant reductions in strength are not seen until temperatures as high as 500-600° are reached. Thus, for the case of repositories in basalt and granite, it will apparently be sufficiently conservative to reduce JCS values by about 5-10%, to allow for the effects of the thermal pulse on the shear strength of the joints.

10.2 THERMAL EFFECTS ON JOINT CLOSURE AND PERMEABILITY

Intuitively, it would seem that the above reductions in JCS values could also be applied to normal closure. The value of JCS is a determining factor in the shape of the loading and unloading hyperbolae, due to its influence on the value of maximum closure (V_m) and initial stiffness (K_{ni}), which determine the asymptotes (a) and (b).

However, the first set of fully controlled hydrothermomechanical tests conducted on rock joints, in Terra Tek's heated block test facility (Figure 10.1) indicate that temperature may have an unexpectedly big effect on joint closure, and therefore also on joint permeability. Flow tests conducted in the diagonal joint depicted in the figure indicated conducting apertures no smaller than 27-30μm at the highest stress levels (6.9 MPa) applied during the four ambient loading tests that were performed. The fourth of these tests is depicted in Figure 10.2 (test numbers 9-10-11). A normal stress of 6.9 MPa without temperature increase, is apparently incapable of closing the diagonal joint to apertures tighter than about 30μm.

However, when both the rock and fluid temperature are increased without change of stress, the aperture is reduced to the extent that permeability falls by an order of magnitude. Upon cooling, the permeability eventually returns nearly to the original value, once normal stresses are released sufficiently for the basically poor fit of asperities to overcome the shear resistance and "spring" apart. Normal stress was controlled throughout the tests by adjusting the pressure in the flatjacks for thermal expansion effects.

The above phenomenon has been interpreted as improved fit between originally "perfectly" mated joint walls. The improved fit is probably the result of thermal expansion of present roughness profiles into something resembling the original joint profile, which was presumeably formed at higher than ambient (12°) temperature. The gneiss in question has anisotropic thermal expansion properties.

Unfortunately, the data shown in Figure 10.2 is at present unique, and further testing in other rock types would be needed before the ambient closure model (Section 8) can be correctly adjusted for temperature effects. The positive influence of this hydrothermomechanical closure phenomenon on near-field repository performance is important, and should be investigated further.

A very interesting point emerges from a comparison of normal stress - permeability tests conducted on artificial tension fractures and those performed on natural joints. Figure 10.3 illustrates three steep curves (Iwai, 1976, 1st and 2nd run, and Witherspoon, Amick and Gale, 1977) obtained from tests on artificial tension fractures in Sierra White Granite (σ_c = JCS = 200 MPa). The considerably shallower sets of curves obtained from in situ block tests on natural joints in gneiss and granite (Terra Tek, 1981, Pratt et al. 1977) contrast strongly with the data on artificial surfaces, leading one to question the use of artificial tension fractures for flow studies. However, when the elevated temperature block test data is plotted on the same figure (dotted

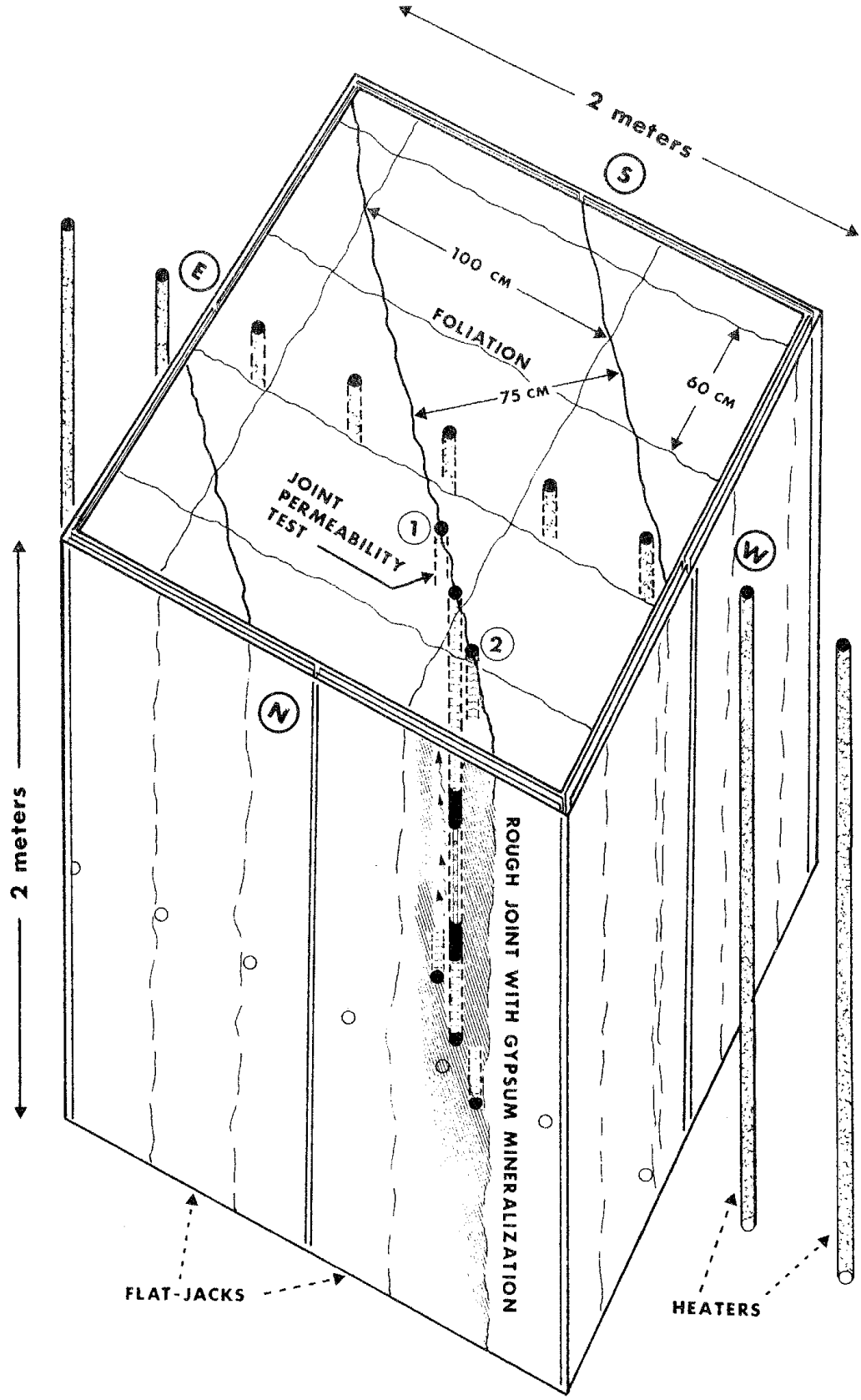

Figure 10.1 The heated block test facility for investigating the hydrothermo-mechanical properties of jointed rock (Terra Tek, 1981).

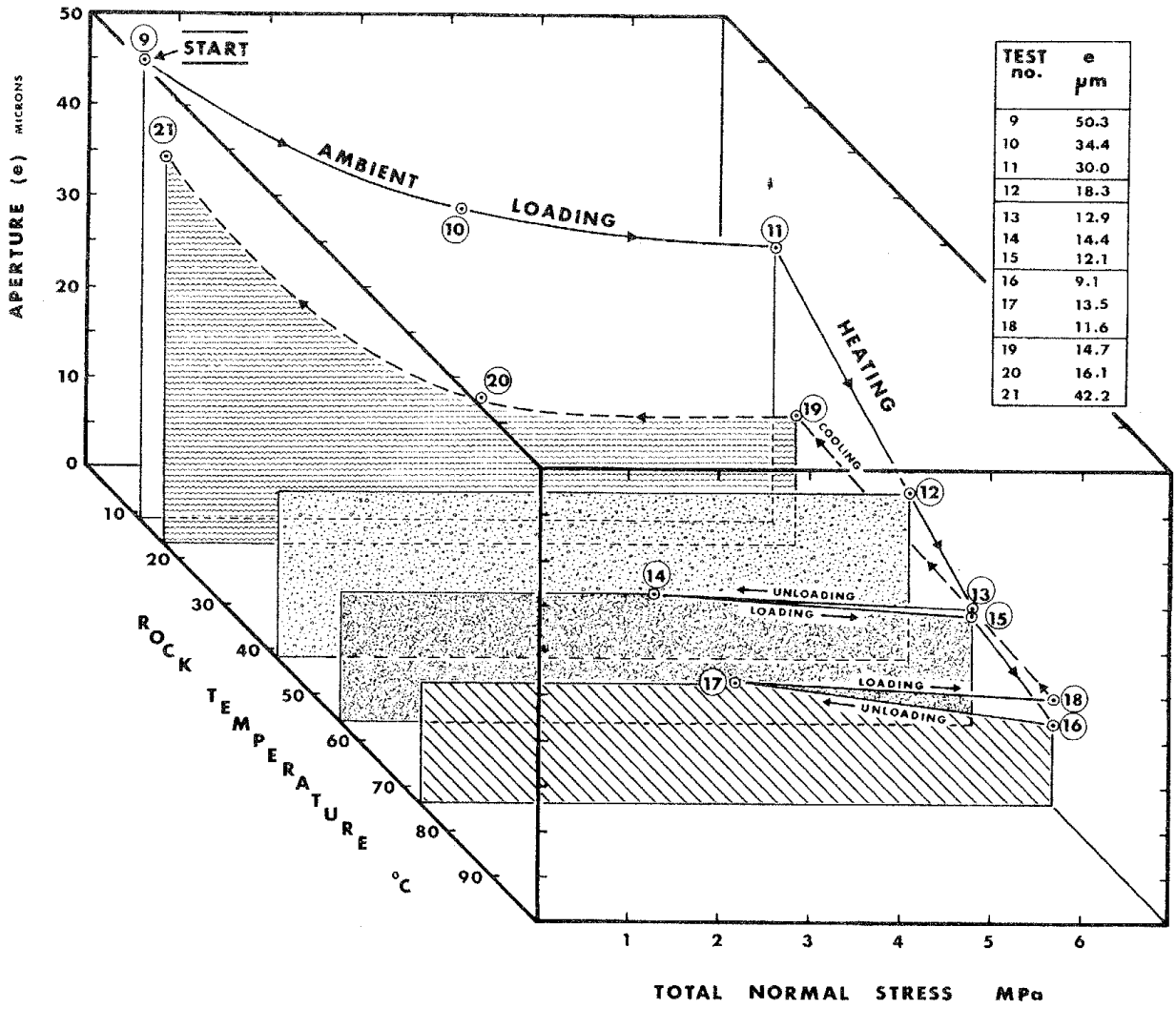

Figure 10.2 Increased temperature causes an unexpected increase in joint closure and a corresponding reduction in conducting aperture and permeability (Terra Tek, 1981).

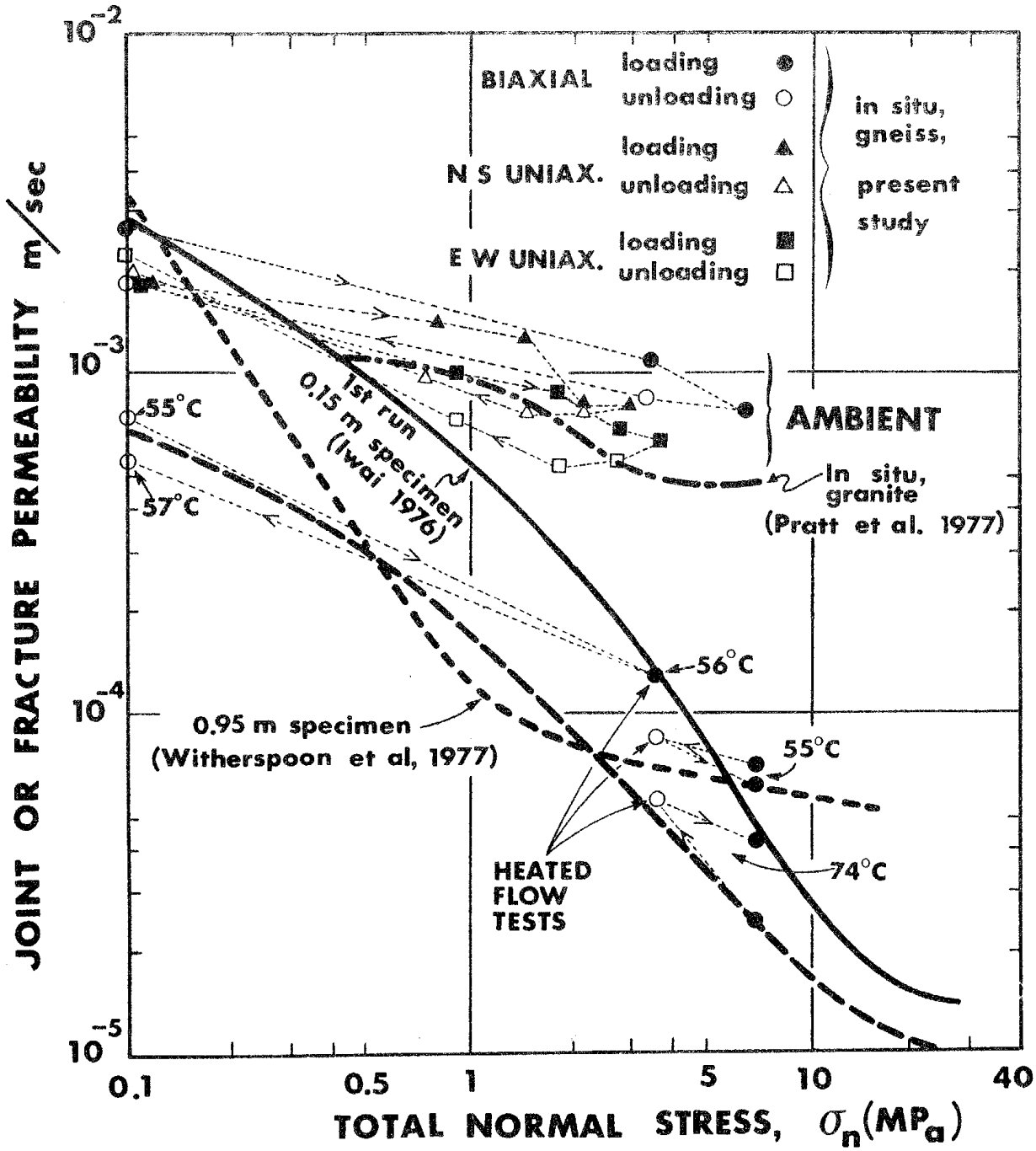

Figure 10.3 Comparison of normal stress-permeability behavior of artificial tension fractures and natural joints, under both ambient and elevated temperature.

lines marked with 55°, 56°, 57°and 75°C), the similarity with tension fracture data is striking. The reason for the similarity is presumeably the fact that artificial tension-fractures are generated and flow tested at the same ambient temperature. Their roughness profiles fit nearly "perfectly".

In view of the relative paucity of data, it is unwise to draw strong conclusions from the above. However, there are grounds for believing that ambient flow tests in tension fractures may approximate elevated temperature flow tests in natural joints. The present uncertainty emphasizes the need for further heated block test facilities, with independent control of stress and temperature.

10.3 INFLUENCE OF LENGTH OF STICK AND SHEARING RATE

Experiments reported by Dieterich (1972) on rough-ground surfaces of sandstone, quartzite, graywacke and granite have indicated that accumulations of powdered rock debris on a shear surface exhibit strongly time dependent properties. Static friction increases with the logarithm of the time that adjacent blocks remain in stationary contact. Over the range of normal stresses from 2-85 MPa, the coefficient of static friction (arctan τ/σ_n) for 10^5 sec. intervals between stick-slip events is 6-10% greater than for 15 sec. intervals. These results appear to be dependent both on the presence of gouge and on periods of stick, rather than on slow shear rates, since Byerlee and Brace (1968) found no detectable variation in frictional strength over a wide range of strain rates. A compilation of data for differential stress ($\sigma_1-\sigma_3$) at failure over as many as 9 log cycles of strain rate (10^{-6} - 10^3 per sec.) given by Brace and Jones (1971) does indicate about 5% increase in strength per log cycle of strain rate. A corresponding increase in JCS at typical repository depths represents only about ½° increase in peak shear strength per three log cycles of strain rate, which confirms Byerlee and Brace's (1968) results.

Dieterich's results are clearly important for any fault surfaces in the neighborhood of a repository, but the question arises whether they need to be considered for the case of essentially gouge free, undisplaced joints. Tests by Dieterich (1972) and Hoskins et al. (1968) on rough, clean rock surfaces showed stable sliding characteristics. It appears that a degree of polish and/or gouge is required before stick-slip mechanisms take over from stable sliding. There are also indications that increased temperature also increases the range of stable sliding (Brace and Byerlee, 1970).

Rough, clean surfaces such as relatively undisplaced rock joints will apparently not be subject to increased shear strength with increased duration

of stationary contact. The methods developed for characterizing joint shear and joint closure therefore appear valid for modelling long-term repository response. However, further work is required to gain an understanding of the effect of temperature on closure and permeability.

11 INEXPENSIVE BLOCK TESTS FOR FULL-SCALE PARAMETER EVALUATION

In view of the inherent variability of all rockmasses, it is important that sampling of joint properties is "extensive" as well as "intensive". Figure 10.1 is an example of an intensive sampling test. The cost and time involved obviously limits their number, even after access to the repository area is established. An example of an "extensive" test is the tilt test on jointed core shown in Figure 3.4. The test can be performed cheaply and in large numbers, once drillcore is available from vertical exploratory drilling and from horizontal holes drilled when access is established. However, an interpretive stage is involved in assessing the appropriate size-correction to apply to JRC_o and JCS_o (Figure 4.6).

11.1 AVOIDANCE OF SIZE EFFECTS

In view of the size effects demonstrated in Section 4, the question arises as to what size of block should be tested to obtain scale-free properties.

Normal closure and permeability mechanisms appear to be governed most strongly by small-scale properties (i.e. JRC_o from laboratory scale samples, JCS_o from Schmidt hammer tests). A theoretical treatment of roughness by Swan (1981) has also indicated that normal stiffness should be virtually independent of the size of the sample, at least for practical size ranges. This lends support to the concept of single value, small-scale parameters for normal closure and permeability effects.

Section 4 indicates very clearly that joint properties are size-dependent when shear displacement is involved, due to the displacement-dependence of strength mobilization. The size dependency may apparently die out in an assembly of rock blocks when a "sample" exceeds the natural block size. Figure 11.1 shows schematically that, for unchanged roughness, the smaller the block size, the higher the shear strength of an assembly of blocks. The spacing of joints intersecting a potential shear plane also defines the distance between potential "hinges" in the assembly. The slightest block rotation allows the finer features of roughness to be felt as opposed to sheared over, hence the scale effect. Details of the tests depicted in Figure 11.1 are given by Bandis et al. 1981.

The above deduction that the natural block size is the correct size of sample for minimizing size-effects leads to the recommendation for performing tilt tests and/or pull tests on natural blocks, as depicted in Figure 11.2. In an

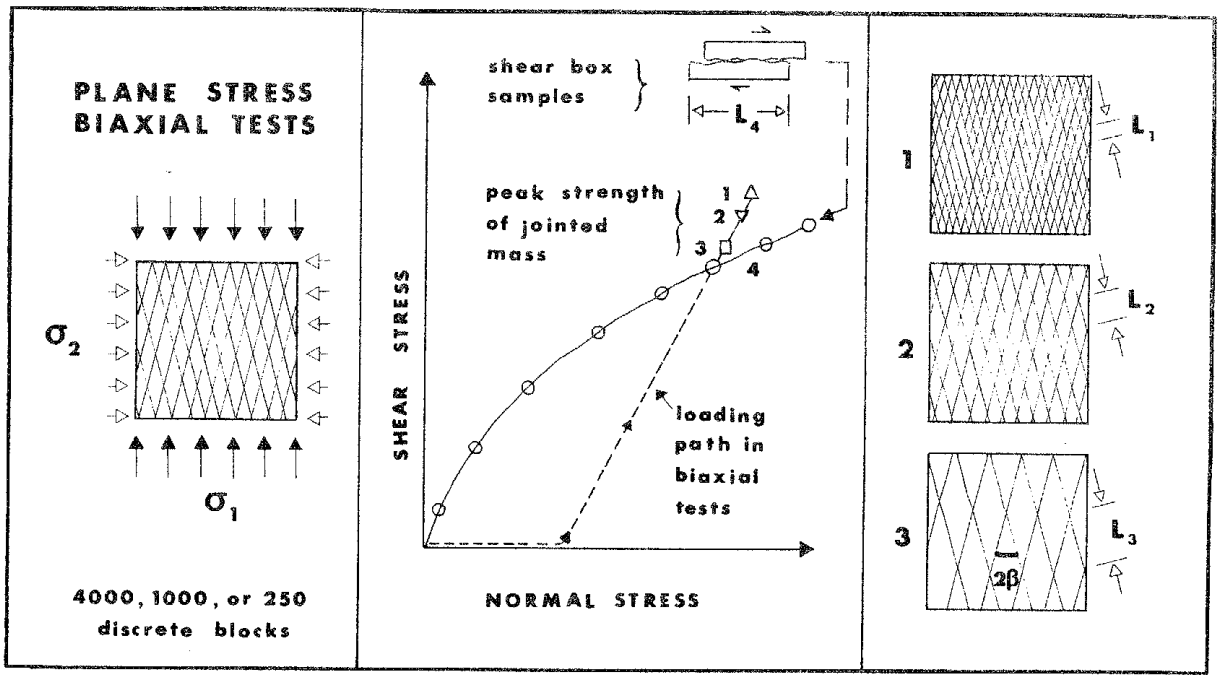

Figure 11.1 Individual block size determines the shear strength of a jointed mass, after Barton and Bandis (1980).

exploratory adit or shaft, it will seldom be possible to extract blocks as easily as from a rock cutting with re-entrant corners, so some form of slot drilling or wire sawing may be required. In the pull-test variation, two sides and the top of the block will usually have to be freed to obtain unambiguous results.

11.2 THE BLOCK TILT TEST

Estimates of JRC can be obtained from tilt tests, using a clinometer to measure the tilt angle (α), and a Schmidt hammer to estimate JCS_o. The value of JRC is back-calculated using equation 3.3, reproduced below:

$$JRC = \frac{\alpha^0 - \phi_r^0}{\log_{10}(JCS/\sigma_{no})} \qquad \text{---------- 11.1}$$

where $\sigma_{no} = \gamma h \cos^2 \alpha$ (=normal stress induced by self-weight of block, see Barton and Choubey, 1977).

γ = rock density

h = thickness of upper block

Example 1. Tilt test

Assume the following values have been measured:

$\alpha = 51^\circ$ (tilt angle)

h = 500 mm (block thickness) $\sigma_{no} = 0.005$ MPa

$\gamma = 25$ kN/m^3

$JCS_o = 50$ MPa (estimated using Schmidt hammer, see Barton and Choubey, 1977 for details).

$\phi_r = 23^\circ$

$$JRC = \frac{51^\circ - 23^\circ}{\log_{10}\left(\frac{50}{0.005}\right)} = 7.0$$

The overestimated value of JCS resulting from use of the Schmidt hammer (small-scale) value JCS_o, causes a corresponding underestimate in JRC. Improved accuracy in the estimation of the full-scale values of JRC and JCS can be obtained by iteration. For example, let us suppose the tilt test was conducted on a 50 cm long naturally joint block. The scaling guidelines given in Figure 4.6 suggest that the laboratory scale (nominal L_o = 10 cm) value of JRC_o will be approximately 10. The ratio JCS_n/JCS_o will therefore be approximately 0.5. Resubstitution of this full-scale estimate of JCS (25 MPa) in equation 11.1 results in an improved estimate of JRC equal to 7.6. The final set of parameters for modelling full-scale shear stress-displacement, dilation, closure, etc. would be as follows:

$$JRC = 7.6, \qquad JCS = 25 \text{ MPa}, \qquad \phi_r = 23^\circ$$

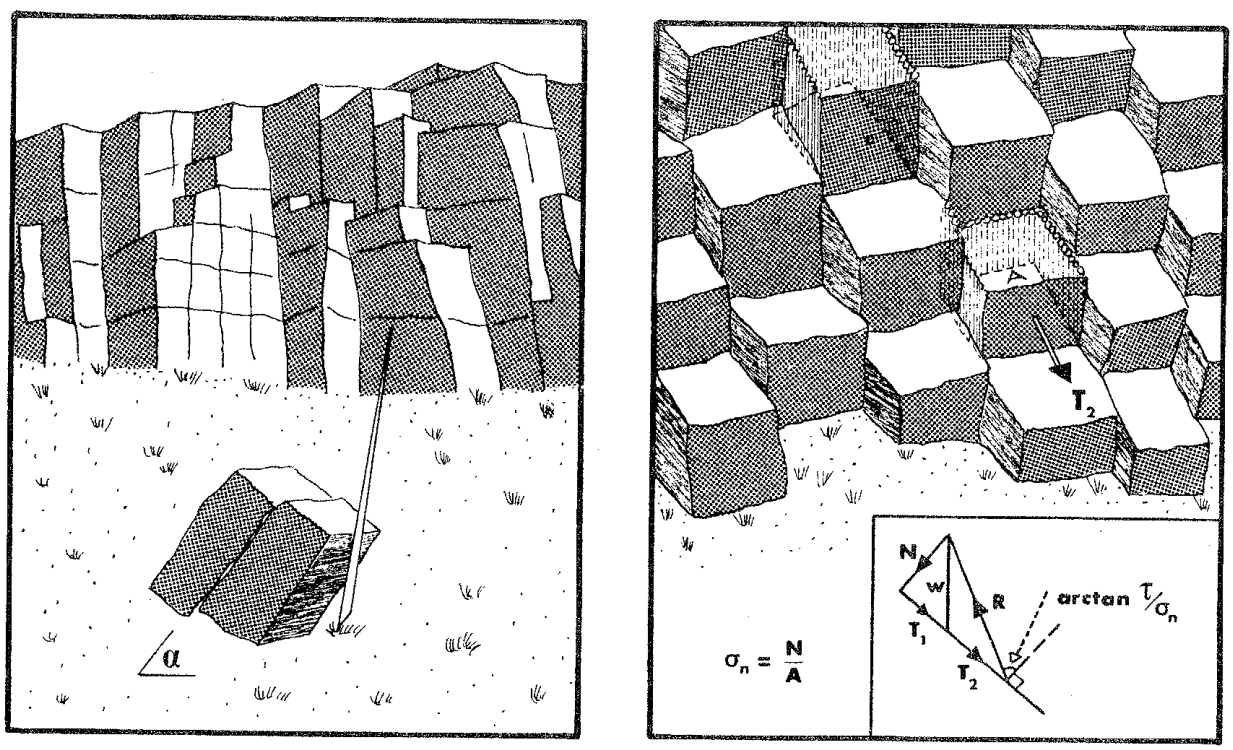

Figure 11.2 Inexpensive block tests for scale-free joint characterization, after Barton and Bandis (1980).

11.3 THE BLOCK PULL TEST

The pull-test arrangement illustrated in Figure 11.2 is appropriate to joint characterization in massive rock, where tilt testing would be impractical due to large natural block sizes, and/or where blocks have to be released by slot-drilling or wire-sawing. In this case, the relevant value of JRC is given by the following relation:

$$JRC = \frac{\arctan\left(\frac{T_1 + T_2}{N}\right)^0 - \phi_r^0}{\log_{10}(JCS.A/N)} \qquad \text{11.2}$$

where

A = the joint area

Example 2. Pull Test

Assume the following values have been measured and/or estimated:

N = 2 tons (normal component of self-weight of upper block, calculated)

T_1 = 1 ton (tangential component of self-weight)

T_2 = 1 ton (applied by means of hydraulic jack)

A = $1m^2$ (area of test surface)

ϕ_r = 24° (estimated using Schmidt hammer, see Barton and Choubey, 1977 for details)

$$JRC = \frac{\arctan\left(\frac{1 + 1}{2}\right)^0 - 24°}{\log_{10}(20/0.02)} = 7.0$$

In this example, the 1m length of joint ($L_n/L_o \approx 10$, Figure 4.6) suggests that JRC_o will again be approximately 10. Resubstitution of the full-scale estimate of JCS (10 MPa) in equation 11.2 results in an improved estimate of JRC equal to 7.8. The final set of parameters for modelling full-scale $\tau - \delta$, d_n, ΔV_j etc. would be as follows:

$$JRC = 7.8, \qquad JCS = 10 \text{ MPa}, \qquad \phi_r = 24°$$

12 CONCLUSIONS

1. The constitutive model of joint behavior described in this report provides realistic simulation of observed phenomena, and involves relatively inexpensive joint data acquisition.
2. Unlike several previous constitutive models, the effect of test sample size and natural block size are specifically addressed, so that size effects can be allowed for in a consistent manner.
3. The constitutive model is based on the acquisition of three key sets of parameters. These consist of the joint-roughness coefficient (JRC) obtained from self-weight tilt or pull tests, the joint wall compression strength (JCS) obtained from Schmidt hammer (and rock density) surveys, and the initial conducting aperture (e_o) of the joints in question, which can be estimated from the results of borehole pumping tests.
4. A key concept in developing realistic shear stress-displacement and dilation data is the mobilization of roughness up to JRC(peak) and its reduction post-peak. This allows consistent modelling of the complete dilation path under any stress level, and a realistic basis for calculating the change of permeability with shear displacement.
5. An important aspect of hydromechanical coupling is the experimental observation that conducting aperture (e) derived from the smooth parallel plate "cubic law", is often considerably smaller than the true mechanical aperture (E). Tortuosity and roughness in the flow path probably accounts for these differences. A constitutive model linking e, E and JRC has been developed.
6. Joint closure tests performed by Bandis (1980) provide an invaluable data base for modelling normal displacement phenomena. The simple hyper-

bolic closure and unloading curves are characterized by abscissa consisting of initial normal stiffness (K_{ni}) and maximum closure (V_m). Both these parameters can be estimated from the relevant values of JRC_o and JCS_o obtained from laboratory scale samples.

7. Evidence has been obtained that artificial tension fractures close under normal stress more readily than natural joints. However, a natural joint in gneis flow tested at high temperature indicated similar closure behavior to artificial tension fractures. Anisotropic contraction of the roughness profiles may be the reason for natural joints not closing under stress as readily as artificial tension fractures.

8. The fully coupled constitutive relationships linking the mechanical and hydraulic behavior of rock joints developed here need to be validated against ambient and elevated temperature hydromechanical tests before they can be used with confidence in modelling the complex response of a saturated rockmass to a slow thermal stress cycle.

REFERENCES

Bandis, S., 1980. "Experimental Studies of Scale Effects on Shear Strength, and Deformation of Rock Joints," Ph.D. Thesis, University of Leeds, Dept. of Earth Sciences.

Bandis, S., A.C. Lumsden, and N. Barton, 1981. "Experimental Studies of Scale Effects on the Shear Behavior of Rock Joints," Int. J. Rock Mech. Sci. and Geomech. Abstr., Vol. 18, pp. 1-21.

Barton, N., 1971. "A relationship Between Joint Roughness and Joint Shear Strength," Rock Fracture, Proceedings of an International Symposium on Rock Mechanics held in Nancy, France, Paper 1-8.

Barton, N., 1972. "A Model Study of Air Transport From Underground Openings Situated Below Ground Water Level," Percolation Through Fissured Rock, Proceedings of an International Symposium on Rock Mechanics held in Stuttgart, W. German, Paper T3-A, 20 p.

Barton, N., 1973. "Review of a New Shear Strength Criterion for Rock Joints," Engineering Geology, Vol. 7, pp. 287-332.

Barton, N., 1976a. "Unsupported Underground Excavations", Rock Mechanics Discussion Meeting, BeFo, held in Stockholm, Sweden, pp. 61-94.

Barton, N., 1976b. "The Shear Strength of Rock and Rock Joints," Int. J. Rock Mech. Min. Sci. and Geomech. Abstr., Vol. 13, pp. 255-279.

Barton, N., and V. Choubey, 1977. "The Shear Strength of Rock Joints in Theory and Practice," Rock Mechanics, Vol. 10, pp. 1-54.

Barton, N., and H. Hansteen, 1979. "Very large Span Openings at Shallow Depth: Deformation Magnitudes from Jointed Models and FE Analysis," Proceedings of Rapid Excavation and Tunneling Conference held in Atlanta, Georgia, Ch. 77, Vol. II, pp. 1331-1353.

Barton, N. and B. Kjaernsli, 1981. "Shear Strength of Rockfill," Journal of the Geotechnical Engineering Division, American Society of Civil Engineers, Vol. 107, No. GT7, Proc. Paper 16374, July, pp. 873-891.

Brace, W.F. and J.D. Byerlee, 1970. "California Earthquakes: Why Only Shallow Focus?", Science, 168, pp. 1573-1575.

Brace, W.F. and A.H. Jones, 1971. "Comparison of Uniaxial Deformation in Shock and Static Loading of Three Rocks", Journal of Geophysical Research, Vol. 76, No. 20, pp. 4913-4921.

Byerlee, J.D., 1968. "Brittle-Ductile Transition in Rocks, "Journal of Geophysical Research, Vol. 73, pp. 4741-4750.

Byerlee, J.D. and W.F. Brace, 1968. "Stick-Slip, Stable Sliding, and Earthquakes - Effect of Rock Type, Pressure, Strain Rate and Stiffness," Journal of Geophysical Research, Vol. 73, pp. 6031-6037.

Byerlee, J.D., 1978. "Friction in Rocks", Journal of Pure and Applied Geophysics, Vol. 116, pp. 615-626.

Celestino, T.B. and R. E. Goodman, 1979. "Path Dependency of Rough Joints in Bi-directional Shearing", Proceedings of 4th International Congress on Rock Mechanics, held in Montreux, Switzerland, Vol. 1, pp. 91-98.

Cundall, P., J. Marti, J. Beresford, P. Last and M. Asagian, 1978. "Computer Modelling of Jointed Rockmasses", Report prepared by Dames and Moore, London, for U.S. Army Engineer Waterways Experiment Station, Vicksburg, 396 p.

Dieterich, J.H., 1972. "Time-Dependent Friction in Rocks", Journal of Geophysical Research, Vol. 77, No. 20, pp. 3690-3697.

Enniss, D., S. Butters, C. McFarland and A. Jones, 1979. "Capabilities to Determine Rock Properties at Simulated Geothermal Conditions", Journal of Energy Resource Technology, Vol. 101, pp. 117-123.

Evdokimov, P.D., and D. D. Sapegin, 1967. "Stability, Shear and Sliding Resistance, and Deformation of Rock Foundations", Moscow, USSR, 1964. Israel Program for Scientific Translations, Jerusalem.

Goodman, R. E., 1970. "Deformability of Joints", Symposium, Determination of the In Situ Modulus of Deformation of Rock, American Society for Testing Materials, S.T.P. 477, pp. 174-196.

Goodman, R. E., 1974. "The Mechanical Properties of Joints," Proceedings of the 3rd International Congress on Rock Mechanics held in Denver, Colorado, Vol. 1, Part A, pp. 127-140.

Goodman, R. E., 1976. "Methods of Geological Engineering," West Publishing Company, 472 p.

Heard, H.C., 1970. "The Influence of Environment on the Inelastic Behavior of Rocks," Proceedings of Symposium on Engineering with Nuclear Explosives, Department of Commerce, Springfield, Virginia. Vol. 1, pp. 127-141, UCRL 72164.

Heimli, P., 1972. "Water and Air Leakage Through Joints in Rock Specimens" (in Norwegian), Fjellsprengningsteknikk, Bergmekanikk, Annual Rock Mechanics Meeting held in Oslo, Norway, pp. 137-142.

Hoskins, E. R., J.C. Jæger and K.J. Rosengren, 1968. "A Medium-Scale Direct Friction Experiment," Int. J. Rock Mech. Min, Sci. Vol. 5, pp. 143-154.

Infanti, N. and M. A. Kanji, 1978. "In Situ Shear Strength, Normal and Shear Stiffness Determinations at Agua Vermelha Project," Proceedings of 3rd International Congress of the International Association of Engineering Geologists, held in Madrid, Spain, Session 2. Vol. 2, pp. 175-183.

Iwai, K., 1976. "Fundamental Studies of Fluid Flow Through a Single Fracture," Ph.D. Thesis, University of California, Berkeley, 208 p.

Kranz, R. L., A.D. Frankel, T. Engelder, and C.H. Scholz, 1979. "The Permeability of Whole and Jointed Barre Granite," Int. J. Rock Mech. Min. Sci. and Geomech. Abstr., Vol. 16, pp. 225-234, and Erratum, Vol. 17, pp. 237-238.

Krsmanovic, D. and M. Popovic, 1966. "Large-Scale Field Tests of the Shear Strength of Limestone," Proceedings of the 1st International Congress on Rock Mechanics, held in Lisboa, Portugal, Vol. 1, pp. 773-779.

Kutter, H. K., 1974. "Results of Laboratory Direct Shear Tests on Four Rock Types," Rock Mechanics Research Report, No. 28, January 1974, Imperial College, London.

Link, H., 1969. "The Sliding Stability of Dams," Water Power, March, April, May 1969, Parts I, II and III.

Maini, T., 1971. "In Situ Hydraulic Parameters in Jointed Rock - Their Measurement and Interpretation," Ph.D. Thesis, Imperial College, London, 312 p.

Maini, T. and G. Hocking, 1977. "An Examination of the Feasibility of Hydrologic Isolation of a High Level Waste Repository in Crystalline Rock," Geologic Disposal of High-Level Radioactive Waste Session, Annual Meeting of the Geological Society of America, held in Seattle, Washington.

Martin, G. R. and P.J. Millar, 1974. "Joint Strength Characteristics of a Weathered Rock," Proceedings of the 3rd International Congress on Rock Mechanics, held in Denver, Colorado, Vol. 2A, pp. 263-270.

Nur, A., 1974. "Tectonophysics: The Study of Relations Between Deformation and Forces in the Earth," Proceedings of the 3rd International Congress on Rock Mechanics, held in Denver, Colorado, Vol. 1A, pp. 243-317.

Pratt, H.R., A.D. Black, and W.F. Brace, 1974. "Friction and Deformation of Jointed Quartz Diorite," Proceedings of the 3rd International Congress on Rock Mechanics, held in Denver, Colorado, Vol. 2A, pp. 306-310.

Pratt, H.R., H.S. Swolfs, W.F. Brace, A.D. Black and J.W. Handin, 1977. "Elastic and Transport Properties of an In Situ Jointed Granite," Int. J. Rock Mech. Min. Sci. and Geomech. Abstr., Vol. 14, pp. 35-45.

Snow, D.T., 1968. "Rock Fracture Spacings, Openings, and Porosities," Proceedings, American Society of Civil Engineers, Vol. 96, No. SM 1, pp. 73-91.

Stetsky, R.M., 1977. "Rock Friction-Effect of Confining Pressure, Temperature and Pore Pressure," Proceedings of 2nd Conference on Experimental Study of Rock Friction with Application to Earthquake Prediction, Geological Survey Open File Report, pp. 329-354.

Swan, G., 1981. "Tribology and the Characterization of Rock Joints," Proceedings of the 22nd U.S. Symposium on Rock Mechanics, held in Boston, Massachusetts, pp. 402-407.

Terra Tek, 1982. "A Heated, Flatjack Test Series to Measure the Thermomechanical and Transport Properties of In Situ Rock Masses ('Heated Block Test')", ONWI-260, prepared for Office of Nuclear Waste Isolation, Battelle Memorial Institute, Columbus, Ohio.

Tsang, Y.W. and P.A. Witherspoon, 1981. "Hydromechanical Behavior of a Deformable Rock Fracture Subject to Normal Stress," preprint of article accepted for publication in the Journal of Geophysical Research.

Wahi, K.K., B.C. Trent, D.E. Maxwell, R.M. Pyke, C. Young and D.M. Ross-Brown, 1980. "Numerical Simulations of Earthquake Effects on Tunnels for Generic Nuclear Waste Repositories," report prepared for the Savannah River Laboratory, Du Pont de Nemours and Co., DP-1579.

Walsh, J.B., 1981. "Effect of Pore Pressure and Confining Pressure on Fracture Permeability," preprint of article accepted for publication in the Journal of Geophysical Research.

Walsh, J.B. and M.A. Grosenbaugh, 1979. "A New Model for Analyzing the Effect of Fractures on Compressibility," Journal of Geophysical Research, Vol. 84, No. B7, pp. 3532-3536.

Weissbach, G. and H.K. Kutter, 1978. "The Influence of Stress and Strain History on the Shear Strength of Rock Joints," Proceedings of the 3rd International Congress of Engineering Geologists, held in Madrid, Spain, Vol. II, 2, pp. 88-94.

Witherspoon, P.A., C.H. Amick, and J.E. Gale, 1977. "Stress-Flow Behavior of a Fault Zone with Fluid Injection and Withdrawal," Mineral Engineering Report No. 77-1, University of California, Berkeley.

Witherspoon, P.A., J.S.Y Wang, K. Iwai and J.E. Gale, 1979. "Validity of Cubic Law for Fluid Flow in a Deformable Rock Fracture," Lawrence Berkeley Laboratory, LBL-9557, SAC-23,28 p.

Voegele, M., E. Hardin, D. Lingle, M. Board, and N. Barton, 1981. "Site Characterization of Joint Permeability Using the Heated Block Test," Proceedings of the 22nd U.S. Symposium on Rock Mechanics, held in Boston, Massachusetts, pp. 120-127.

DISTRIBUTION LIST

ACRES AMERICAN INC
A. S. BURGESS
R. STRUBLE
ALABAMA DEPT OF ENERGY
CAMERON MCDONALD
ALABAMA STATE GEOLOGICAL SURVEY
THORNTON L. NEATHERY
ALLIED GENERAL NUCLEAR SERVICES
P.F. HIGHBERGER
AMERICAN FRIENDS SERVICE COMMITTEE
WILLIAM REYNOLDS
AMERICAN NUCLEAR INSURERS
DOTTIE SHERMAN
ANALYTIC & COMPUTATIONAL RESEARCH INC
B. SAGAR
APPLIED MECHANICS INC
JOHN R. WILLIAMS
ARGONNE NATIONAL LABORATORY
REX COUTURE
KEVIN FLYNN
WYMAN HARRISON
J. HOWARD KITTEL
MARTIN SEITZ
MARTIN J. STEINDLER
ARINC RESEARCH CORP
H. P. HIMPLER
ARIZONA PUBLIC SERVICE COMMISSION
HENRY W. RILEY, JR.
ARIZONA STATE UNIVERSITY
PAUL KNAUTH
ARKANSAS GEOLOGICAL COMMISSION
WILLIAM V. BUSH
ARTHUR D. LITTLE INC
CHARLES R. HADLOCK
ATOMIC ENERGY CONTROL BOARD
J. L. WALLACH
ATOMIC ENERGY COUNCIL, ROC
KUO-YUEH LIU
ATOMIC ENERGY OF CANADA LTD
M.O. LUKE
ANN QUINN
F. P. SARGENT
ATOMIC ENERGY RESEARCH ESTABLISHMENT
P. J. BOURKE
R. L. NELSON
ATOMIC INDUSTRIAL FORUM INC
EMANUEL GORDON
AUSTRALIAN ATOMIC ENERGY COMMISSION
BABCOCK & WILCOX
INFORMATION SERVICES
BAKER, TOUHILL, SHUCKROW & ASSOCIATES INC
C. J. TOUHILL
BATTELLE COLUMBUS DIVISION
JOHN T. MCGINNIS
JEFFREY L. MEANS
STEPHEN NICOLOSI
THOMAS M. TRAINER
BECHTEL GROUP INC
THOMAS S. BAER
DON B. CRANDALL
D. S. DUNCAN
R. C. LOVINGTON
N. A. NORMAN
RICHARD J. TOSETTI
BENDIX FIELD ENGINEERING CORP
BILL GRAHAM
CHARLES A. JONES
JOHN C. PACER
BHABHA ATOMIC RESEARCH CENTRE
K. T. THOMAS
BLACK & VEATCH
M. JOHN ROBINSON
BRITISH NUCLEAR FUELS LTD
R. S. WILKS
BROOKHAVEN NATIONAL LABORATORY
GERALD BIDA
DONALD E. CLARK
M. S. DAVIS
SANDRA G. LANE
P. W. LEVY
PETER SOO
HELEN TODOSOW (2)
BUNDESANSTALT FUR GEOWISSENSCHAFTEN UND ROHSTOFFE
MICHAEL LANGER
HELMUT VENZLAFF
BUNDESMINISTERIUM FUR FORSCHUNG
ROLF-PETER RANDL
BUREAU DE RECHERCHES GEOLOGIQUES ET MINIERES
BERNARD D. FEUGA
PIERRE F. PEAUDECERF
BURNS AND ROE INDUSTRIAL SERVICES CORP
JOHN PIRRO
C.R. WATTS ASSOCIATES
CURTIS WATTS
CALIFORNIA DEPT OF CONSERVATION
PERRY AMIMITO
CALIFORNIA INSTITUTE OF TECHNOLOGY
LEON T. SILVER
CAMBOURNE SCHOOL OF MINES
TREVENSON, POOL, REDRUTH
CAMP, DRESSER, AND MCKEE INC
WATER RESOURCES DIVISION
DAVID A. WOODRUFF
CANADIAN DEPT OF ENERGY, MINES AND RESOURCES
A. S. JUDGE
CANYONLANDS NATIONAL PARK
PETER L. PARRY
CAPITAL AREA GROUND WATER CONSERVATION COMMISSION
A. N. TURCAN JR.
CAPITAL UNIVERSITY
VICTOR M. SHOWALTER
CARNEGIE-MELLON UNIVERSITY
STEPHEN G. ZEMBA
CASTUS VALLEY ORCHARDS
CARL ANDERSON
CAYUGA LAKE CONSERVATION ASSOCIATION INC
D. S. KIEFER
CENTRAL WASHINGTON UNIVERSITY
J.R. HINTHORNE
CENTRE D ETUDE DE L ENERGIE NUCLEAIRE
RENE HEREMANS
CENTRE D'INFORMATIQUE GEOLOGIQUE
GHISLAIN DE MARSILY
CGS INC
E. DONALD MCKAY, III
CHALMERS UNIVERSITY OF TECHNOLOGY
BERT ALLARD
CITIZENS ASSOCIATION FOR SOUND ENERGY
JUANITA ELLIS
COLORADO GEOLOGICAL SURVEY
JOHN W. ROLD
COLORADO SCHOOL OF MINES
W. HUSTRULID
COLUMBIA UNIVERSITY
HUBERT STAUDIGEL
CONSERVATION COUNCIL OF NORTH CAROLINA
JANE SHARP
CONSOIL ASSOCIATES
DAVID A. LEE
CORNELL UNIVERSITY
JOHN BIRD
ARTHUR L. BLOOM
DUANE CHAPMAN
FRED H. KULHAWY
ROBERT POHL
CORTLAND COUNTY HEALTH DEPT
J. V. FEUSS
COUNCIL ON ECONOMIC PRIORITIES
MARVIN RESNIKOFF
D.R.E.
KARL J. ANANIA
DALTON, DALTON & NEWPORT
MARIA R. EIGERMAN
STEVE NACHT
DAMES & MOORE
PETER CONROY
RON KEAR
CHARLES R. LEWIS
O. L. OZTUNOLI
DAPPOLONIA CONSULTING ENGINEERS INC
LISA K. DONOHUE
ABBY FORREST
AMIRA HAMDY
JO JANET D. HOLCOMB
PETER C. KELSALL
CARL E. SCHUBERT
DELAWARE CUSTOM MATERIEL INC
HOWARD NOVITCH
DEPT OF THE ENVIRONMENT
F. S. FEATES
DIVISION OF ENVIRONMENTAL SAFETY RESEARCH
HARUTO NAKAMURA
DRAVO ENGINEERS AND CONSTRUCTORS
KEN BEALL
DUKE UNIVERSITY
THOMAS DAVIS
DUNN GEOSCIENCE CORP
WM E. CUTCLIFFE
DYNATECH R/D COMPANY
STEPHEN E. SMITH
E.I. DU PONT DE NEMOURS & COMPANY
DONALD E. GORDON
E.L.H. PUBLICATIONS - THE RADIOACTIVE EXCHANGE
EDWARD L. HELMINSKI
E.R. JOHNSON ASSOCIATES INC
E. R. JOHNSON
G.L. JOHNSON
EARTH RESOURCE ASSOCIATES INC
SERGE GONZALES
EARTH SCIENCE AND ENGINEERING INC
LOU BLANCK
EARTH SCIENCES CONSULTANTS INC
HARRY L. CROUSE
EBASCO SERVICES INC
ZUBAIR SALEEM
RAYMOND H. SHUM
ECOLOGY CENTER OF LOUISIANA
ROSS VINCENT
EDISON ELECTRIC INSTITUTE
R. E. L. STANFORD

EDS NUCLEAR INC
C. SUNDARARAJAN
EG & G IDAHO INC
M. D. MCCORMACK
RICHARD FALLMAN
ELECTROWATT ENGINEERING SERVICE
H. N. PATAK
ELSAM
A. V. JOSHI
ARNE PEDERSEN
EMBASSY OF THE UNITED STATES
MAUD LI HAIJLEN-RYLANDER
ENERCOR INC
JOHN RODOSEVICH
ENERGY FUELS NUCLEAR INC
DON M. PILLMORE
ENERGY INC
ENERGY RESEARCH GROUP INC
MARC GOLDSMITH
ENVIRONMENT CANADA
CLAUDE BARRAUD
ENVIRONMENTAL POLICY INSTITUTE
DAVID M. BERICK
ENVIRONMENTAL RESEARCH GROUP INC
PETER G. COLLINS
ENVIROSPHERE COMPANY
ROGER G. ANDERSON
BOB HAINES
ERIE COUNTY ENVIRONMENTAL MANAGEMENT COUNCIL
JOAN P. SCHMIDT
ERTEC WESTERN INC
J. CARL STEPP
MATT WERNER
EXXON PRODUCTION RESEARCH
GARY WAYMIRE
F.B.A.B.
OTTO BROZEN
F.M. FOX AND ASSOCIATES INC
MIKE E. BRAZIE
FENIX AND SCISSON INC
PATRICIA A. BOLLING
FLORIDA DEPT OF ENVIRONMENTAL REGULATION
HAMILTON OVEN
FLORIDA INSTITUTE OF TECHNOLOGY
JOSEPH A. ANGELO, JR.
FLUOR ADVANCED TECHNOLOGY DIVISION
JOAN V. MCCURRY
FLUOR ENGINEERS & CONSTRUCTORS INC
RAYMOND J. DUGAL
VINCENT J. KAVLICK
FORD, BACON & DAVIS UTAH INC
PRESTON H. HUNTER
FOSTER-MILLER ASSOCIATES INC
NORBERT PAAS
FREESTONE COUNTY COURTHOUSE
SAM BOURNIAS
FREIE UNIVERSITAET BERLIN
HANSKARL BRUEHL
FRIENDS OF THE EARTH
LOUIS BUCKLIN
GARTNER LEE ASSOCIATES LTD
ROBERT E. J. LEECH
GENERAL ATOMIC COMPANY
ROBERT J. CAMPANA
H. C. CARNEY
MICHAEL STAMATELATOS
GEO/RESOURCE CONSULTANTS INC
ALVIN K. JOE, JR.
GEOLOGICAL SURVEY OF IRELAND
MICHAEL D. MAX
GEOLOGICAL SURVEY OF NORWAY
SIGURD HUSEBY
GEOLOGICAL SURVEY OF SWEDEN (SGU)
KAJ AHLBOM
LEIF CARLSSON
GEORESULTS INC
DAVID SNOW
GEORGETOWN CONSULTING GROUP
SUSAN SHALAGAN
GEORGIA INSTITUTE OF TECHNOLOGY
MELVIN W. CARTER
GEOFFREY G. EICHHOLZ
ALFRED SCHNEIDER
CHARLES E. WEAVER
GEOTECHNICAL ENGINEERS INC
RICHARD W. TURNBULL
GEOTHERMAL ENERGY INSTITUTE
DONALD F. X. FINN
GEOTRONS
JAMES MERCER
GERMANTOWN FRIENDS SCHOOL
HERB BASSOW
GESELLSCHAFT F. STRAHLEN U. UMWELTFORSCHUNG M.B.H.
WOLFGANG BODE
HERMANN GIES
HANS W. LEVI
H. MOSER
GIBBS & HILL INC
ROBERT PRIETO
GILBERT/COMMONWEALTH
JERRY L. ELLIS
GOLDER ASSOCIATES
ELIZABETH EISENHOOD
LAWRENCE A. WHITE
GRIMCO
DONALD H. KUPFER
GRUY COMPANIES
NED TILLMAN
GTC GEOLOGIC TESTING CONSULTANTS LTD
JOHN F. PICKENS
GULF MINERAL RESOURCES
THOMAS R. SCOTESE
H & R TECHNICAL ASSOCIATES INC
WILLIAM R. RHYNE
H-TECH LABORATORIES INC
BRUCE HARTENBAUM
HAHN-MEITNER-INSTITUT FUR KERNFORSCHUNG BERLIN
KLAUS ECKART MAASS
HALEY AND ALDRICH INC
JAMES R. LAMBRECHTS
HANFORD ENGINEERING DEVELOPMENT LABORATORY
ROBERT EINZIGER
R. L. KNECHT
JOHN MACLAREN
HARDING LAWSON ASSOCIATES
FRANK C. KRESSE
HARVARD UNIVERSITY
CHARLES W. BURNHAM
DADE W. MOELLER
RAYMOND SIEVER
HDR SCIENCES
MARY S. MORAN
HIRAM COLLEGE
JAMES W. COWDEN
HOUGH-NORWOOD HEALTH CARE CENTER
GEORGE H. BROWN, M.D.
IDAHO BUREAU OF MINES AND GEOLOGY
EARL H. BENNETT
CHARLES R. KNOWLES
IDAHO DEPT OF HEALTH AND WELFARE
ROBERT D. FUNDERBURG
ILLINOIS STATE GEOLOGICAL SURVEY
KEROS CARTWRIGHT
IMPERIAL COLLEGE OF SCIENCE AND TECHNOLOGY
B. K. ATKINSON
INDIANA GEOLOGICAL SURVEY
MAURICE BIGGS
INDIANA UNIVERSITY
HAYDN H. MURRAY
CHARLES J. VITALIANO
INSTITUT FUR TIEFLAGERUNG
KLAUS KUHN
E. R. SOLTER
PETER UERPMANN
INSTITUTE FOR CHEMICAL TECHNOLOGY
REINHARD ODOJ
INSTITUTE OF GEOLOGICAL SCIENCES
NEIL A. CHAPMAN
STEPHEN THOMAS HORSEMAN
INSTITUTE OF RADIATION PROTECTION
KAI JAKOBSSON
INTERA ENVIRONMENTAL CONSULTANTS INC
F. J. PEARSON, JR.
ROBERT WILEMS
INTERA ENVIRONMENTAL CONSULTANTS LTD
T. CHAN
INTERNATIONAL ATOMIC ENERGY AGENCY
EVERETT R. IRISH
INTERNATIONAL ENERGY ASSOCIATES LTD
BLYTHE K. LYONS
INTERNATIONAL ENGINEERING COMPANY INC
TERRY L. STEINBORN
MAX ZASLAWSKY
INTERNATIONAL RESEARCH AND EVALUATION
R. DANFORD
INTERNATIONAL SALT COMPANY
LEWIS P. BUSH
IOWA GEOLOGICAL SURVEY
DONALD L. KOCH
IOWA STATE COMMERCE COMMISSION
ROBERT J. BUCKLEY
IOWA STATE UNIVERSITY
MARTIN C. EDELSON
IRT CORP
J. STOKES
ISTITUTO SPERIMENTALE MODELLI E STRUTTURE S.P.A.
F. GERA
J.F.T. AGAPITO & ASSOCIATES INC
MICHAEL P. HARDY
JACKSON STATE UNIVERSITY
ESTUS SMITH
JACOBY AND COMPANY
CHARLES H. JACOBY
JAPAN ATOMIC ENERGY RESEARCH INSTITUTE
TARO ITO
JAY L. SMITH COMPANY INC
JAY L. SMITH
JGC CORPORATION
MASAHIKO MAKINO
JOHNS HOPKINS UNIVERSITY
JARED L. COHON
KENNETH N. WEAVER
JOINT RESEARCH CENTRE
GIRARDI FRANCESCO
JORDAN GORRILL ASSOCIATES
JOHN D. TEWHEY

KAISER ENGINEERS INC
W. J. DODSON
J. S. RITCHIE
KALAMAZOO COLLEGE
RALPH M. DEAL
KANSAS DEPT OF HEALTH AND ENVIRONMENT
GERALD W. ALLEN
KANSAS STATE GEOLOGICAL SURVEY
WILLIAM W. HAMBLETON
KBS
LARS B. NILSSON
KELLER WREATH ASSOCIATES
FRANK WREATH
KERNFORSCHUNGSZENTRUM KARLSRUHE GMBH
K. D. CLOSS
KIHN ASSOCIATES
HARRY KIHN
KLOHN LEONOFF LTD
CRAIG FORSTER
KOREA INSTITUTE OF ENERGY AND RESOURCES (KIER)
CHONG SU KIM
LACHEL HANSEN & ASSOCIATES INC
DOUGLAS E. HANSEN
LAKE MICHIGAN FEDERATION
JANE SCHAEFER
LANCASTER AVENUE LIBRARY
F.M. CALVARESI
LAWRENCE BERKELEY LABORATORY
JOHN A. APPS
THOMAS DOE
NORMAN M. EDELSTEIN
ORAH GOLDMAN
BRIAN KANEHIRO
S. KLAINER
E. MAJER
ROBIN SPENCER
J. WANG
HAROLD WOLLENBERG
LAWRENCE LIVERMORE NATIONAL LABORATORY
LYNDEN B. BALLOU
JOHN H. CAMPBELL
HUGH HEARD
FRANCOIS E. HEUZE
DANA ISHERWOOD
R. CARROLL MANINGER
PAUL L. PHELPS
LAWRENCE D. RAMSPOTT (2)
FRANK ROGUE
R. N. SCHOCK
W. G. SUTCLIFFE
TECHNICAL INFORMATION DEPARTMENT L-53
DALE G. WILDER
LOS ALAMOS NATIONAL LABORATORY
DONALD W. BROWN
ERNEST A. BRYANT
GEORGE A. COWAN
BRUCE R. ERDAL
WAYNE R. HANSEN
L. E. LANHAM
DONALD T. OAKLEY
ROBERT E. RIECKER
JOE SMYTH
JOHN T. WHETTEN
KURT WOLFSBERG
LOS ALAMOS TECHNICAL ASSOCIATES INC
R. J. KINGSBURY
LOUISIANA DEPT OF NATURAL RESOURCES
B. JIM PORTER
LOUISIANA DEPT OF TRANSPORTATION & DEVELOPMENT
GEORGE H. CRAMER, II
LOUISIANA GEOLOGICAL SURVEY
CHARLES S. GROAT
LEE W. JENNINGS
LOUISIANA NUCLEAR ENERGY DIVISION
L. HALL BOHLINGER (3)
LOUISIANA STATE UNIVERSITY
ROBERT L. THOMS
LOUISIANA TECH UNIVERSITY
LIBRARY
NORMAN WITRIAL
LOWENSTEIN, NEWMAN, REIS & AXELRAD
MICHAEL A. BAUSER
MACLAREN PLANSEARCH INC
ALEX BUCHNEA
MAINE BUREAU OF HEALTH
DONALD C. HOXIE
MAINE GEOLOGICAL SURVEY
WALTER ANDERSON
MARQUETTE UNIVERSITY
DOUGLAS H. GREENLEE
MASSACHUSETTS INSTITUTE OF TECHNOLOGY
JOHN DEUTCH
TED GREENWOOD
RICHARD K. LESTER
MARSHA LEVINE
MCMASTER UNIVERSITY
L. W. SHEMILT
MECHANICAL TECHNOLOGY INC
WARREN BESSLER
MELLEN GEOLOGICAL ASSOCIATES INC
FREDERIC F. MELLEN
MEMBERS OF THE GENERAL PUBLIC
MORRIS A. BALDERMAN
W. VON BLACK
DAVID H. BOLTZ
JAMES BOYD
LARRY BRADLEY
WILLIAM V. CONN
D.P. DAUTOVICH
DANNELLE D. DUDEK
FRANCES FARLEY
DOROTHY FORD
RICHARD L. FOUKE
STEVE FRISHMAN
JOHN H. GERVERS
CARL A. GIESE
SHIRLEY M. GIFFORD
DARYL GLAMANN
OSWALD H. GREAGER
C. F. HAJEK
HAROLD L. JAMES
KENNETH S. JOHNSON
THOMAS H. LANGEVIN
GRANT W. LAPIER
TERRY R. LASH
HARRY E. LEGRAND
DAVID LYLE
MAX MCDOWELL
JAMES B. MUCKERHEIDE
ALAN D. PASTERNAK
SHAILER S. PHILBRICK
ROGER E. POWERS
MARTIN RATHKE
CHRIS RICH
GUNTHER SCHWARZ
JERRY SHEPPARD
M. J. SZULINSKI
ROBERT WEESE
JIMMY L. WHITE
MICHIGAN DEPT OF NATURAL RESOURCES
R. THOMAS SEGALL
MICHIGAN DEPT OF PUBLIC HEALTH
DON VAN FAROWE
MICHIGAN DISTRICT HEALTH DEPT NO 4
EDGAR KREFT
MICHIGAN GEOLOGICAL SURVEY
ROBERT C. REED
MICHIGAN GOVERNORS OFFICE
WILLIAM C. TAYLOR
MICHIGAN TECHNOLOGICAL UNIVERSITY
GARY L. DOWNEY
MINISTRY OF THE ENVIRONMENT
JAAK VIIRLAND
MINNESOTA GEOLOGICAL SURVEY
MATT S. WALTON
MINNESOTA STATE ENERGY AGENCY
MISSISSIPPI ATTORNEY GENERALS OFFICE
MACK CAMERON
MISSISSIPPI BUREAU OF GEOLOGY
MICHAEL B. E. BOGRAD
MISSISSIPPI CITIZENS AGAINST NUCLEAR DISPOSAL
STANLEY DEAN FLINT
MISSISSIPPI DEPT OF ENERGY AND TRANSPORTATION
JOHN W. GREEN (3)
MISSISSIPPI DEPT OF NATURAL RESOURCES
ALVIN R. BICKER, JR.
CHARLES L. BLALOCK
CURTIS W. STOVER
MISSISSIPPI DEPT OF WILDLIFE CONSERVATION
JOSEPH W. JACOB, JR.
MISSISSIPPI EMERGENCY MANAGEMENT AGENCY
JAMES E. MAHER
MISSISSIPPI MINERAL RESOURCES INSTITUTE
MISSISSIPPI POWER & LIGHT
ROBERT SHADDIX
MISSISSIPPI STATE BOARD OF HEALTH
EDDIE S. FUENTE
J. WARREN GREEN
MISSISSIPPI STATE HOUSE OF REPRESENTATIVES
E. FRED DOBBINS
JERRY OKEEFE
MITRE CORP
LESTER A. ETTLINGER
MONTANA BUREAU OF MINES AND GEOLOGY
S. L. GROFF
MORRISON-KNUDSEN COMPANY INC
SERGI KAMINSKY
NASA JOHNSON SPACE CENTER
MICHAEL R. HELFERT
NATIONAL ACADEMY OF SCIENCES
JOHN T. HOLLOWAY
PETER B. MYERS
NATIONAL AERONAUTICS AND SPACE ADMINISTRATION - HEADQUARTERS
PHILIP R. COMPTON
NATIONAL ATOMIC MUSEUM
GWEN SCHREINER
NATIONAL BOARD FOR SPENT NUCLEAR FUEL, KARNBRANSLENAMDEN
NILS RYDELL
NATIONAL BUREAU OF STANDARDS
RILEY M. CHUNG
LEWIS H. GEVANTMAN
WILLIAM P. REED

NATIONAL HYDROLOGY RESEARCH INSTITUTE
DENNIS J. BOTTOMLEY
NATIONAL OCEANOGRAPHIC AND ATMOSPHERIC ADMINISTRATION
ALEXANDER MALAHOFF
NATIONALE GENOSSENSCHAFT FUR DIE LAGERUNG RADIOAKTIVER ABFALLE
MARLIES KUHN
NATURAL RESOURCES DEFENSE COUNCIL
THOMAS B. COCHRAN
NEVADA DEPT OF ENERGY
ROBERT R. LOUX
NEW ENGLAND NUCLEAR CORP
KERRY BENNERT
CHARLES B. KILLIAN
NEW JERSEY DEPT OF ENVIRONMENTAL PROTECTION
JEANETTE ENG
NEW MEXICO BUREAU OF MINES AND MINERAL RESOURCES
FRANK E. KOTTLOWSKI
NEW MEXICO ENVIRONMENTAL EVALUATION GROUP
ROBERT H. NEILL
NEW YORK DEPT OF HEALTH
DAVID AXELROD,M.D.
NEW YORK STATE ATTORNEY GENERALS OFFICE
EZRA I. BIALIK
NEW YORK STATE ENERGY OFFICE
JOHN P. SPATH (15)
NEW YORK STATE ERDA
JOHN C. DEMPSEY
NEW YORK STATE GEOLOGICAL SURVEY
ROBERT H. FAKUNDINY
ROBERT H. FICKIES
NEW YORK STATE PUBLIC SERVICE COMMISSION
FRED HAAG
NIEDERSACHSISCHES SOZIALMINISTERIUM
HORST SCHNEIDER
NORTH CAROLINA DEPT OF NATURAL RESOURCES & COMMUNITY DEVELOPMENT
STEPHEN G. CONRAD
NORTH CAROLINA STATE UNIVERSITY
M. KIMBERLEY
NORTHEAST FOUR COUNTY REGIONAL PLANNING & DEVELOPMENT ORGANIZATION
JOHN C. PIERSON
NTR GOVERNMENT SERVICES
THOMAS V. REYNOLDS
NUCLEAR ASSURANCE CORP
ANDREW J. FRANKEL
RHONNIE L. SMITH
NUCLEAR INFORMATION AND RESOURCE SERVICE
GARY HZKOWITZ
NUCLEAR SAFETY ASSOCIATES INC
JOSEPH A. LIEBERMAN
NUCLEAR SAFETY RESEARCH ASSOCIATION
KAZUMORI MATSUO
NUCLEAR WASTE WATCHERS
HELEN LETARTE
NUS CORP
W. G. BELTER
JOSEPH J. DINUNNO
BARRY N. NAFT
DOUGLAS D. ORVIS
DOUGLAS W. TONKAY
OAK RIDGE NATIONAL LABORATORY
J. O. BLOMEKE
H. C. CLAIBORNE
ALLEN G. CROFF
LESLIE R. DOLE
JOHN T. ENSMINGER
CATHY S. FORE
DAVID C. KOCHER
ARTHUR J. SHOR
ELLEN D. SMITH
E. G. ST. CLAIR
OFFICE OF NWTS INTEGRATION
ROBERT E. HEINEMAN
OHIO DEPT OF NATURAL RESOURCES
SCOTT KEIL
OHIO ENVIRONMENTAL COUNCIL
STEPHEN H. SEDAM
OHIO STATE UNIVERSITY
R. N. CHRISTENSEN
A. T. CONLISK
M. A. CORNWELL
OKLAHOMA GEOLOGICAL SURVEY
CHARLES J. MANKIN
ONTARIO HYDRO
R. W. BARNES
C. F. LEE
CRAIG J. SIMPSON
OPEN EARTH
PETER J. SMITH
ORANGE COUNTY COMMUNITY COLLEGE
LAWRENCE E. OBRIEN
OREGON DEPT OF ENERGY
MICHAEL W. GRAINEY
OREGON STATE UNIVERSITY
U. C. RINGLE
ORGANIZATION FOR ECONOMIC COOPERATION AND DEVELOPMENT
J. P. OLIVIER
PACIFIC GAS AND ELECTRIC COMPANY
ADRIAN C. SMITH, JR
PACIFIC NORTHWEST LABORATORY
DON J. BRADLEY
H. C. BURKHOLDER
L. L. CLARK
JOHN P. CORLEY
HARVEY DOVE
FLOYD N. HODGES
J. H. JARRETT
MAX R. KREITER
DONALD E. LARSON
ROBERT MCCALLUM
J. M. RUSIN
E. C. WATSON
R. E. WESTERMAN
PARSONS, BRINCKERHOFF, QUADE, & DOUGLAS, INC.
T. R. KUESEL
PB-KBB INC
DILIP K. PAUL
MARK E. STEINER
PENBERTHY ELECTROMELT INTERNATIONAL INC.
LARRY PENBERTHY
PENNSYLVANIA GEOLOGICAL SURVEY
ARTHUR A. SOCOLOW
PENNSYLVANIA STATE UNIVERSITY
MICHAEL GRUTZECK
GERALD L. PALAU
DELLA M. ROY
PERMIAN BASIN REGIONAL PLANNING COMMISSION
E. W. CRAWFORD
PERRY COUNTY BOARD OF SUPERVISORS
PAUL D. JOHNSTON,SR
PERRY COUNTY SCHOOLS
MANIEL A. COCHRAN
PHYSIKALISCH-TECHNISCHE BUNDESANSTALT
PETER BRENNECKE
PINCOCK, ALLEN & HOLT INC
LUTZ KUNZE
PORTLAND GENERAL ELECTRIC
J. W. LENTSCH
POTASH CORP OF SASKATCHEWAN
GRAEME G. STRATHDEE
POWER AUTHORITY OF THE STATE OF NEW YORK
MYRON M. KACZMARSKY
POWER REACTOR AND NUCLEAR FUEL DEVELOPMENT CORPORATION
PRESQUE ISLE COURTHOUSE
PRINCETON UNIVERSITY
PETER MONTAGUE
PUBLIC LAW UTILITIES GROUP
DORIS FALKENHEINER
PUBLIC SERVICE INDIANA
ROBERT S. WEGENG
QUADREX CORP
FRANCIS J. KENESHEA
R & M CONSULTANTS INC
ROBERT SYDNOR
RADIATION PROTECTION COUNCIL
TERI L. VIERIMA
RALPH M. PARSONS COMPANY
JERROLD A. HAGEL
RE/SPEC INC
GARY D. CALLAHAN
PAUL F. GNIRK
WILLIAM C. MCCLAIN
RENSSELAER POLYTECHNIC INSTITUTE
JAMES WU
RICHTON CITY HALL
R. RAHAIM
RISO NATIONAL LABORATORY
LARS CARLSEN
ROCKWELL HANFORD OPERATIONS
RONALD C. ARNETT
HARRY BABAD
R. A. DEJU
GEORGE C. EVANS (2)
R. J. GIMERA
KUNSOO KIM
KARL M. LA RUE
ROCKWELL INTERNATIONAL
MICHAEL J. SMITH
NORMAN A. STEGER
K. THIRUMALAI
DAVE A. TURNER
ROCKWELL INTERNATIONAL ENERGY SYSTEMS GROUP
W. S. BENNETT
HOWARD L. RECHT
LAWRENCE J. SMITH
ROGERS & ASSOCIATES ENGINEERING CORP
ARTHUR SUTHERLAND
ROYAL INSTITUTE OF TECHNOLOGY
IVARS NERETNIEKS
ROGER THUNVIK
S.E. LOGAN & ASSOCIATES INC
STANLEY E. LOGAN
S.M. STOLLER CORP
ROBERT W. KUPP
SAN DIEGO GAS & ELECTRIC COMPANY
LOUIS BERNATH
SAN JOSE STATE UNIVERSITY SCHOOL OF ENGINEERING
R. N. ANDERSON
SANCANA INC.
RALPH L. HOPKINS

SANDIA NATIONAL LABORATORIES
G. C. ALLEN
SHARLA BERTRAM
JOE A. FERNANDEZ
THOMAS O. HUNTER
J. KEITH JOHNSTONE
O. E. JONES
LIBRARY
R. L. LINK
R. W. LYNCH
RUDOLPH V. MATALUCCI
ANTHONY MULLER
RICHARD E. PEPPING
G. F. RUDOLFO
ALLAN R. SATTLER
LEO W. SCULLY
SCOTT SINNOCK
A. W. SNYDER
A. E. STEPHENSON
DANIEL M. TALBERT
LYNN D. TYLER
WOLFGANG WAWERSIK
WENDELL D. WEART
WIPP CENTRAL FILES
SANTA FE INTERNATIONAL
ROBERT J. PLISKA
SAVANNAH RIVER LABORATORY
E. J. HENNELLY
CAROL JANTZEN
J. WENDELL MARINE
WILLIAM R. MCDONELL
S. W. OREAR SR
DONALD ORTH
S. V. TOPP
SCIENCE APPLICATIONS INC
A. A. BAKR
JERRY J. COHEN
J. DONALD DIXON
RALPH FULLWOOD
JAMES E. HAMMELMAN
RONALD HOFMANN
J. ROBERT LARIVIERE
DAVID H. LESTER
PETER E. MCGRATH
JOHN E. MOSIER
HOWARD PRATT
M. D. VOEGELE
KRISHAN K. WAHI
ROBERT A. YODER
HOMER YOOK
SCRIPPS INSTITUTE OF OCEANOGRAPHY
EDWARD WINTERER
SENECA COUNTY PLANNING BOARD
SHANNON & WILSON INC
HARVEY W. PARKER
SHIMIZU CONSTRUCTION COMPANY LTD
TAKASHI ISHII
JUN SHIMADA
SIERRA CLUB - MISSISSIPPI CHAPTER
SIERRA CLUB - RADIOACTIVE WASTE CAMPAIGN
LISA FINALDI
MINA HAMILTON
SIERRA GEOPHYSICS INC
STEPHEN L. GILLETT
SNAKE RIVER ALLIANCE
TIM MCNEIL
SOUTH CAROLINA GEOLOGICAL SURVEY
NORMAN K. OLSON
SOUTH DAKOTA GEOLOGICAL SURVEY
RICHARD BRETZ
SOUTH DAKOTA OFFICE OF ENERGY POLICY
STEVEN M. WEGMAN
SOUTHWEST RESEARCH AND INFORMATION CENTER
DON HANCOCK
ALISON P. MONROE
ST BONAVENTURE UNIVERSITY
CARL J. TWAROG
ST JOSEPH COLLEGE
CLAIRE MARKHAM
ST MARTIN HIGH SCHOOL
RAYMOND J. WERTHNER
STANFORD UNIVERSITY
KONRAD B. KRAUSKOPF
GEORGE A. PARKS
IRWIN REMSON
STEARNS-ROGER SERVICES INC
VERYL ESCHEN
STONE & WEBSTER ENGINEERING CORP
J. PECK
A. PORT
EVERETT N. WASHER
STUDIO GEOLOGICO FOMAR
A. MARTORANA
STUDSVIK ENERGITEKNIK AB
AKE HULTGREN
ROLF SJOBLOM
SUMMIT COUNTY ENVIRONMENTAL SERVICES
JAMES T. KING
SWISS FEDERAL OFFICE OF ENERGY
U. NIEDERER
SYRACUSE UNIVERSITY
STEPHEN S. BRIGGS
SYSTEMS SCIENCE AND SOFTWARE
PETER LAGUS
T.M. GATES INC
TODD M. GATES
T.T.I. ENGINEERING CORP
DONALD C. TONIKA
TECHNICAL INFORMATION PROJECT
DONALD PAY
TECHNICAL RESEARCH CENTRE OF FINLAND
OLLI J. HEINONEN
SILJA RUMMUKAINEN
KARI SAARI
SEPPO VUORI
TEKNEKRON RESEARCH INC
ANTHONY F. MOSCATI
TERRA TEK INC
NICK BARTON
RICHARD LINGLE
TEXAS A&M UNIVERSITY
JOHN HANDIN
STEVE MURDOCK
JAMES E. RUSSELL
TEXAS BUREAU OF RADIATION CONTROL
DONALD G. ANDERSON
TEXAS DEPT OF HEALTH
DAVID K. LACKER
TEXAS DEPT OF WATER RESOURCES
C. R. BASKIN
TEXAS ENERGY & NATURAL RESOURCES ADVISORY COUNCIL
TERRY BARRON
MILTON L. HOLLOWAY (5)
CAROL KING
ROBERT D. SMITH
TEXAS HOUSE OF REPRESENTATIVES
BRINCK KERR
TEXAS STATE REPRESENTATIVE
PETE LANEY
THE ANALYTIC SCIENCES CORP
JOHN W. BARTLETT
CHARLES M. KOPLIK
THE CHRONICLE
CHRIS BRAITHWAITE
THE CLARION-LEDGER
MARK SCHLEIFSTEIN
THOMSEN ASSOCIATES
C. T. GAYNOR, II
TRENDS PUBLISHING INC
TRINITY EPISCOPAL CHURCH
BENJAMIN F. BELL
TRW INC
PETER ALEXANDER
E. R. CHRISTIE
TUN ISMAIL ATOMIC RESEARCH CENTRE
PUSPATI LIBRARY
TVO POWER COMPANY
VEIJO RYHANEN
U.H.D.E.
FRANK STEINBRUNN
U.K. DEPT. OF THE ENVIRONMENT
RADIOACTIVE WASTE MANAGEMENT DIVISION
U.S. ARMY CORPS OF ENGINEERS
DON BANKS
KATHARINE MATHER
U.S. ARMY CORPS OF ENGINEERS, MX PROGRAM AGENCY
JOHN BOWMAN, JR.
U.S. BUREAU OF LAND MANAGEMENT
LYNN JACKSON
MARY PLUMB
EDWARD R. SCHERICK
GREGORY F. THAYN
U.S. BUREAU OF MINES
GEORGE E. NIEWIADOMSKI
U.S. DEPT OF COMMERCE
PETER A. RONA
U.S. DEPT OF ENERGY - ALBUQUERQUE OPERATIONS OFFICE
R. LOWERY
JOSEPH M. MCGOUGH
DORNER T. SCHUELER
U.S. DEPT OF ENERGY - AMERICAN SOCIETY FOR ENVIRONMENTAL PROTECTION
R. COOPERSTEIN
U.S. DEPT OF ENERGY - ASSISTANT GENERAL COUNSEL FOR ENVIRONMENT
S. H. GREENLEIGH
U.S. DEPT OF ENERGY - CHICAGO OPERATIONS OFFICE
D. BRAY
PUBLIC READING ROOM
R. SELBY
U.S. DEPT OF ENERGY - DALLAS SUPPORT OFFICE
CURTIS E. CARLSON, JR.
U.S. DEPT OF ENERGY - DIVISION OF WASTE REPOSITORY DEPLOYMENT
W. WADE BALLARD, JR.
J. W. BENNETT
C. R. COOLEY (2)
WARREN EISTER
MARK W. FREI
CRITZ H. GEORGE
THOMAS P. LONGO
HARRY W. SMEDES
RALPH STEIN
U.S. DEPT OF ENERGY - HEADQUARTERS
PUBLIC READING ROOM
U.S. DEPT OF ENERGY - IDAHO OPERATIONS OFFICE
PUBLIC READING ROOM
JOHN B. WHITSETT

U.S. DEPT OF ENERGY - NEVADA OPERATIONS OFFICE
J. B. COTTER
M.P. KUNICH
PUBLIC READING ROOM
U.S. DEPT OF ENERGY - NUCLEAR ENVIRONMENTAL APPLICATION BRANCH
ROBERT W. BARBER
U.S. DEPT OF ENERGY - NWTS PROGRAM OFFICE
T. BAILLIEUL
M. BLANCHARD
L. A. CASEY
MICHAEL T. FIELD
R. LAHOTI
L. K. MCCLAIN
J. O. NEFF
K. K. WU
R. C. WUNDERLICH
U.S. DEPT OF ENERGY - OAK RIDGE OPERATIONS OFFICE
PUBLIC READING ROOM
U.S. DEPT OF ENERGY - OFFICE OF BASIC ENERGY SCIENCES
MARK W. WITTELS
U.S. DEPT OF ENERGY - OFFICE OF NUCLEAR WASTE MANAGEMENT
STEPHEN LANES
EARL WAHLQUIST
U.S. DEPT OF ENERGY - OFFICE OF PROJECT AND FACILITIES MANAGEMENT
D. L. HARTMAN
U.S. DEPT OF ENERGY - OFFICE OF WASTE ISOLATION
JANIE SHAHEEN
U.S. DEPT OF ENERGY - OFFICE OF WASTE PRODUCTS
JAMES TURI
U.S. DEPT OF ENERGY - REGION VIII
SIGRID HIGDON
U.S. DEPT OF ENERGY - RICHLAND OPERATIONS OFFICE
R. B. GORANSON
PUBLIC READING ROOM
J. SCHREIBER
U.S. DEPT OF ENERGY - SAN FRANCISCO OPERATIONS OFFICE
ENERGY RESOURCES CENTER
LEN LANNI
PUBLIC READING ROOM
U.S. DEPT OF ENERGY - SAVANNAH RIVER OPERATIONS OFFICE
REGINA T. HARRIS
T. B. HINDMAN
U.S. DEPT OF ENERGY - WIPP PROGRAM
LAWRENCE H. HARMON
U.S. DEPT OF LABOR
ALEX G. SCIULLI
KELVIN K. WU
U.S. ENVIRONMENTAL PROTECTION AGENCY
DIVISION OF CRITERIA & STANDARDS
DONALD HUNTER
JAMES NEIHEISEL
U.S. GENERAL ACCOUNTING OFFICE
WILLIAM DAVID BROOKS
U.S. GEOLOGICAL SURVEY - COLUMBUS
A. M. LA SALA, JR.
U.S. GEOLOGICAL SURVEY - DENVER
JESS M. CLEVELAND
G. L. DIXON
S.S. GOLDICH
W. SCOTT KEYS
WILLIAM WILSON
ROBERT A. ZIELINSKI
U.S. GEOLOGICAL SURVEY - JACKSON
GARALD G. PARKER, JR.
U.S. GEOLOGICAL SURVEY - MENLO PARK
JOHN BREDEHOEFT
J. BYERLEE
JACOB RUBIN
U.S. GEOLOGICAL SURVEY - RESTON
I-MING CHOU
JOHN ROBERTSON
EDWIN ROEDDER
EUGENE H. ROSEBOOM JR
PETER R. STEVENS
DAVID B. STEWART
NEWELL J. TRASK JR
U.S. HOUSE SUBCOMMITTEE ON ENERGY AND THE ENVIRONMENT
MORRIS K. UDALL
U.S. NUCLEAR REGULATORY COMMISSION
J. CALVIN BELOTE
R. BOYLE
ENRICO F. CONTI
MICHAEL C. CULLINGFORD
J. J. DAVIS
JOSEPH F. DONOGHUE
F. L. DOYLE
FREDERICK FORSCHER
RICHARD F. FOSTER
PAUL F. GOLDBERG
HIGH-LEVEL WASTE LICENSING BRANCH
HIGH-LEVEL WASTE TECHNICAL
CLYDE JUPITER
PHILIP S. JUSTUS
LIBRARY
JAMES C. MALARO
JOHN B. MARTIN (3)
JOHN C. MCKINLEY
HUBERT MILLER
THOMAS J. NICKOLSON
EDWARD ODONNELL
JAY E. RHODERICK
U.S. SENATE COMMITTEE ON ENERGY AND NATURAL RESOURCES
WILLIS D. SMITH
UNION CARBIDE CORP
JOHN D. SHERMAN
UNION OF CONCERNED SCIENTISTS
MICHAEL FADEN
UNIVERSITY OF ALBERTA
F.W. SCHWARTZ
UNIVERSITY OF ARIZONA
JAAK DAEMEN
STANLEY N. DAVIS
JAMES G. MCCRAY
SHLOMO P. NEUMAN
ROY G. POST
DAVID L. SOUTH
UNIVERSITY OF CALIFORNIA AT BERKELEY
NEVILLE G. W. COOK
TODD LAPORTE
BJORN PAULSSON
THOMAS H. PIGFORD
UNIVERSITY OF CALIFORNIA AT LOS ANGELES
D. OKRENT
UNIVERSITY OF CALIFORNIA AT RIVERSIDE
LEWIS COHEN
DON STIERMAN
UNIVERSITY OF CALIFORNIA AT SAN DIEGO
RICHARD J. WILLIS
UNIVERSITY OF CALIFORNIA AT SANTA CRUZ
JOEL PRIMACK
UNIVERSITY OF CHICAGO
BARRETT R. FRITZ
UNIVERSITY OF DELAWARE
ROBERT R. JORDAN
FRANK A. KULACKI
UNIVERSITY OF FLORIDA
DAVID E. CLARK
DOLORES C. JENKINS
M. J. OHANIAN
UNIVERSITY OF HAWAII AT MANOA
DAVID EPP
MURLI H. MANGHNANI
UNIVERSITY OF ILLINOIS AT URBANA - CHAMPAIGN
MAGDI RAGHEB
UNIVERSITY OF LOWELL
JAMES R. SHEFF
UNIVERSITY OF MARYLAND
MARVIN ROUSH
UNIVERSITY OF MINNESOTA
E. N. LINDNER
RAYMOND STERLING
D. H. YARDLEY
UNIVERSITY OF MISSOURI AT COLUMBIA
W.D. KELLER
UNIVERSITY OF MISSOURI AT KANSAS CITY
EDWIN D. GOEBEL
SYED E. HASAN
UNIVERSITY OF MISSOURI AT ROLLA
ALLEN W. HATHEWAY
NICK TSOULFANIDIS
UNIVERSITY OF NEVADA AT RENO
RODNEY J. WEICK
BECKY WEIMER
UNIVERSITY OF NEW HAMPSHIRE
ROBERT I. DAVIS
UNIVERSITY OF NEW MEXICO
DOUGLAS G. BROOKINS
UNIVERSITY OF NORTH CAROLINA
PAUL D. FULLAGAR
UNIVERSITY OF OKLAHOMA
DANIEL T. BOATRIGHT
UNIVERSITY OF OTTAWA
TUNCER OREN
UNIVERSITY OF PITTSBURGH
B. L. COHEN
UNIVERSITY OF SOUTHERN MISSISSIPPI
CHARLES R. BRENT
ROBERT E. BURKS
JAMES W. PINSON
DANIEL A. SUNDEEN
GARY L. WILDMAN
UNIVERSITY OF TENNESSEE AT KNOXVILLE
DON W. BYERLY
J.B. FUSSELL
UNIVERSITY OF TEXAS AT AUSTIN
BUREAU OF ECONOMIC GEOLOGY
THOMAS C. GUSTAVSON
MARTIN P. A. JACKSON
DALE KLEIN
JOE D. LEDBETTER
E. G. WERMUND
UNIVERSITY OF TEXAS AT SAN ANTONIO
DONALD R. LEWIS
UNIVERSITY OF TOKYO
RYOMEI KIYOSE
UNIVERSITY OF TORONTO
N. S. BRAR
R. M. STESKY
UNIVERSITY OF UTAH
RODGER WEAVER
UNIVERSITY OF UTAH MEDICAL CENTER
JAMES A. SORENSON

UNIVERSITY OF UTAH RESEARCH INSTITUTE
DUNCAN FOLEY
UNIVERSITY OF WASHINGTON
DAVID BODANSKY
KAI N. LEE
M. A. ROBKIN
UNIVERSITY OF WATERLOO
JOHN E. GALE
UNIVERSITY OF WESTERN ONTARIO
WILLIAM S. FYLE
P. W. M. JACOBS
UNIVERSITY OF WISCONSIN
B. C. HAIMSON
UNIVERSITY OF WISCONSIN AT MILWAUKEE
HOWARD PINCUS
URS/JOHN A. BLUME & ASSOCIATES, ENGINEERS
ANDREW B. CUNNINGHAM
UTAH BUREAU OF RADIATION CONTROL
DARRELL M. WARREN
UTAH GEOLOGICAL AND MINERAL SURVEY
GENEVIEVE ATWOOD
MAGE YONETANI
UTAH NUCLEAR WASTE REPOSITORY TASK FORCE
JAMES O. MASON, M.D., DR. P. H.
UTAH SOUTHEASTERN DISTRICT HEALTH DEPARTMENT
ROBERT L. FURLOW
UTAH STATE UNIVERSITY
DEPT OF GEOLOGY
UTILITY DATA INSTITUTE
FRED YOST
VANDERBILT UNIVERSITY
FRANK L. PARKER
VERMONT AGENCY OF ENVIRONMENTAL CONSERVATION
CHARLES A. RATTE
VERMONT STATE NUCLEAR ADVISORY PANEL
VIRGINIA CALLAN
VIRGINIA DIVISION OF MINERAL RESOURCES
ROBERT C. MILICI
VIRGINIA POLYTECHNIC INSTITUTE AND STATE UNIVERSITY
DAVID R. WONES
WASHINGTON DEPT OF SOCIAL AND HEALTH SERVICES
T. STRONG
WASHINGTON HOUSE OF REPRESENTATIVES
RAY ISAACSON
WASHINGTON STATE SENATE
DONN CHARNLEY
WASHINGTON STATE UNIVERSITY
GEORGIA YUAN
WATTLAB
BOB E. WATT
WAYNE STATE UNIVERSITY
JAMES A. WOODYARD
WBAI-FM
WARREN LIEBOLD
WEST VALLEY NUCLEAR SERVICES COMPANY INC
RICHARD M. WINAR
WEST VIRGINIA GEOLOGICAL AND ECONOMIC SURVEY
ROBERT B. ERWIN
WESTINGHOUSE ELECTRIC CORP
GEORGE V. B. HALL
D. NEWBY
GEORGE P. SABOL
JAMES H. SALING
WESTINGHOUSE WIPP PROJECT
WESTINGHOUSE ELECTRIC CORPORATION
WISCONSIN DIVISION OF STATE ENERGY
ROBERT HALSTEAD
WISCONSIN GEOLOGICAL AND NATURAL HISTORY SURVEY
MICHAEL G. MUDREY, JR.
MEREDITH E. OSTROM
WISCONSIN PUBLIC SERVICE CORP
PAUL WOZNIAK
WOODWARD-CLYDE CONSULTANTS
F. R. CONWELL (2)
ASHOK PATWARDHAN
WP-SYSTEM AB
IVAR SAGEFORS
WYOMING GEOLOGICAL SURVEY
DANIEL N. MILLER
YALE UNIVERSITY
BRIAN SKINNER

☆USGPO: 1982 — 559-099/1315

BATTELLE Project Management Division
505 King Avenue
Columbus, Ohio 43201